Technical Report Documentation Page

1. Report No.	2. Government Accession No.	3. Recipient's Catalog No.
FHWA/TX-03/9-558-1		

4. Title and Subtitle	5. Report Date
EVALUATION OF SIMPLE PERFORMANCE TESTS ON HMA MIXTURES FROM THE SOUTH CENTRAL UNITED STATES	June 2003 Resubmitted: March 2004
	6. Performing Organization Code

7. Author(s)	8. Performing Organization Report No.
Amit Bhasin, Joe W. Button, and Arif Chowdhury	Report 9-558-1

9. Performing Organization Name and Address	10. Work Unit No. (TRAIS)
Texas Transportation Institute The Texas A&M University System College Station, Texas 77843-3135	11. Contract or Grant No. Project No. 9-558

12. Sponsoring Agency Name and Address	13. Type of Report and Period Covered
Texas Department of Transportation Research and Technology Implementation Office P. O. Box 5080 Austin, Texas 78763-5080	Research: January 2002- April 2003
	14. Sponsoring Agency Code

15. Supplementary Notes

Research performed in cooperation with the Texas Department of Transportation and the U.S. Department of Transportation, Federal Highway Administration.
Research Project Title: Superpave Performance Testing

16. Abstract

A wide variety of hot mix asphalt (HMA) materials and mixture designs were obtained from the six states in the south central region of the United States. Three additional mixtures were designed and produced in the laboratory to provide modified mixtures in this project. All mixtures were characterized using the three simple performance tests (dynamic modulus, flow number, and flow time), Superpave shear test - frequency sweep at constant height (SST-FSCH), and the Asphalt Pavement Analyzer (APA) as a torture test. The Hamburg wheel-tracking device (HWTD) was also conducted on selected mixtures.

Objectives included the following: evaluate applicability of current test procedures and equipment for measuring HMA mixture properties with particular emphasis on complex modulus; provide state departments of transportation in the south central United States familiarity with the proposed |E*| parameter; generate information on performance of selected HMA mixtures with the new tests; extend the application of the protocols to gap-graded (e.g., stone mastic asphalt or Texas department of transportation coarse matrix high binder) mixtures; compare results from |E*| test results with other established tests (e.g., SST-FSCH, APA); evaluate specially designed HMA mixtures which may exhibit low dynamic modulus but high recovery of strains (i.e., HMA containing a highly polymer-modified soft asphalt, e.g., PG 64-40). A limited study was conducted to characterize the cracking potential of the selected mixtures using parameters from the indirect creep test in addition to the dynamic modulus test parameters.

Results showed that flow number value and flow time slope correlated better with laboratory rutting (APA and HWTD) than dynamic modulus. The correlations of |E*| or |G*| with APA were better at lower frequencies than at higher frequencies. Flow time slope, flow number value, $|E^*|/\sin\phi$ at 1 Hz, flow number slope, and flow time value were among the best five correlations both with HWTD and the APA rut depths.

17. Key Words	18. Distribution Statement
Simple Performance Test, Dynamic Modulus, Flow Time, Flow Number	No restrictions. This document is available to the public through NTIS: National Technical Information Service 5285 Port Royal Road Springfield, Virginia 22161

19. Security Classification (of this report)	20. Security Classification (of this page)	21. No. of Pages	22. Price
Unclassified	Unclassified	152	

Form DOT F 1700.7 (8-72) **Reproduction of completed page authorized**

EVALUATION OF SIMPLE PERFORMANCE TESTS ON HMA MIXTURES FROM THE SOUTH CENTRAL UNITED STATES

by

Amit Bhasin
Graduate Research Assistant
Texas Transportation Institute

Joe W. Button, P.E.
Senior Research Engineer
Texas Transportation Institute

and

Arif Chowdhury, P.E.
Associate Transportation Researcher
Texas Transportation Institute

Report 9-558-1
Project Number 9-558
Research Project Title: Superpave Performance Testing

Sponsored by the
Texas Department of Transportation
In Cooperation with the
U.S. Department of Transportation
Federal Highway Administration

June 2003
Resubmitted: March 2004

TEXAS TRANSPORTATION INSTITUTE
The Texas A&M University System
College Station, Texas 77843-3135

DISCLAIMER

The contents of this report reflect the views of the authors, who are responsible for the facts and the accuracy of the data presented herein. The contents do not necessarily reflect the official view or policies of the Federal Highway Administration (FHWA) or the Texas Department of Transportation (TxDOT). This report does not constitute a standard, specification, or regulation. The engineer in charge of the project was Joe W. Button, P.E. (Texas, # 40874).

ACKNOWLEDGMENTS

This project was funded by FHWA and conducted in cooperation with TxDOT and FHWA.

Mr. John Bukowski of FHWA in Washington, D.C., was instrumental in establishing this project. His efforts are hereby gratefully acknowledged.

The project directors for the sponsoring agencies were Mr. Jim Travis of FHWA and Mr. Dale Rand of TxDOT, both in Austin, Texas. Mr. Greg Cleveland of TxDOT also assisted in the direction of this work. The guidance and assistance provided by these gentlemen during prosecution of this work was very helpful and is much appreciated.

TABLE OF CONTENTS

Page

LIST OF FIGURES

Page

LIST OF TABLES

Page

CHAPTER 1
INTRODUCTION

BACKGROUND

The Federal Highway Administration (FHWA) and, particularly, the National Cooperative Highway Research Program (NCHRP) have sponsored or are sponsoring research projects that will lead to the development and validation of advanced materials characterization models and associated laboratory testing procedures for hot mix asphalt (HMA) (i.e., NCHRP Projects 1-37A, 1-40, 9-19, 9-29, and 9-30). They are sponsoring development of a product currently called the 2002 Pavement Design Guide, which will lead, in part, to improved methods of characterizing HMA material properties. The recommended test methods for the design guide focus on the complex modulus (E*) or dynamic modulus (|E*|) of compacted HMA materials but also involve accumulated axial strain from a repetitive loading test (flow number) and tertiary axial strain from a static test (flow time). This series of three tests has been termed simple performance tests (SPTs) for rutting (Witczak et al. 2002).

FHWA desires to study these SPT procedures using commonly employed HMA materials from departments of transportation (DOTs) within the central U.S. region and compare |E*| of these mixtures with results from other established laboratory tests. The North Central, Southeast, and South Central Superpave Centers, located at Purdue University, the National Center for Asphalt Technology, and the Texas Transportation Institute (TTI), respectively, are conducting similar studies simultaneously for FHWA.

The results of this research project will provide practical information to state DOTs in the central region of the United States regarding how their standard mixes respond to the SPTs. And just as importantly, if not more so, the results will show how standard mixtures respond to the new test procedures and may provide information useful for subsequently setting or adjusting criteria.

Researchers obtained a wide variety of HMA materials and mixture designs from the six states in the central region of the United States and three special mixtures were designed and produced in the laboratory to provide additional dimensions to this study. Rutting potential of all mixtures were characterized using the three SPTs (dynamic modulus, flow time and flow number), Superpave shear test-frequency sweep at constant height (SST-FSCH), and the Asphalt

Pavement Analyzer (APA) as a torture test. Additionally, five selected mixture designs were tested using the Hamburg Wheel Tracking Device (HWTD).

Cracking potential of the mixtures was estimated using indirect tensile strength and indirect tensile creep tests.

OBJECTIVES

Specific objectives of this research project were to:

- evaluate applicability of current test procedures and equipment for measuring HMA mixture properties with particular emphasis on complex modulus;
- provide state DOTs in the south central region familiarity with the proposed E*/sin N parameter and generate information on performance of selected HMA mixtures in the new tests;
- extend the application of the protocols to gap-graded or coarse graded mixtures (e.g., TxDOT coarse matrix-high binder [CMHB] and stone-filled mixtures);
- compare results from dynamic modulus tests with those from other established tests (e.g., SST-FSCH, APA, and HWTD for rutting potential and indirect tension and indirect tensile creep for cracking potential);
- evaluate specially designed HMA mixtures, which exhibit low dynamic moduli but high recovery of strains (i.e., HMA containing a highly polymer-modified soft asphalt; and
- provide feedback to FHWA and others regarding the practical issues associated with implementation of the new SPT procedures.

CHAPTER 2
SELECTION OF TESTS AND MIXTURES

SELECTED MIXTURES

Nine HMA mixtures were obtained from state DOTs in the South Central Region of the United States including states of Arkansas, Arizona, Louisiana, New Mexico, Oklahoma, and Texas with varied degrees of reported field performances. One mixture was designed in the TTI laboratory using rounded gravel and sand with a PG 64-22, which was intended to be rut susceptible. Two additional mixtures were designed using a highly polymer-modified asphalt, PG 64-40, to evaluate the tests using mixtures with low modulus but high recovery. The selected asphalt had a polymer content near 6 percent; whereas, a usual value is about 1 to 2 percent. One of the mixtures containing PG 64-40 asphalt was designed using crushed river gravel aggregate and the other using rhyolite aggregate. A summary of the twelve selected mixtures is shown in Table 2.1.

The selected mixtures also had a wide range of gradations varying from dense to coarse graded mixtures. The gradations for the HMA mixtures are shown in Appendix A.

A variety of mixture parameters, such as binder grade and aggregate size, were selected to ascertain if the rutting performance predicted using various test procedures was consistent irrespective of these variables.

TEST PROCEDURES

The following five tests for evaluating the rutting potential of the mixtures were included in this study:

- Asphalt Pavement Analyzer (APA),
- Superpave Shear Test-Frequency Sweep at Constant Height,
- dynamic modulus,
- flow time (static creep), and
- flow number (dynamic creep).

In addition, indirect tension and indirect tensile creep tests were conducted to study cracking potential of the selected mixtures.

Table 2.1. Details of Selected Mixtures.

State (Mix Code)	Max Nom. Agg. Size, mm	Aggregate Type	Binder Grade	Additives	Design AC[1], %	Design Air Voids, %	Remarks
Arkansas DOT (ARTL)	9.5	Twin Lakes Gravel	Tosco PG 64-22	None	6.0	4.5	--
Arkansas DOT (ARLR)	9.5	Granite Mountain	Mtn. Lyon PG 64-22	0.5% Morelife 300	5.8	4.5	--
Arizona DOT (AZ)	19	Basalt	PG 64-22	1.5% Type II Cement	5.0	5.0	Below restricted zone
Louisiana DOT (LA)	12.5	Nova Scotia Granite	PG 70-22M	0.6% Anti-strip	4.7	4.0	Level 1 Design
New Mexico DOT (NM Bingham)	12.5	Hard Rock Crushed Gravel	PG 70-22	1.5% Lime	4.3	4.0	--
New Mexico DOT (NMVado)	19	Monzo-nite, Vado	PG 82-16	None	4.8	4.0	--
Oklahoma DOT (OK)	12.5	Granite + Limestone	PG 70-28	None	4.8	4.0	--
Texas DOT Wichita Falls (TXWF)	12.5	Limestone	PG 76-22	1% Lime	4.8	4.0	Stone-Filled Gradation
Texas DOT Bryan (TXBryan)	16	Limestone	PG 64-22	None	4.6	3.5	TxDOT Type CMHB-C (coarse matrix-high binder)
Lab Mix (ROG)	9.5	Rounded River Gravel	PG 64-22	None	5.5	4.0	Designed to be Rut Susceptible
Lab Mix (64-40RG)	9.5	Crushed River Gravel	PG 64-40	None	5.5	4.0	Low Modulus High Recovery
Lab Mix (64-40RHY)	9.5	Rhyolite	PG 64-40	None	7.8	3.5	Low Modulus High Recovery

[1]AC = asphalt content

Due to the lack of field performance data, the researchers chose the APA to represent a simulative type of performance prediction test or torture test. Selected mixtures were also tested using the HWTD. The researchers realize that these laboratory devices cannot always accurately predict actual pavement rutting but they should rank mixtures generally similar to their field rutting and/or identify mixtures that are rut susceptible. The SST-FSCH was developed as a part of the original performance prediction model in the strategic highway research program (SHRP) studies. The dynamic modulus, flow time and flow number tests were some of the "Simple Performance Tests" evaluated in NCHRP Project 9-19 (Witczak et al. 2002).

Each of these tests is further described in the following subsections. A description of the parameters from the test results that can be related to rutting performance is also provided.

Asphalt Pavement Analyzer

The APA is a loaded wheel tester which has been adopted by several state DOTs as a torture test device to evaluate or qualify their HMA paving mixtures. Independent studies (Williams and Prowell, 1999 and Zhang et al. 2002) have established a strong correlation between APA results and actual field rutting.

The APA test typically involves running a loaded grooved wheel over a pressurized rubber hose that rests on the test specimens. The APA test was conducted in a dry condition at 60°C (140°F) with a pressure of 0.689 MPa (100 psi) in the hose and a vertical load of 0.44 KN (100 lb). Three pairs (or replicates) of samples were tested. Data from each pair were recorded to one channel resulting in three replicate data sets. All specimens were molded using the Superpave gyratory compactor and were 75 mm (3 inches) in height and 150 mm (6 inches) in diameter.

The relevant parameters from the APA results used for evaluation are:

- Final rut depth at 8000 passes: One forward and one backward stroke comprise one cycle of the loaded wheel. The APA machine stops running the test at either 8000 passes or when the recorded rut depth is 12.5 mm (0.5 inch). In cases where the test was terminated before completing 8000 passes, the extrapolated value of the rut depth was computed for purposes of comparison.

- Creep slope of the linear portion of the rut depth versus number of passes curve: During the first two to three thousand passes, typically, the sample undergoes initial consolidation, and the deformation with respect to number of load passes becomes linear after that. The slope is determined for this linear segment of the response expressed in terms of millimeters of rut depth/thousand passes. The creep slope therefore gives a measure of deformation with respect to the number of load passes, irrespective of the amount of initial consolidation.

Superpave Shear Test-Frequency Sweep at Constant Height Test

The performance prediction model developed in the SHRP study included the Superpave shear tester in various modes, such as repeated shear at constant stress, simple shear at constant height, and frequency sweep at constant height. For laboratory experiments, these tests are typically performed at 4, 20, and 40°C (39, 68, and 104°F).

The parameters that are evaluated from these tests include the complex shear modulus (G*) and the phase angle (δ). The magnitude of the complex shear modulus is represented as:

$$|G^*| = \frac{\tau_0}{\gamma_0}$$

where,

|G*| = shear dynamic modulus

τ_0 = shear stress, and

γ_0 = shear strain.

Witczak et al. (2002) compared the |G*| and |G*|/sin δ values obtained by performing the shear test at constant height with the actual rutting for mixtures that were used in the Accelerated Loading Facility (ALF), MnRoad, and WesTrack test sections. They tested the mixes at different temperatures (38°C and 54°C) and strain levels (100, 150 and 200 microstrain). Good correlations (R^2 = 0.70 to 0.79) for strain levels at 100 microstrain and fair correlations (R^2 = 0.51 to 0.67) for strain levels at 150 and 200 microstrain were found.

Zhang et al. (2002) confirmed a sound correlation between APA rut tests and fundamental tests such as the repeated shear at constant height.

The SST-FSCH test was performed at 10, 5, 2, 1, 0.5, 0.2, 0.1, 0.05, 0.02, and 0.01 Hz. A constant and controlled shear strain (100 microstrain) was applied while the corresponding

shearing stress was recorded and the height of the specimen was kept constant by applying varying levels of axial load through a feedback-controlled system.

The parameters related to rutting that were evaluated in this study are:

- |G*| and |G*|/sin δ at 10 Hz and 40°C. This frequency was selected because it is the frequency that most closely represents highway speeds of about 60 miles per hour based on Barksdale's (1971) equivalent pulse time conversion for sinusoidal loading.
- |G*| and |G*|/sin δ at 1 Hz and 40°C. This frequency was used in order to compare the parameters of the SST with the APA. Since the APA loading arm moves at a stroke rate of 60 strokes per minute with a travel of about 300 mm (11.8 inch), the equivalent pulse time based on the Barksdale (1971) conversion is about 1 Hz.

Dynamic Modulus Test

The dynamic modulus test is not a new test on paving materials. A typical test is performed over a range of different temperatures by applying sinusoidal loading at different frequencies to a confined or unconfined sample.

The typical parameters resulting from such a test are the complex modulus (E*) and the phase angle (ϕ). The complex modulus is a function of the storage modulus and loss modulus. Typically, the magnitude of the complex modulus is represented as:

$$|E^*| = \frac{\sigma_0}{\varepsilon_0}$$

where,

|E*| = dynamic modulus

σ_0 = axial stress, and

ε_0 = axial strain.

Witczak et al. (2002) compared the |E*| and |E*|/sin ϕ values from dynamic modulus tests with actual field rutting using the WesTrack, ALF, and MnRoad test data. Comparisons were made for a wide variety of frequencies, temperatures, and test conditions (confined and unconfined), and correlations of varying degrees were found.

All SPT procedures were conducted in accordance with NCHRP 1-37A, "Draft Test Method for Dynamic Modulus Test," at 25, 10, 5, 1, 0.5, and 0.1 Hz and -10, 4, 20, 38, and 54.4°C. The stress level for measuring the dynamic modulus was chosen in order to maintain the

measured resilient strain within 50 to 150 microstrain. The order for conducting each test was from lowest to highest temperature and highest to lowest frequency of loading at each temperature to minimize specimen damage.

The data generated were used for plotting a master curve using the sigmoidal curve fitting function as demonstrated by Pellinen (2002). The sigmoidal function used is shown below:

$$\log(|E^*|) = \delta + \frac{\alpha}{1 + e^{\beta - \gamma \log(\xi)}}$$

where,

|E*| = dynamic modulus,

ξ = reduced frequency,

δ = minimum modulus value,

α = span of modulus values, and

β, γ = shape parameters.

The parameters related to rutting from the dynamic modulus test that were used for evaluation in this study are:

- |E*| and |E*|/sin ϕ at 10 Hz and 54.4°C (130°F). Similar to the SST, a frequency of 10 Hz was selected as it most closely corresponds to highway speeds of about 60 miles per hour.
- |E*| and |E*|/sin ϕ at 1 Hz and 54.4°C (130°F). This frequency was used for comparison with APA parameters as the loading frequency most closely matched the APA test conditions.

Shenoy and Romero (2002) recommended a standardized method for analyzing data from the dynamic modulus test using data from different frequencies and temperatures. They have proposed a method to develop a standardized curve. The slope of this standardized curve was found to correspond with the rutting performance of the mixture. The detailed analysis based on this procedure is beyond the scope of this current report. The data contained herein, however, can be used for such analyses.

The |E*| sin ϕ parameter at 21°C (70°F) from the dynamic modulus test was used to characterize the cracking potential of the mixes.

Flow Time Test

The flow time test has been recognized as one of the tests to measure the fundamental properties of HMA related to rutting performance by Witczak et al. (2002) in NCHRP Project 9-19. The test aims at measuring the visco-elastic response of an HMA specimen under a static stress level. This test can be performed in confined or unconfined conditions. The total compliance at any given point in time, D(t), is calculated as the ratio of the measured strain ε_t to the applied stress σ_0.

$$D(t) = \frac{\varepsilon_t}{\sigma_0}$$

Kaloush and Witczak (2002) described three basic zones in a typical plot of the compliance versus time graph on a log-log scale, i.e., primary, secondary, and tertiary. The primary zone is where the strain rate decreases sharply under static load and tends to stabilize reaching the secondary zone. In the secondary zone, the strain rate remains almost constant under the applied static load and starts increasing in the tertiary zone. These three zones are shown in Figure 2.1. Since the applied stress level is constant, the rate of change of compliance corresponds to the strain rate. A graph of rate of change of compliance versus loading time on a log-log scale (Figure 2.2) clearly shows the point of minimal rate of change, which corresponds to the starting point of the tertiary zone. The time corresponding to the start of the tertiary zone is referred to as the flow time. Based on the above description, flow time can therefore be considered as the time when the rate of change of compliance is the lowest.

Typically, the total compliance in the secondary zone at any given time, D(t), can be expressed as a power function as follows:

$D(t) = at^m$,

where,

t = time, and

a, b = regression constants.

The regression constants are obtained by plotting compliance versus time on a log-log scale in the secondary zone.

The above expression on a log-log scale can be rewritten as:

$\log D(t) = m \log(t) + \log(a)$,

where,

m = slope of the curve on a log-log scale, and

log(a) = intercept.

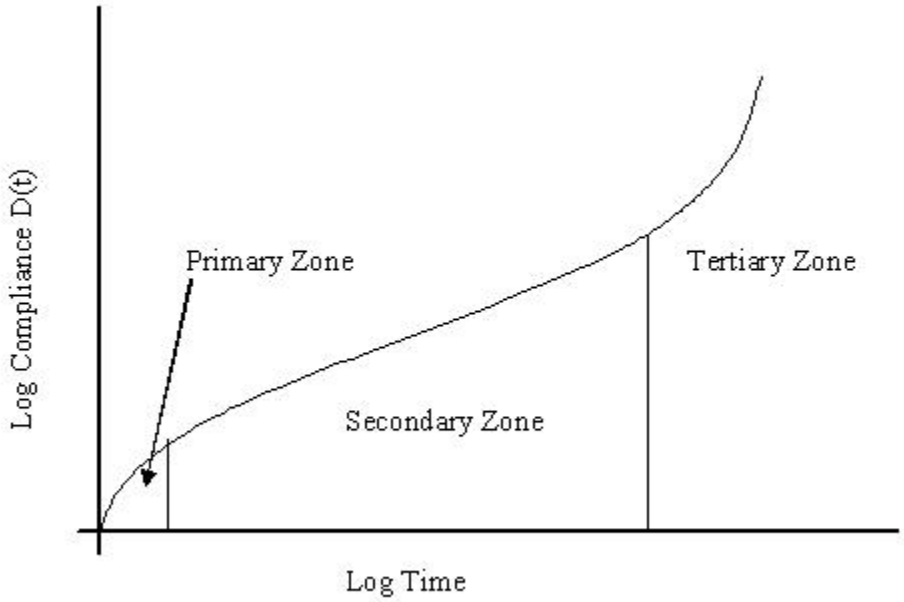

Figure 2.1. Compliance versus Time Curve on Log Scale.

The flow time test herein was conducted at 54.4°C (130°F). All the samples were tested at this temperature in order to provide a uniform basis for comparison.

The stress level selected for the test was 0.207 MPa (30 psi). This stress level was selected based on trial tests conducted on various samples in order to ensure that most specimens would exhibit tertiary flow within a reasonable testing time.

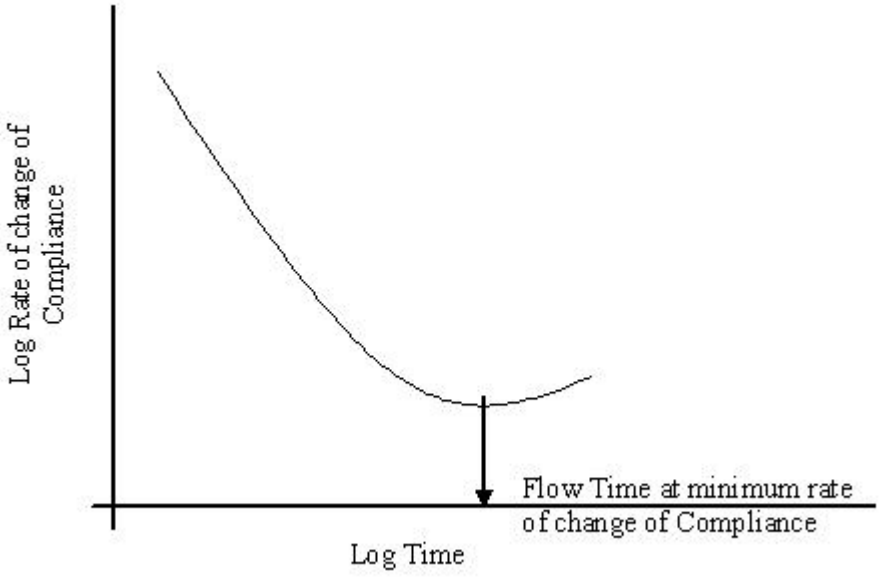

Figure 2.2. Rate of Change of Compliance versus Time on a Log Scale.

Some of the parameters related to rutting performance that were evaluated from the flow time tests are:

- flow time value, which corresponds to the start of the tertiary flow or the time at which the rate of change of compliance is minimum,
- slope parameter: m, and
- intercept parameter: a.

Witczak et al. (2002) as a part of Task C of NCHRP Project 9-19 correlated rutting performance with compliance at "short time" and "long time" in addition to the above parameters. These correlations were not very good. The present analysis, however, made comparisons between mixtures using the three bulleted parameters only.

Flow Number Test

The flow number test captures fundamental material properties of an HMA mixture that correlate with rutting performance. This test involves application of a specific stress level in a

dynamic form. The stress is typically applied in a haversine waveform with a wavelength of 0.1 seconds followed by a rest or dwell period of 0.9 seconds. All tests were conducted at 54.4°C (130°F). This test is different from the flow time test because it applies a dynamic load and provides periodic recovery periods for the test specimen.

Permanent strain data from the test results can be recorded and plotted against the number of load cycles. This plot is similar to that in the flow time test with primary, secondary, and tertiary zones. The permanent strain is also expressed as a power function in terms of the number of cycles as follows:

$\varepsilon_p = aN^b$

where,

ε_p = permanent strain,

a, b = regression constants, and

N = number of load cycles at which the permanent strain is recorded.

On a log-log scale the equation is,

$\log \varepsilon_p = \log a + b \log N$

where,

log a = intercept on log-log plot of permanent strain versus number of load cycles, and

b = slope on log-log plot of permanent strain versus number of load cycles.

Witczak et al. (2002) selected several parameters from the flow number test for evaluation. These included the intercept and slope, resilient modulus, resilient strain, μ parameter, flow number value, permanent strain, and ratio of permanent to resilient strain. The degree of correlation obtained with respect to field rutting varied for each of these parameters ranging from "poor" to "excellent." However, only the following parameters were considered:

- flow number value, which corresponds to the number of cycles at which the tertiary flow starts or the number of cycles at which the rate of change of compliance is minimum, and
- slope parameter, b.

The above parameters were found to have better correlations with field rutting as compared to the remaining parameters considered in the NCHRP study.

Hamburg Wheel Tracking Device

HWTD testing was performed on five HMA mixtures that included two from TxDOT (TXBryan from the Bryan District and TXWF from the Wichita Falls District) and three laboratory mixes (64-40RHY, 64-40RG, and ROG).

HWTD testing consisted of oscillating a 200-mm (8.0-inch) diameter and 47-mm (1.85-inch) wide steel wheel loaded with 705 N (158 lb) over a Superpave gyratory compactor (SGC) compacted specimen 63 mm (2.5 inches) in height submerged in water at 50°C (122°F). Permanent deformation of each specimen was recorded with reference to the number of passes of the loaded wheel. TxDOT typically records HWTD rutting in terms of a specified number of passes depending on the grade of the asphalt. Mixtures showing excessive susceptibility to moisture damage tend to undergo stripping and may exhibit a sudden increase in the slope of a plot of rut depth versus the number of passes after a certain number of cycles. If a mixture is found to undergo stripping, then the final deformation value cannot be used directly for comparison of permanent deformation characteristics with other tests. Typical HWTD results are shown in Figure 2.3.

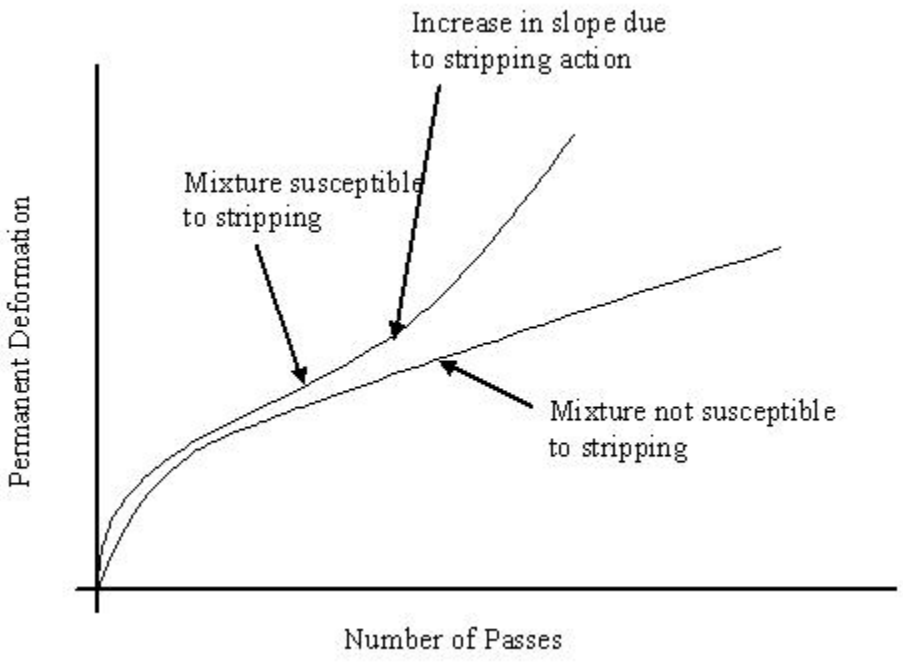

Figure 2.3. Typical Hamburg Wheel Tracking Device Results.

Indirect Tension Creep Test

The indirect tension creep test was recognized as one of the simple performance tests to characterize the cracking potential of the HMA mixtures by Witczak et al. (2002) in the NCHRP project 9-19. Further, this test provides information regarding the elastic and viscoelastic components of the mixture properties.

Indirect tensile creep testing was conducted at 21°C (70°F). Two replicates of a 150-mm (6-inch) diameter and 38-mm (1.5-inch) thick specimen were subjected to a static diametral loading of 200 N (45 lbf). This load level was selected because it was within the range of 1% to 3% of the indirect tensile strength of the mixtures being tested. Indirect tensile strength tests were performed on other specimens before the indirect tensile creep tests in order to estimate this load level. The static load was applied for a period of 1000 seconds after which the load was removed, and the loading axis was free of any contact with the test specimen. Lateral tensile strain at the center of the specimen was recorded using a gauge length of 76.2 mm (3 inches) during the 1000-second loading period and for another 1000 seconds after the load was removed. These tests resulted in typical static creep curves for viscoelastic materials exhibiting elastic strain, plastic strain, viscoelastic strain, and viscoplastic strain.

Viscoelastic and viscoplastic components of the strain were computed from a typical strain vs. time response curve for a static creep test as shown in Figure 2.4. The final permanent deformation at the end of each test was attributed to the plastic and viscoplastic strains. This is based on the assumption that the final strain becomes asymptotically parallel with time and there is no viscoelastic recovery after 1000secs. The calculated viscoplastic strain would be conservative if this assumption is not entirely true.

Poisson's ratio and creep compliance were calculated based on the formulae recommended by Witczak et al. (2002):

$$\mu = 0.15 + \frac{0.35}{1 + \exp(3.1849 - 0.04233 x Temp)}$$

where,

μ = Poisson's ratio, and

Temp = temperature in Fahrenheit,

$$D(t) = E(t)^{-1} = \frac{T\delta_{xx}}{P(0.2339 + 0.7801\mu)}$$

where,

D(t) = compliance at time t,

T = thickness of the specimen,

D = lateral deformation at the center,

P = diametral load, and

0.2339 and 0.7801 are regression constants for 76.2-mm (3-inch) gauge length at center of the specimen.

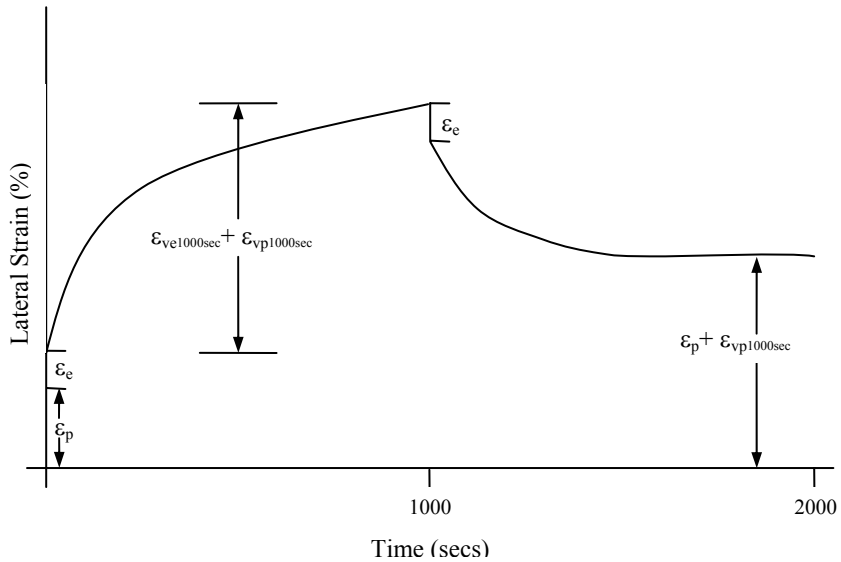

Figure 2.4. Typical Response from a Indirect Tensile Creep Test

The parameters selected for characterizing the cracking potential of the mixes from the indirect tensile creep test were:

- compliance at 1000 seconds,
- viscoelastic strain, and
- viscoplastic strain.

SPECIMEN PROPERTIES AND CONDITIONING FOR ALL TESTS

All test specimens were fabricated using the same mixture design developed by the individual agency (DOT). For the dynamic modulus, flow time, and flow number tests, the specimens were 100 mm (4 inches) in diameter and 150 mm (6 inches) in height with a gauge length of 100 mm (4 inches). Technicians prepared the specimens by coring and sawing the ends of a 150-mm (6-inches) diameter and 175-mm (7-inches) height specimen, which was compacted using a SGC. Technicians ensured that the air voids in the cored and finished specimen were between 6 and 8 percent. Studies conducted by Witczak et al. (2002) indicate that the standard error for testing using two replicates with three linear variable displacement transformers (LVDTs) is approximately the same as that for testing using three replicates with two LVDTs for mixtures with maximum nominal aggregate size of 19 mm (3/4th inch) or less. Therefore, two replicates with three LVDTs glued on each specimen were used for each of these tests.

For the APA and SST tests the samples were prepared using the SGC. Two replicates were used for the SST and three replicates (three pairs of six specimens) were used for the APA.

The dynamic modulus test was conducted at five different temperatures, i.e., -10, 4, 20, 38, and 54.4°C. For each test temperature, the samples were conditioned to ensure that the core of the specimen had reached the desired testing temperature. This was accomplished using a dummy sample in the environmental chamber with a thermocouple near its center. Care was taken to avoid prolonged heating of samples at higher temperatures. All flow time and flow number tests were conducted at 54.4°C. SST-FSCH tests were conducted at both 20 and 40°C. APA tests were conducted at 60°C. In all tests, similar preconditioning procedures were adopted.

CHAPTER 3
RESULTS AND ANALYSIS

GENERAL

This chapter discusses results obtained from the various tests. In general, various parameters (identified in Chapter 2) from the fundamental tests, such as SST-FSCH, dynamic modulus, flow time, and flow number, were compared with the data obtained from the empirical torture tests.

The SHRP procedure recommends that the performance prediction tests for comparing various mixtures be performed at an effective temperature. The effective test temperature is a single test temperature at which the amount of permanent deformation that would occur would be equivalent to that measured by considering each season separately throughout the year. Mixture designs were obtained from different geographic locations with a different effective temperature applicable to each region. In order to provide a uniform basis for evaluating the test results, all the mixtures (e.g., mixtures containing PG64 to PG82 binder) were tested at the same temperature. Hence, it is important to note that although some of the mixtures demonstrated extremely poor performance as compared to other mixes, this may not necessarily be representative of the actual field performance of the mix.

ASPHALT PAVEMENT ANALYZER

Three replicate tests were performed for each mixture design in the APA under dry conditions at 60°C. Data were recorded in terms of rut depth versus the number of strokes for each replicate. A summary of the results is shown in Table 3.1.

Mixtures ARLR and ROG were unable to complete 8000 passes in the APA. Recall that Mix ROG was designed to be rut susceptible. In both of these cases, the rut depth value at 8000 passes was determined by extrapolation to facilitate comparison with other test values. By extrapolation, the final rut depth at 8000 passes for Mix ARLR was 18.9 mm (0.74 inches) and for Mix ROG was 19.1 mm (0.75 inches).

APA creep slopes were computed for all mixtures. The linear portion of the curve indicating rut depth versus number of passes was identified. Values from this portion of the curve were then used with a best-fit method to find a straight-line slope in terms of millimeters

of rutting per thousand strokes. Graphs showing creep slopes are located in Appendix B. A summary of the creep slopes for various mixtures is indicated in Table 3.2.

Table 3.1. Summary of APA Rut Depth Results.

Mix Identity	Final Permanent Deformation (mm)				CV[1], %	No. APA Passes
	Left	Middle	Right	Average		
ARTL	8.6	8.0	7.9	8.2	5	8000
ARLR	11.5	12.1	10.5	11.3 (18.9)[2]	7	3865 (8000)
AZ	4.2	4.3	4.7	4.4	6	8000
LA	7.5	7.9	6.2	7.2	12	8000
NMBingham	2.6	2.9	2.1	2.5	16	8000
NMVado	---	2.3	1.8	2.0	18	8000
OK	4.7	4.3	3.8	4.2	11	8000
TXWF	3.3	4.0	3.5	3.6	10	8000
TXBryan	5.3	4.9	3.9	4.7	15	8000
ROG	19.8	17.0	16.8	17.9 (19.1)	9	6201 (8000)
64-40RG	6.4	6.5	6.1	6.3	3	8000
64-40RHY	3.8	3.7	3.8	3.8	1	8000

[1] CV – Coefficient of Variation
[2] ( ) – Indicates projected rut depth at 8000 passes

The value of creep slope as an independent parameter for evaluation is clear from Figure 3.1. A mixture with high rut depth does not necessarily indicate a mixture with higher creep slope in the linear region. This outcome is because as the wheel tracking test starts, the rut depth increases nonlinearly over the first one to two thousand passes, usually indicating consolidation in the sample.

After the initial deformation of a sample, the rate of rutting normally remains constant for the remainder of the test on a typical mixture. The total deformation value at 8000 passes is therefore a function of both the initial rut formation (consolidation) and the creep slope.

Table 3.2. Summary of APA Creep Slope Values.

Mix Identity	Slope (mm/thousand passes)				CV, %
	Left	Middle	Right	Average	
ARTL	0.528	0.438	0.491	0.49	9.4
ARLR	2.011	1.741	1.554	1.77	13.0
AZ	0.207	0.158	0.248	0.20	21.9
LA	0.268	0.282	0.302	0.28	5.9
NMBingham	0.147	0.292	0.151	0.20	41.9
NMVado	---	0.100	0.079	0.09	16.4
OK	0.281	0.299	0.202	0.26	19.7
TXWF	0.273	0.284	0.330	0.30	10.2
TXBryan	0.181	0.113	0.134	0.14	24.1
ROG	0.622	0.703	0.628	0.65	6.9
64-40RG	0.557	0.422	0.468	0.48	14.2
64-40RHY	0.155	0.189	0.242	0.19	22.6

CV – Coefficient of Variation

For example, consider mixtures TXWF and 64-40RHY. These mixes exhibited final APA rut depths of 3.6 and 3.8 mm, respectively. This test result indicates that TXWF performed equivalent to or slightly better than the 64-40RHY. But, if the rut rates are considered, then the creep slope for TXWF is 0.30 mm/thousand strokes and the creep slope for 64-40RHY is 0.19 mm per thousand strokes. This indicates that, if the test was conducted beyond 8000 passes, say for 9000 passes, the final rut depth for the 64-40RHY would likely be less than that for TXWF. Therefore, slope of the creep curve in addition to rut depth should be considered for comparing APA results with the various fundamental tests.

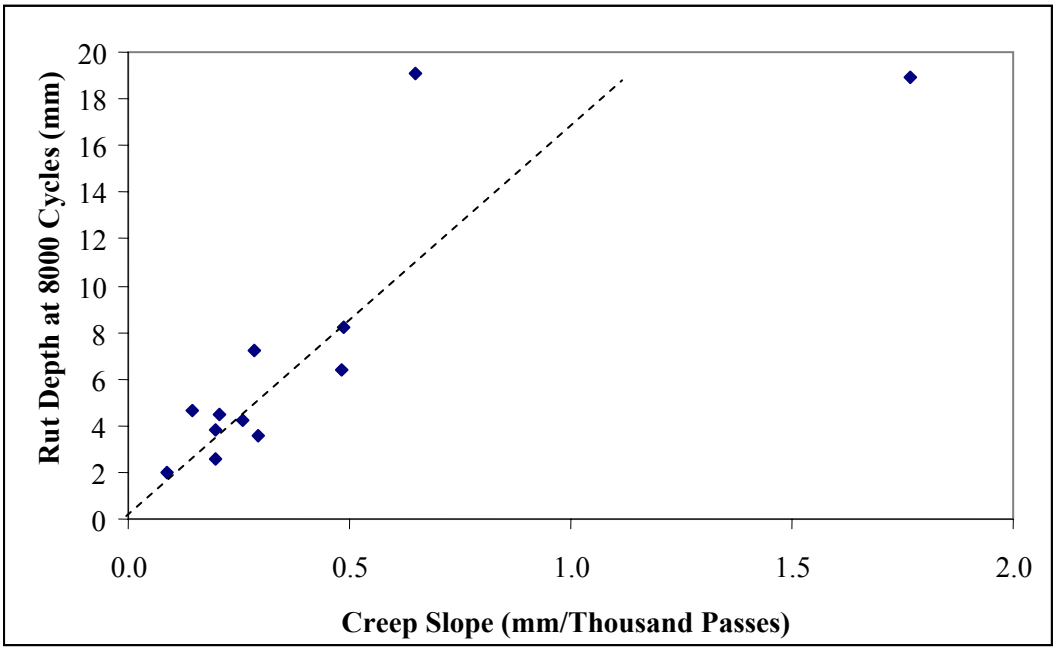

Figure 3.1. APA Rut Depth versus Creep Slope.

SST-FSCH TEST

Two replicates for each mixture design were tested using the SST at two temperatures (20 and 40°C) and ten different frequencies (10, 5, 2, 1, 0.5, 0.2, 0.1, 0.05, 0.02, and 0.01 Hz). For the purpose of comparing mixtures with respect to the rutting performance, the higher temperature of 40°C and frequencies of 10 Hz and 1.0 Hz were selected for data analysis. The frequency of 10 Hz, applied in sinusoidal form, was selected since it closely represents a highway speed of about 60 mph. A frequency of 1 Hz was selected in order to simulate the loading rate at which the APA wheel runs over the samples, for a more appropriate comparison with the APA results.

The parameters used for comparative analysis include |G*| and |G*|/sin δ at the above mentioned frequencies and temperature. Tables 3.3 through 3.6 give a summary of these data. All of the data for the SST tests at both temperatures and all frequencies are provided in Appendix C.

High variability in results was observed, particularly (but not necessarily) when the shear modulus values were toward the lower end (i.e., at high temperatures and/or low frequencies).

This indicates the test is not as sensitive for mixtures with lower shear modulus. This variability was exhibited in spite of the fact that the air voids for the tested specimens were within 7±0.5 percent.

Table 3.3. Summary of |G*| at 40°C and 10 Hz.

Mix Identity	|G*| (MPa)			CV, %
	Sample 1	Sample 2	Average 1000 MPa	
ARTL	29865	56629	43	44
ARLR	29524	34174	32	10
AZ	36884	35757	36	2
LA	46393	41339	44	8
NMBingham	72198	54706	63	19
NMVado	151066	110063	131	22
OK	49815	56280	53	9
TXWF	51645	44354	48	11
TXBryan	67367	65693	67	2
ROG	45657	43436	45	4
64-40RG	35757	15221	25	57
64-40RHY	8181	15276	12	43

CV – Coefficient of Variation

Table 3.4. Summary of |G*|/sin δ at 40°C and 10 Hz.

Mix Identity	|G*|/sin δ (MPa)			CV, %
	Sample 1	Sample 2	Average 1000 MPa	
ARTL	34867	73665	54	51
ARLR	33792	39601	37	11
AZ	45949	44254	45	3
LA	55816	52829	54	4
NMBingham	119995	84338	102	25
NMVado	330153	257258	294	18
OK	74840	84125	79	8
TXWF	74889	62336	69	13
TXBryan	92369	82246	87	8
ROG	65690	60608	63	6
64-40RG	44254	23990	34	42
64-40RHY	10752	28981	20	65

CV – Coefficient of Variation

Table 3.5. Summary of |G*| at 40°C and 1 Hz.

Mix Identity	|G*| (MPa)			CV, %
	Sample 1	Sample 2	Average 1000 MPa	
ARTL	10407	19075	15	42
ARLR	8528	9913	9	11
AZ	14296	12039	13	12
LA	14141	15308	15	6
NMBingham	34118	33910	34	0.4
NMVado	86288	63868	75	21
OK	22695	24005	23	4
TXWF	19880	17087	18	11
TXBryan	24934	22102	24	9
ROG	17410	17674	18	1
64-40RG	12039	8999	11	20
64-40RHY	4227	11145	8	64

CV – Coefficient of Variation

Table 3.6. Summary of |G*|/sin δ at 40°C and 1 Hz.

Mix Identity	|G*|/sin δ (MPa)			CV, %
	Sample 1	Sample 2	Average 1000 MPa	
ARTL	12945	23527	18	41
ARLR	10272	11784	11	10
AZ	18326	14517	16	16
LA	18276	21848	20	13
NMBingham	60528	63813	62	4
NMVado	187691	137994	163	22
OK	38127	41603	40	6
TXWF	29254	24056	27	14
TXBryan	36336	30250	33	13
ROG	26125	24891	26	3
64-40RG	14517	17063	16	11
64-40RHY	5694	30222	18	97

CV – Coefficient of Variation

DYNAMIC MODULUS TEST

Dynamic modulus testing on two replicates of each mixture design used five different temperatures and six frequencies. The temperatures used for testing were -10, 4, 20, 38, and 54.4°C, and the frequencies of loading were 25, 10, 5, 1, 0.5, and 0.1 Hz.

Previous studies (Witczak [2002] and Pellinen [2002]) found that the parameters |E*| and |E*|/sin ϕ at higher temperatures, i.e., 40 and 54.4°C, correlate with pavement rutting. In this study, the samples were tested at various frequencies and temperatures in order to develop a master curve using the sigmoidal function. As mentioned in Chapter 2, other parameters, such as slope function at slower loading rates from the standardized curve, could be further analyzed for other correlations with rutting performance. However, the scope of this report is restricted to measurement and comparison of |E*| and |E*|/sin ϕ parameters only. The frequencies used for comparative analyses are, again, 10 Hz and 1 Hz, which correspond to typical traffic speeds and the speed of APA loading, respectively.

A summary of results for |E*| and |E*|/sin ϕ at 54.4°C and at 10 and 1 Hz are presented in Tables 3.7 through 3.10. The master curve for all the mixes plotted using the sigmoidal function is shown in Figure 3.2. The detailed test data for the complete set of frequencies and temperatures are provided in Appendix D.

Table 3.7. Summary of |E*| at 54.4°C and 10 Hz.

Mix Identity	|E*| (MPa)			CV, %
	Sample 1	Sample 2	Average 1000 MPa	
ARTL	1323	848	1.1	31
ARLR	390	480	0.4	15
AZ	826	913	0.9	7
LA	712	794	0.8	8
NMBingham	1518	1771	1.6	11
NMVado	1625	1978	1.8	14
OK	629	406	0.5	31
TXWF	1120	1035	1.1	6
TXBryan	1145	1312	1.2	10
ROG	591	786	0.7	20
64-40RG	211	231	0.2	6
64-40RHY	507	405	0.5	16

CV – Coefficient of Variation

Table 3.8. Summary of |E*|/sin ϕ at 54.4°C and 10 Hz.

Mix Identity	|E*|/sin ϕ (MPa)			CV, %
	Sample 1	Sample 2	Average 1000 MPa	
ARTL	2753	1475	2.1	43
ARLR	734	864	0.8	12
AZ	1792	1798	1.8	0.2
LA	1402	1367	1.4	2
NMBingham	3896	4982	4.4	17
NMVado	4915	5159	5.0	3
OK	1140	855	1.0	20
TXWF	3037	2327	2.7	19
TXBryan	2421	2517	2.5	3
ROG	1180	1773	1.5	28
64-40RG	872	729	0.8	13
64-40RHY	1673	1250	1.5	21

CV – Coefficient of Variation

Table 3.9. Summary of |E*| at 54.4°C and 1 Hz.

Mix Identity	|E*| (MPa)			CV, %
	Sample 1	Sample 2	Average 1000 MPa	
ARTL	453	263	0.4	37
ARLR	135	147	0.1	6
AZ	333	347	0.3	3
LA	239	272	0.3	9
NMBingham	769	894	0.8	11
NMVado	854	992	0.9	11
OK	228	181	0.2	16
TXWF	544	430	0.5	17
TXBryan	528	503	0.5	3
ROG	231	323	0.3	23
64-40RG	152	145	0.1	3
64-40RHY	311	218	0.3	25

CV – Coefficient of Variation

Table 3.10. Summary of |E*|/sin ϕ at 54.4°C and 1 Hz.

Mix Identity	|E*|/sin ϕ (MPa)			CV, %
	Sample 1	Sample 2	Average 1000 MPa	
ARTL	876	413	0.6	51
ARLR	274	312	0.3	9
AZ	649	622	0.6	3
LA	417	511	0.5	14
NMBingham	1512	1810	1.7	13
NMVado	1792	1869	1.8	3
OK	427	411	0.4	3
TXWF	1158	799	1.0	26
TXBryan	1079	900	1.0	13
ROG	420	613	0.5	26
64-40RG	678	460	0.6	27
64-40RHY	845	628	0.7	21

CV – Coefficient of Variation

A summary of |E*| sin ϕ at 21°C and 10 Hz, which will be used for cracking characterization of the mixes, is provided in Table 3.11. The master curves for the mixes containing PG 64-40 asphalt are significantly different from the remaining curves. Further comparisons of the dynamic modulus test results with results from other tests are included in the analysis section later in this chapter.

Table 3.11. Summary of |E*| Sinϕ at 21°C and 10 Hz

Mix Identity	|E*| Sinϕ (MPa)			CV, %
	Sample 1	Sample 2	Average 1000 MPa	
ARTL	2566	2639	2603	2%
ARLR	2960	2717	2838	6%
AZ	3928	3135	3531	16%
LA	2952	2908	2930	1%
NMBingham	2432	2596	2514	5%
NMVado	1802	1585	1693	9%
OK	2062	2202	2132	5%
TXWF	2707	2417	2562	8%
TXBryan	2325	2488	2407	5%
ROG	2798	2394	2596	11%
64-40RG	752	1276	1014	37%
64-40RHY	1095	1328	1212	14%

CV – Coefficient of Variation

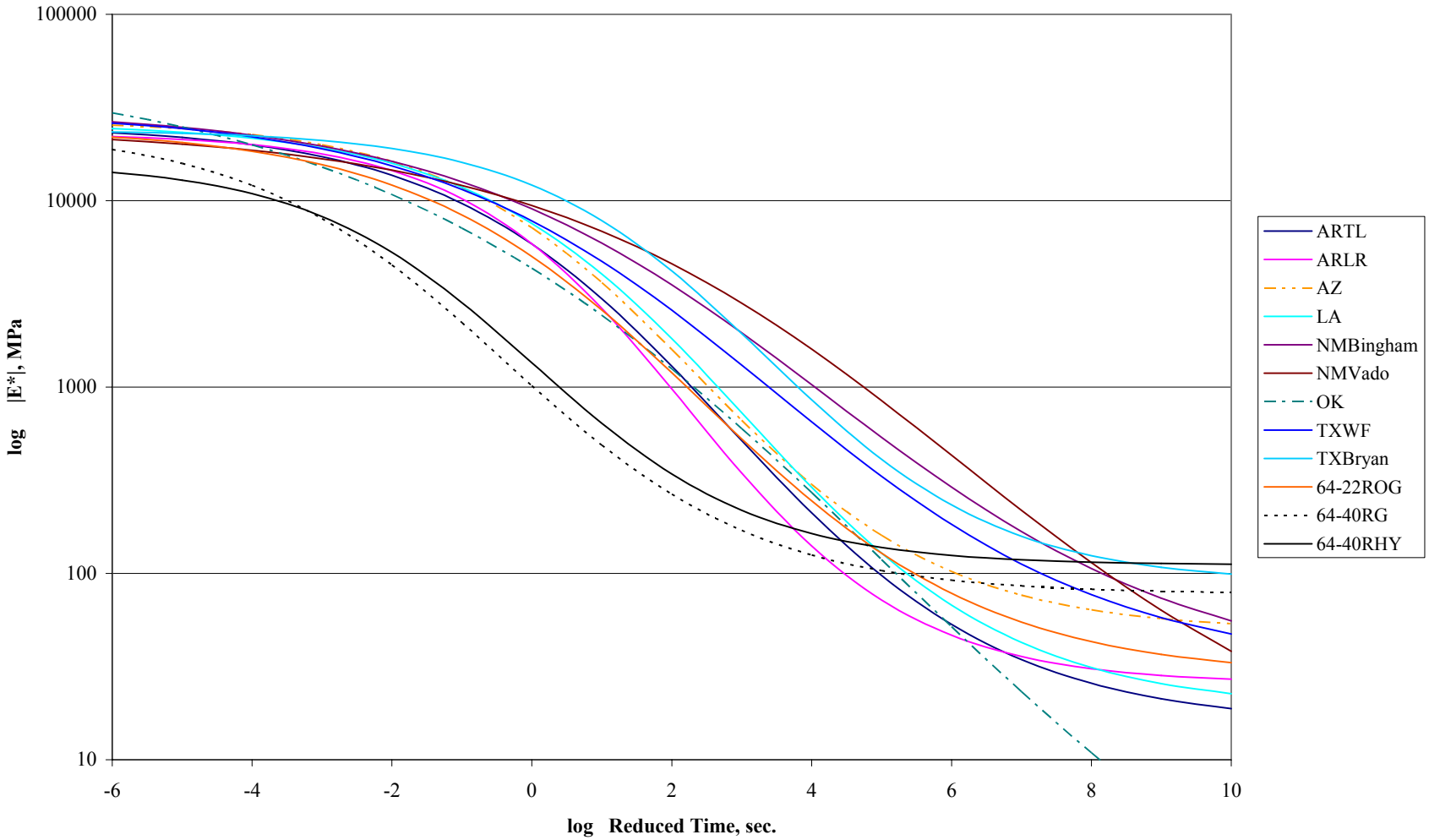

Figure 3.2. Master Curve for Mixtures.

FLOW TIME TEST

The flow time test was performed on two replicates of each mix using a static stress level of 0.0207 MPa (30 psi) and 54.4°C (130°F). This stress and temperature were selected after performing trial runs on "dummy" samples. The goal was to capture all three stages of deformation (i.e., primary, secondary, and tertiary) for all the mixes in a reasonable time limit in a common stress and temperature window.

The parameters used for analysis in the flow time test are the flow time value; slope parameter, m; and the intercept parameter, a. Results from these tests are summarized in Tables 3.12 through 3.14.

Variability in the flow time values was high for samples with lower values. Use of lower stress levels and temperatures can decrease the variability and thus improve the precision of the test. In general, the coefficient of variation values for flow time slope was relatively less than the coefficient of variation of the flow time value.

Table 3.12. Summary of Flow Time Values.

Mix Identity	Flow Time (sec)			CV, %
	Sample 1	Sample 2	Average	
ARTL	44	51	48	10
ARLR	24	20	22	13
AZ	298	297	298	0.2
LA	56	125	91	54
NMBingham	29950	21445	25698	23
NMVado	30942	25585	28263	13
OK	1849	1224	1537	29
TXWF	997	489	743	48
TXBryan	2824	3108	2966	7
ROG	7	9	8	18
64-40RG	136	84	110	33
64-40RHY	164	62	113	64

CV – Coefficient of Variation

Table 3.13. Summary of Flow Time Intercept (a) Values.

Mix Identity	Flow Time Intercept: a			CV, %
	Sample 1	Sample 2	Average 0.001x	
ARTL	0.01410	0.01310	14	5
ARLR	0.01220	0.01370	13	8
AZ	0.01450	0.00920	12	32
LA	0.00830	0.01390	11	36
NMBingham	0.00750	0.00820	8	6
NMVado	0.00460	0.01290	9	67
OK	0.00333	0.01160	8	78
TXWF	0.01060	0.00780	9	22
TXBryan	0.00830	0.00700	8	12
ROG	0.00940	0.01410	12	28
64-40RG	0.00960	0.01230	11	17
64-40RHY	0.01370	0.01320	13	3

CV – Coefficient of Variation

Table 3.14. Summary of Flow Time Slope (m) Values.

Mix Identity	Flow Time Slope: m			CV, %
	Sample 1	Sample 2	Average	
ARTL	0.243	0.282	0.26	10
ARLR	0.378	0.323	0.35	11
AZ	0.229	0.235	0.23	2
LA	0.361	0.267	0.31	21
NMBingham	0.149	0.156	0.15	3
NMVado	0.200	0.117	0.16	37
OK	0.225	0.189	0.21	12
TXWF	0.181	0.225	0.20	15
TXBryan	0.192	0.178	0.18	5
ROG	0.682	0.556	0.62	14
64-40RG	0.295	0.312	0.30	3
64-40RHY	0.176	0.246	0.21	23

CV – Coefficient of Variation

The flow time values were obtained by plotting the rate of change of creep compliance versus time on a log-log scale and determining the time when the rate of change of compliance was lowest along with the slope and intercept parameters. Appendix E shows curves for the different mixes. The slope and intercept parameters were obtained by using a best-fit line on the secondary creep portion of the compliance versus time curves. The tests were conducted on an IPC Servopac UTM-25 machine. The testing equipment incorporates software that enables the user to manually select the linear portion of the curve for which the slope and intercept are calculated and returned as outputs. Typical output curves from the Servopac machine are shown in Figures 3.3 and 3.4.

Flow time was normally conducted for 40,000 seconds or until the sample failed due to crack initiation in the tertiary zone. Mixes NMBingham and NMVado demonstrated relatively much higher flow time values for reaching the tertiary flow stage as compared to the remaining mixes. In most cases, the samples failed when the strain approached 1.5 to 2 percent.

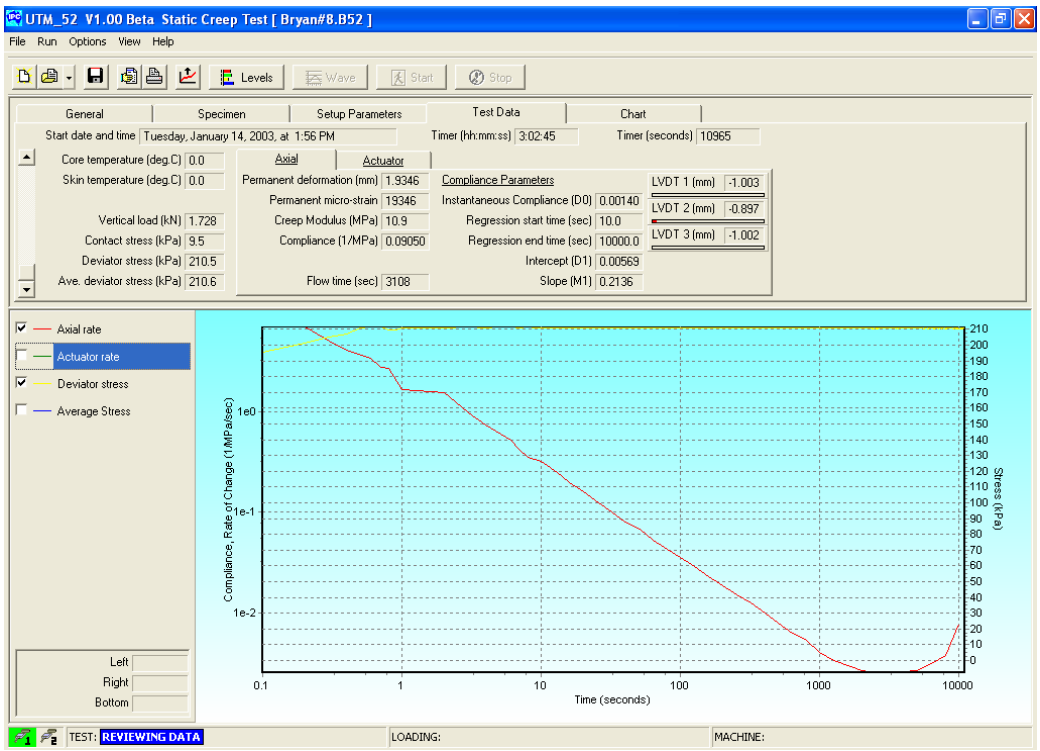

Figure 3.3. Typical Rate of Change of Compliance versus Time Curve.

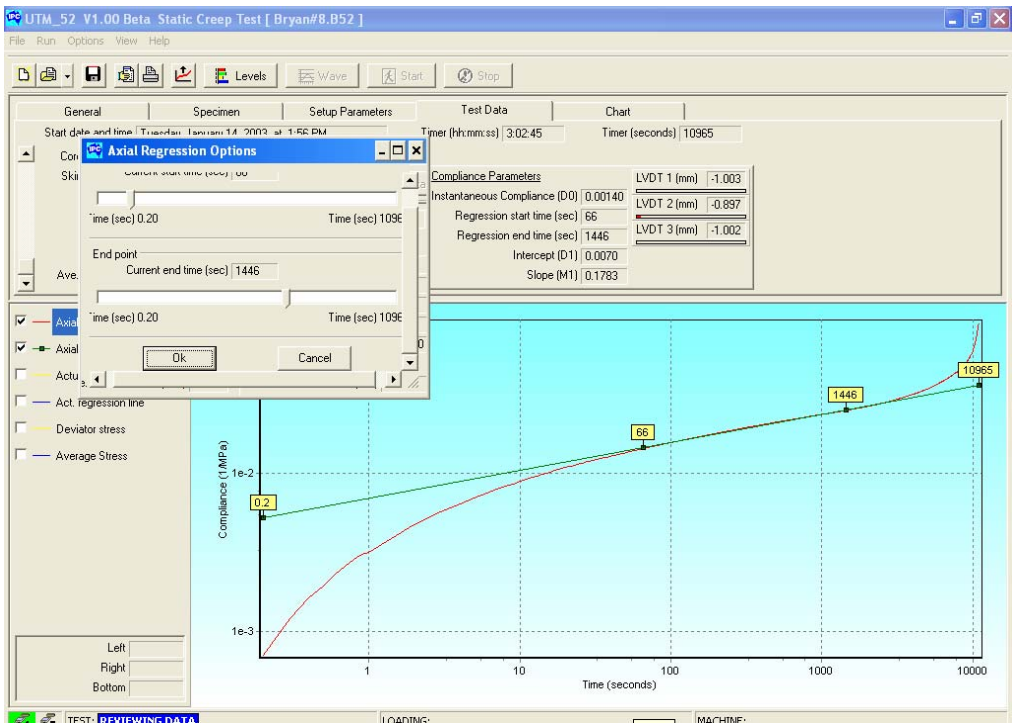

Figure 3.4. Typical Straight-Line Fitting for Secondary Creep to Determine Slope and Intercept Parameters.

FLOW NUMBER TEST

The flow number test was conducted on two replicates for each mixture design at 54.4°C (130°F) and a stress level of 0.0207 MPa (30 psi). The repeated dynamic load was applied in a sinusoidal waveform with a wavelength 0.1 seconds and followed by a dwell or rest period of 0.9 seconds. As for flow time, the stress and temperature levels were selected in order to capture the primary, secondary, and tertiary deformation or creep characteristics of all the mixtures in a reasonable time span.

The flow number corresponds to the minimum value of rate of change of compliance when plotted against the number of cycles on a log-log scale. The slope parameter, b, was determined in a way similar to the slope parameter in the flow time test using the IPC Servopac software. Figure 3.5 shows a typical curve for rate of change of compliance versus number of cycles. Figure 3.6 shows a typical curve used for fitting the straight-line portion in the secondary creep zone to determine the slope parameter.

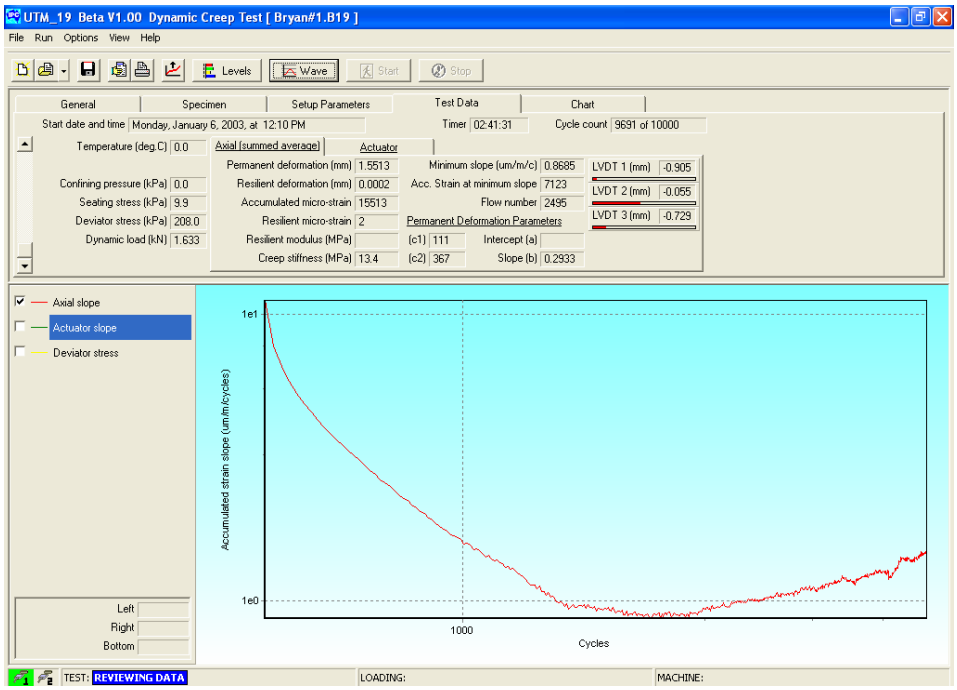

Figure 3.5. Typical Output of Rate of Change of Compliance versus Number of Cycles.

The tests continued until the sample failed in the tertiary zone or until 15,000 cycles. In the case of the NMBingham and NMVado mixes, no tertiary flow was observed even at 15,000 cycles; therefore, the test was stopped. Because of this, the exact flow numbers for these mixtures could not be ascertained. At this stage, the total strain in these mixtures was less than 1.5 percent.

The parameters used for analysis in the flow number tests are the flow number value and the slope parameter, b. Results from these tests are summarized in Tables 3.15 and 3.16.

Variability of the flow number values was generally, but not necessarily, high when the actual flow number values were small. Further, the variability in flow number slope was relatively less than the variability in the flow number values.

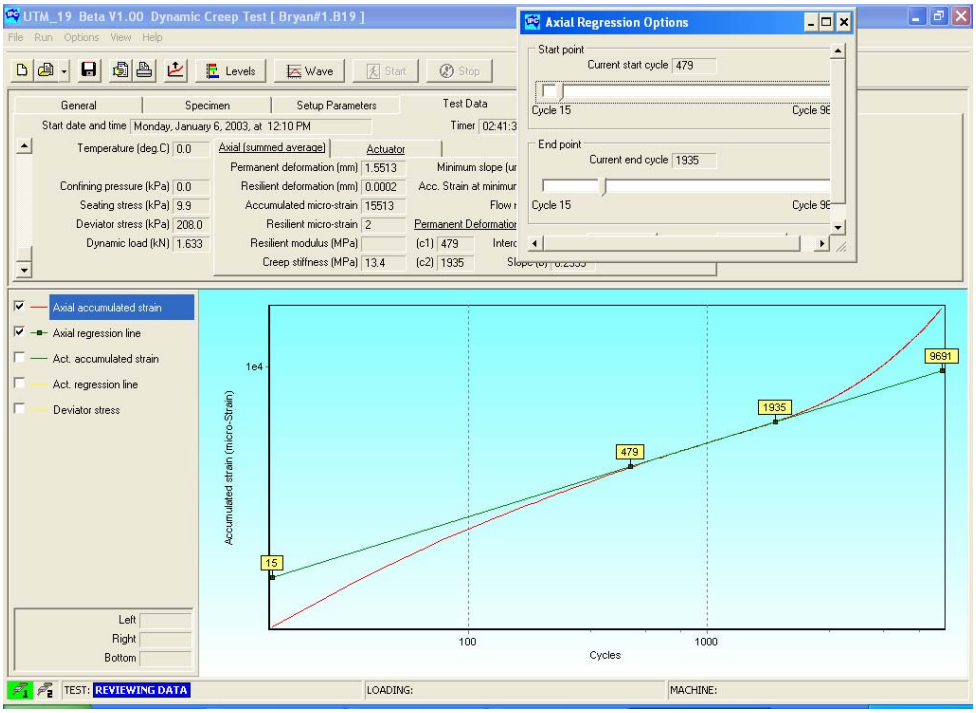

Figure 3.6. Typical Straight Line Fitting for Secondary Creep to Determine Slope and Intercept Parameters.

Table 3.15. Summary of Flow Number Values.

Mix Identity	Flow Number			CV, %
	Sample 1	Sample 2	Average 1000x	
ARTL	235	201	0.2	11
ARLR	227	111	0.2	49
AZ	667	401	0.5	35
LA	395	461	0.4	11
NMBingham	15000	15001	15.0	--
NMVado	15001	15001	15.0	--
OK	3455	3663	3.6	4
TXWF	1527	4791	3.2	73
TXBryan	2495	9119	5.8	81
ROG	225	179	0.2	16
64-40RG	227	167	0.2	22
64-40RHY	2119	1115	1.6	44

CV – Coefficient of Variation

Table 3.16. Summary of Flow Number Slope Parameter Values.

Mix Identity	Flow Number Slope: b			CV, %
	Sample 1	Sample 2	Average	
ARTL	0.4120	0.4561	0.43	7
ARLR	0.5367	0.5480	0.54	1
AZ	0.4740	0.4165	0.44	9
LA	0.4753	0.3909	0.43	14
NMBingham	0.2710	0.3157	0.29	11
NMVado	0.3043	0.3254	0.31	5
OK	0.2810	0.3437	0.31	14
TXWF	0.4328	0.3695	0.40	11
TXBryan	0.2933	0.4180	0.36	25
ROG	0.5578	0.6004	0.58	5
64-40RG	0.3805	0.3657	0.37	3
64-40RHY	0.1758	0.2611	0.22	28

CV – Coefficient of Variation

HAMBURG WHEEL TRACKING DEVICE

The HWTD test used two pairs of samples for certain mixture designs. Test results for the two TxDOT mixtures were collected from the respective district sources. The three laboratory mixes were tested as part of another study. These results are summarized below in Table 3.17. All the mixes were tested at 50°C (122°F) except for mixture TXBryan, which was tested at 40°C (104°F).

Table 3.17. Summary of HWTD Test Results at 50°C .

Mix Identity	HWTD Rut Depth (mm)	Number of Passes
TXWF	8.9	20,000
TXBryan	5.8*	20,000
ROG	12.1 (47.6)**	4,541 (20,000)
64-40RG	9.2 (38.1)**	4,300 (20,000)
64-40RHY	5.4	20,000

* 40°C (104°F) test temperature

** Extrapolated values assuming no stripping occurred

INDIRECT TENSILE CREEP TEST

Indirect tensile creep tests were conducted on two replicates for each mixture design. Parameters from the tests that were used for characterizing the cracking potential are summarized in Tables 3.18 through 3.20.

Table 3.18. Summary of Compliance at 1000 seconds.

Mix Identity	Complaince at 1000 sec (1/MPa)			CV, %
	Sample 1	Sample 2	Average	
ARTL	0.15	0.19	0.17	18%
ARLR[1]	-	0.03	0.03	-
AZ	0.09	0.10	0.095	12%
LA	0.07	0.05	0.06	14%
NMBingham	0.01	0.01	0.01	11%
NMVado	0.01	0.01	0.01	58%
OK	0.08	0.08	0.08	4%
TXWF	0.03	0.04	0.035	8%
TXBryan	0.02	0.02	0.02	2%
ROG	0.22	0.20	0.21	5%
64-40RG	0.31	0.28	0.29	7%
64-40RHY	0.25	0.42	0.34	36%

[1] – Replicate data not available
CV – Coefficient of Variation

Table 3.19. Summary of Viscoplastic Strain.

Mix Identity	Visco Plasticstrain (%)			CV, %
	Sample 1	Sample 2	Average	
ARTL[1]	-	0.280	0.28	-
ARLR[1]	0.173	-	0.17	-
AZ	0.110	0.127	0.12	11%
LA	0.077	0.061	0.07	16%
NMBingham	0.007	0.012	0.01	34%
NMVado	0.004	0.004	0.004	7%
OK	0.079	0.089	0.084	9%
TXWF	0.033	0.037	0.04	8%
TXBryan	0.020	0.019	0.02	1%
ROG	0.278	0.256	0.27	6%
64-40RG	0.285	0.257	0.27	7%
64-40RHY	0.229	0.394	0.31	38%

[1] – Replicate data not available
CV – Coefficient of Variation

Table 3.20 Summary of Viscoelastic Strain.

Mix Identity	Visco Elastic Strain (%)			CV, %
	Sample 1	Sample 2	Average	
ARTL[1]	-	0.026	0.03	-
ARLR[1]	0.023	-	0.02	-
AZ	0.025	0.027	0.03	4%
LA	0.028	0.023	0.03	13%
NMBingham	0.006	0.004	0.01	23%
NMVado	0.004	0.004	0.004	4%
OK	0.037	0.035	0.04	5%
TXWF	0.016	0.017	0.02	3%
TXBryan	0.009	0.007	0.01	23%
ROG	0.052	0.051	0.05	2%
64-40RG	0.142	0.126	0.13	9%
64-40RHY	0.137	0.205	0.17	28%

[1] – Replicate data not available
CV – Coefficient of Variation

ANALYSIS OF TEST RESULTS

Due to a lack of quantitative objective data related to the rutting performance of the mixtures in the field, analyses were performed using APA rut depth and creep slope as the basis for rutting performance. Different approaches were used to perform the analyses.

One approach was to rank the mixtures in terms of rut resistance based on various parameters from different tests. The ranking assigned to each mix by the different parameters can therefore be used as a basis for comparing the results of the various tests. A correlation coefficient for each ranking was computed by comparing the APA results with the remainder of the parameters. The correlation was performed using the Kendall Tau coefficient. This coefficient ranges from -1 to +1, where -1 indicates that the rankings are perfectly inverse of each other, and +1 indicates that the rankings are perfectly correlated with each other. A coefficient value of 0 means that there is absolutely no correlation between the rankings. This coefficient can be determined for any two pairs of ranks. In general, a coefficient value of about 0.6 or higher or -0.6 or lower would indicate a good relationship between the two systems of ranking.

The second approach that was used to compare the results of each parameter was to group the mixtures based on the comparisons of their means. The Duncan grouping procedure

was used for this purpose. Statistically equivalent groups were established for the different parameters that were evaluated and compared.

A third approach was to determine direct correlations between APA results and the other test parameters. With this procedure, correlation coefficients can be used to compare the relative degree of each correlation.

Analysis Based on Rankings (Kendall's τ)

Rankings of the different mixtures based on various parameters are summarized in Table 3.21.

Table 3.21. Comparisons of Rankings by Parameters from the Different Tests.

Mixture Identity	APA Rut Depth	APA Creep Slope	|G*| at 10 Hz	|G*|/sin δ at 10 Hz	|G*| at 1Hz	|G*|/sin δ at 1Hz	|E*| at 10 Hz	|E*|/sin ϕ at 10 Hz	|E*| at 1 Hz	|E*|/sin ϕ at 1 Hz	Flow Time	Flow Time Intercept	Flow Time Slope	Flow Number	Flow Number Slope
NMVado	1	1	1	1	1	1	1	1	1	1	1	4	2	1	4
NMBingham	2	4	3	2	2	2	2	2	2	2	2	3	1	2	2
TXWF	3	8	5	5	5	5	5	3	4	4	5	5	4	5	7
64-40RHY	4	3	12	12	12	9	10	8	8	5	7	11	6	6	1
OK	5	6	4	4	4	3	9	10	10	11	4	1	5	4	3
AZ	6	5	9	9	9	10	6	6	6	7	6	9	7	7	10
TXBryan	7	2	2	3	3	4	3	4	3	3	3	2	3	3	5
64-40RG	8	9	11	11	10	11	12	11	11	8	8	6	9	11	6
LA	9	7	7	7	8	7	7	9	9	10	9	7	10	8	8
ARTL	10	10	8	8	7	8	4	5	5	6	10	12	8	9	9
ARLR	11	12	10	10	11	12	11	12	12	12	11	10	11	12	11
ROG	12	11	6	6	6	6	8	7	7	9	12	8	12	10	12

Although the exact flow number values for the two mixtures from New Mexico could not be ascertained, a value of 15,000 and 15,001 was assigned to the mixtures NMBingham and NMVado, respectively, for the purpose of the ranking analysis.

The Kendall Tau coefficients of correlation were obtained by comparing the rankings of the different test parameters with the APA rut depth results and the APA creep slope results. The findings are summarized in Table 3.22.

Table 3.22. Kendall Tau Coefficients of Correlation – All Test Parameters versus APA Rut Depth or Creep Slope.

Test Parameter	APA Rut Depth	APA Creep Slope
Flow Time	0.79	0.70
Flow Time Slope, m	-0.76	-0.61
Flow Number	0.70	0.73
Flow Number Slope, b	-0.64	-0.55
$\|E^*\|/\sin\phi$ at 1 Hz	0.55	0.58
$\|G^*\|/\sin\delta$ at 1 Hz	0.49	0.46
$\|E^*\|/\sin\phi$ at 10 Hz	0.49	0.46
$\|E^*\|$ at 1 Hz	0.46	0.49
$\|G^*\|/\sin\delta$ at 10 Hz	0.39	0.36
$\|E^*\|$ at 10 Hz	0.39	0.39
Flow Time Intercept, a	-0.36	-0.33
$\|G^*\|$ at 1 Hz	0.33	0.36
$\|G^*\|$ at 10 Hz	0.30	0.42

Based on this analysis, the following observations are made:

- For the 64-40RHY mixture, APA rut depth and creep slope indicate a relatively sound mix in terms of rutting resistance. However, the dynamic modulus and the shear modulus tests indicate a relatively poor mix when the rankings are compared at 10 Hz. Further, $|E^*|/\sin\phi$ at 1 Hz ranks the mixture similar to the APA result. Furthermore, flow time slope, flow number, and flow number slope parameters for the 64-40RHY mixture rank more closely to APA rut depth than the other parameters.

- The Kendall Tau correlation coefficients show that the flow number and flow time parameters correlate most closely with APA rut depth and APA creep slope. Dynamic modulus and shear modulus exhibit slightly to significantly weaker correlations than the flow tests. The poorer correlations may be due, in part, to the different APA rut depths of the mixes containing the PG 64-40. It must also be noted that, since there were only two mixtures using highly modified asphalt, the difference in the strength of the correlations cannot be attributed to this factor alone. However, at the same time, it should be remembered that the PG 64-40 amplifies the affect of polymer modification in an HMA mixture. It is also possible that mixtures containing asphalt with a lower polymer content would exhibit similar trends but probably with lesser intensity.

- Evidence indicates the dynamic modulus test may be recommended in the 2002 Design Guide as the main test to characterize HMA. This experiment was designed, in part, to evaluate the ability of the dynamic modulus test to properly characterize or rank HMA mixtures, including some containing polymer-modified binders. The dynamic modulus test ranked the PG64-40 mixtures as relatively poorer in performance when compared to torture tests such as the APA and the HWTD. This may be due, in part, to the fact that the torture tests allow a brief rest period at any given point on the specimen between every consecutive pass. The final permanent deformation recorded in these tests thus accommodates the effect of any recovery that may have occurred during the rest period. On the other hand, there is no significant rest period in the dynamic modulus test.
- For the PG 64-40 mixtures, the $|E^*|/\sin\phi$ at 1Hz correlated better with the APA results than the $|E^*|/\sin\phi$ at 10 Hz. Although there is no significant rest period with zero strain in the dynamic modulus test, the amount of time during which the stress decreases in a sinusoidal form varies based on the test frequency. For example, the duration during which the stress level decreases from peak to zero is 0.05 seconds when the test is conducted at 10 Hz as compared to 0.5 seconds when the test is conducted at 1Hz. This variation in correlation at different frequencies again suggests that the polymer modification might effect the interpretation of dynamic modulus test results because these materials normally exhibiting high recovery are not allowed time to recover.

Analyses Based on Statistically Equivalent Groupings (Duncan Multiple Range Test)

The analyses based on rankings are associated with the drawback that rankings are not representative of the range of the data. For example, the difference between the values of any two consecutive rankings is not necessarily the same as the difference between any other two consecutive rankings. Therefore, when mixture properties are relatively similar, the rankings may change for such sets of mixtures based on the sensitivity of the test being conducted.

To address the above limitation, Duncan grouping was preferred for each of the test parameters using all the test replicates. Analyses were performed at a significance level of $\alpha = 0.05$ and assuming equal variance of the mixture property considered. Details of the statistical analysis are presented in Appendix F. For the Duncan test of a particular parameter,

the values within a given group are statistically equivalent, but the individual groups are not necessarily statistically different from each other.

As is common with the Duncan Multiple Range Test, the number of groups formed for each parameter varied. For example, APA rut depth classified the 12 samples into six groups of statistically equivalent values; whereas, flow time intercept data classified the same 12 samples into only one group. The test parameter and the number of Duncan groups that could be distinguished for each parameter for the 12 mixtures are shown in Table 3.23.

The Duncan groupings show that the flow time and flow number classify all the mixes into only two to three groups of statistically equivalent values, as compared to the APA rut depth test which classifies the mixtures into six different groups. This shows that the APA is comparatively more sensitive to differences in mixture properties than flow time and flow number values.

The rankings based on Duncan groupings are presented in Table 3.24. Based on the sensitivity of the test, each mixture might have more than one rank or a given rank may be assigned to more than one mixture.

Table 3.23. Number of Duncan Groups for Each Test Parameter.

Test Parameter	Number of Duncan Groups
APA Rut Depth	6
APA Creep Slope	4
|E*| at 10 Hz	6
|E*| at 1 Hz	5
|E*|/sinϕ at 10 Hz	4
|E*|/sinϕ at 1 Hz	4
|G*| at 10 Hz	5
|G*| at 1 Hz	4
|G*|/sinδ at 10 Hz	5
|G*|/sinδ at 1 Hz	3
Flow Number	3
Flow Number Slope	6
Flow Time	2
Flow Time Intercept	1
Flow Time Slope	6

Table 3.24. Rankings Based on Duncan Groups for Each Test Parameter.

Mixture Identity	APA Rut Depth	APA Creep Slope	|G*| at 10 Hz	|G*|/sin δ at 10 Hz	|G*| at 1 Hz	|G*|/sin δ at 1 Hz	|E*| at 10 Hz	|E*|/sin ϕ at 10 Hz	|E*| at 1 Hz	|E*|/sin ϕ at 1 Hz	Flow Time	Flow Time Intercept	Flow Time Slope	Flow Number	Flow Number Slope
NMVado	1	1	1	1	1	1	1	1	1	1	1	1	1-2	1	1-3
NMBingham	1-2	1-2	2-3	2	2	2	1	1	1	1	1	1	1	1	1-2
64-40RHY	2-3	1-2	5	5	4	3	5-6	3-4	4-5	2-3	2	1	1-3	3	1
TXWF	2-3	2	2-4	2-4	3-4	3	2-3	2	2-3	2	2	1	1-3	2-3	3-4
AZ	3	1-2	3-5	3-5	3-4	3	2-4	2-4	3-4	2-4	2	1	1-4	3	4-5
OK	3	1-2	2-4	2-4	2-3	2-3	4-6	4	4-5	3-4	2	1	1-3	2-3	1-3
TXBryan	3	1-2	2	2-3	2-3	3	2	2	2	2	2	1	1-2	2	2-4
64-40RG	4	3	4-5	4-5	4	3	6	4	5	3-4	2	1	3-5	3	2-4
LA	4-5	2	2-4	3-5	3-4	3	3-5	2-4	4-5	3-4	2	1	4-5	3	4
ARTL	5	3	2-4	3-5	3-4	3	2-3	2-3	3-4	2-4	2	1	2-5	3	4
ARLR	6	4	4-5	4-5	4	3	5-6	4	5	4	2	1	5	3	5-6
ROG	6	3	2-4	2-5	3-4	3	4-5	3-4	4-5	3-4	2	1	6	3	6
TOTAL GROUPS	**6**	**4**	**5**	**5**	**4**	**3**	**6**	**4**	**5**	**4**	**2**	**1**	**6**	**3**	**6**

Based on the above analysis, the following observations are made:

- The number of groups in the case of flow time value, flow time intercept, and flow number value were very few (one to three). The following could be some of the reasons for this: The mixtures selected had a wide range of resulting values from very low to very high, thus minimizing the number of groups of statistically equivalent values. The differences between the performance levels of some of the mixtures (specifically those from New Mexico) were much higher than those of other mixtures. For example, the flow time value for the two mixtures from New Mexico was about 30,000, and the flow time value for the next best performing mixture (TXBryan) was about 3000. The flow time value for the rest of the mixtures was below this value. Therefore, the results were "cluttered" at the lower end of the rankings for most of the mixes within a relatively small range of values. This situation could be avoided by using a lower stress level for testing and thereby amplifying the sensitivity of the test. However, the researchers were trying to capture the tertiary flow phenomenon for all the mixes (PG 64 to PG 76) in the same reasonable stress and temperature window. This could only be done, as the results indicated, at the expense of sensitivity.
- Flow time and flow number slopes were able to separate the mixes into six groups, which was much better than the flow time or flow number values.
- Mixture 64-40RHY (rhyolite) performed much better than the mixture 64-40RG (gravel) in the APA test, both in terms of the total rut depth and creep slope. Both of them contained highly polymer-modified asphalt.
- Based on the APA rut depth, the 64-40RHY was placed in the second or third of six groups. The mix can therefore be said to perform better than most of the other mixes, since it is in the top 33 to 50 percent of the mixtures. The 64-40RG, on the other hand, ranked fourth in the six groups.
- Based on the dynamic modulus grouping, 64-40RHY was placed in the fifth and sixth of six groups when |E*| values are compared at 10 Hz and in the fourth and fifth of the five groups when |E*| values are compared at 1 Hz. This means that the |E*| values placed this mix in the last 33 percent of the mixtures. Mix 64-40RG was

placed in the sixth of six groups and fifth of the five groups when |E*| values are compared at 10 and 1 Hz, respectively.

- The results using |E*|/sin ϕ were similar to those using |E*| with the difference that there were only four different groups and the PG 64-40 mixes were placed in the last two groups.
- Similarly, when considering the SST-FSCH results, the PG 64-40 mixes were always placed in the latter groups.
- Flow time slope and flow number slope categorized 64-40RHY in the top groups similar to APA rut depth. Based on this finding and assuming that APA relates well to pavement rutting, flow number slope and flow time slope appear to relate well to simulated rutting in a pavement.

Correlations of Different Test Parameters with APA and HWTD Rut Depth

Based on the correlation coefficients of the rankings and Duncan groupings, it is apparent that the APA rut depth has much better correlations with the flow number and flow time slopes as compared to the |E*| or |G*| values. Correlations with the APA parameters are shown in Appendices G and H. A summary of the correlation coefficients (R^2) is shown in descending order for APA rut depth in Table 3.25.

For determining the different R^2 values, a log scale was used for all the parameters. This was because the permanent deformations observed in the APA tests are related to the visco-elastic properties of the HMA mixtures, which is most commonly expressed in terms of a power function in mechanistic analyses of these mixtures. The correlation for the flow number value with the APA results was developed based on only 10 mixture designs. The two mixture designs from New Mexico were excluded because these samples never reached the point of tertiary flow within the tested range of 15,000 cycles.

Table 3.25. R^2 Values for Correlations between Various Parameters with APA Results.

Parameter	R^2 Values	
	versus APA Rut Depth	versus APA Creep Slope
Flow Time Slope	0.84	0.56
Flow Number Value	0.72	0.63
|E*|/sin ϕ at 1Hz	0.63	0.59
Flow Number Slope	0.62	0.46
Flow Time Value	0.61	0.61
|E*| at 1 Hz	0.48	0.53
|G*|/sin δ at 1 Hz	0.46	0.50
|E*|/sin ϕ at 10 Hz	0.45	0.48
Flow Time Intercept	0.34	0.31
|G*| at 1 Hz	0.33	0.38
|E*| at 10 Hz	0.24	0.32
|G*|/sin δ at 10 Hz	0.22	0.28
|G*| at 10 Hz	0.11	0.16

In addition to the above correlations, a comparison was made between the HWTD rut depth and APA rut depth for certain mixtures. Correlation coefficients were also derived for HWTD rut depth versus the other parameters used for the comparison with the APA rut depth. These coefficients are shown in descending order in Table 3.26. Detailed correlation graphs for HWTD are shown in Appendix I.

These observations are based on the results of HWTD tests conducted on only five of the mixtures. It should also be noted that extrapolated data were used for two of the mixtures that failed before completion of 20,000 passes.

Table 3.26. Correlation Coefficients between Various Parameters and HWTD Rut Depth.

Parameter	R^2 Values
Flow Number Value	0.87
Flow Time Slope	0.77
|E*|/sin ϕ at 1 Hz	0.74
APA Rut Depth	0.68
Flow Time Value	0.56
Flow Number Slope	0.52
|E*|/sin ϕ at 10 Hz	0.42
|E*| at 1 Hz	0.42
|E*| at 10 Hz	0.25
|G*|/sin δ at 1 Hz	0.10
Flow time intercept	0.10
|G*| at 10 Hz	0.01
|G*|/sin δ at 10 Hz	0.003
|G*| at 1 Hz	0.0001

The following observations are made from Tables 3.25 and 3.26:

- Flow time slope, flow number value, and |E*|/sin ϕ at 1 Hz provided the best correlations with the APA rut depth. Further, the correlation between the APA rut depth and the flow time value was better than the correlation between flow number slope and APA rut depth.
- Flow number and flow time correlated better with APA rut depth than they correlated with APA creep slope.
- Correlations of dynamic modulus and SST-FSCH with the APA test parameters were not as good as correlations of the flow time and flow number test parameters with the APA test parameters. Zhou and Scullion (2001) obtained similar results when relatively low dynamic modulus values were observed for heavy-duty asphalt mixes in contradiction with field performance, APA, and permanent strain test results.

- The correlations of |E*|/sin ϕ or |G*|/sin δ were relatively better than correlations of |E*| and |G*| alone with the APA test parameters. This is likely because the phase angle captures the viscous behavior of the mix, which is also responsible for the permanent deformation.
- The correlations of |E*| or |G*| were relatively better when a lower frequency such as 1 Hz was considered in place of a higher frequency such as 10 Hz. Again, these values did not show any strong correlations with APA. This could be because: (1) 1 Hz is closer to the rate at which the APA loading arm operates, and (2) the lower loading frequency allows more time for the sample to recover. However, if the first case is true, assuming that sample recovery has no influence on its rutting behavior, then the correlations with the flow number test should also have been poor because the frequency in this test was also 10 Hz. Therefore, the second suggested cause seems to be more likely. The second suggested cause can once again be supported by the flow number test which applies a load at a rate of 10 Hz but also allows a dwell or rest period of 0.9 seconds before the next load application, thereby allowing the specimen to recover, at any one point on a specimen during the APA test.
- In general, it was found that the overall rut depth from APA at 8000 strokes correlated better with the remaining parameters rather than with the creep slope.
- Correlations of HWTD rutting with the rest of the test parameters were similar to the correlations between the APA rut depth and those same test parameters. Flow number value, flow time slope, |E*|/sin ϕ at 1 Hz, flow number slope, and flow time value were among the best five correlations both with HWTD and APA rut depths.

In the aforementioned observations, one of the reasons for the poor correlations of |E*| and |E*|/sin ϕ parameters at 10 Hz and the |G*| and |G*|/sin δ parameters at 10 Hz and 1Hz with the APA results is attributed to the fact that these parameters were unable to characterize the rut resistance of the mixes with low modulus but high recovery, i.e., highly polymer-modified mixes containing PG 64-40. In order to assess the impact of the two mixes containing PG 64-40 asphalt, the Kendall Tau coefficients of the rank correlation and the R^2 values of the direct correlation for all the test parameters with APA rut depth were determined excluding the

PG 64-40 mixes. These values were then compared with the original values obtained by considering all twelve mixes. Comparisons of the R^2 values including and excluding the mixes with PG 64-40 asphalt are summarized in Table 3.27 and Figure 3.7. Comparisons of the Kendall Tau coefficient including and excluding the mixes containing PG 64-40 asphalt are summarized in Table 3.28 and Figure 3.8.

The Kendall Tau coefficient is a non-parametric tool for analysis and does not account for the actual quantitative values of the test parameters. Therefore, the impact of removing two mixes from a set of twelve mixes in determining the Kendall Tau coefficient will usually be much less than the impact of removing the same mixes from the determination of the R^2 values due to the "leverage effect" of the values.

Table 3.27. Comparison of R^2 Values Including and Excluding PG 64-40 Mixes.

Parameter	R^2 Values of Direct Correlation for APA Rut Depth versus Listed Test Parameters	
	with PG 64-40 mixes	without PG 64-40 mixes
Flow Time Slope	0.84	0.85
Flow Number Value	0.72	0.79
$\|E^*\|/\sin\phi$ at 1Hz	0.63	0.65
Flow Number Slope	0.62	0.81
Flow Time Value	0.61	0.87
$\|E^*\|$ at 1 Hz	0.48	0.62
$G^*/\sin\delta$ at 1 Hz	0.46	0.55
$\|E^*\|/\sin\phi$ at 10 Hz	0.45	0.57
Flow Time Intercept	0.34	0.50
G^* at 1 Hz	0.33	0.57
$\|E^*\|$ at 10 Hz	0.24	0.54
$G^*/\sin\delta$ at 10 Hz	0.22	0.50
G^* at 10 Hz	0.11	0.50

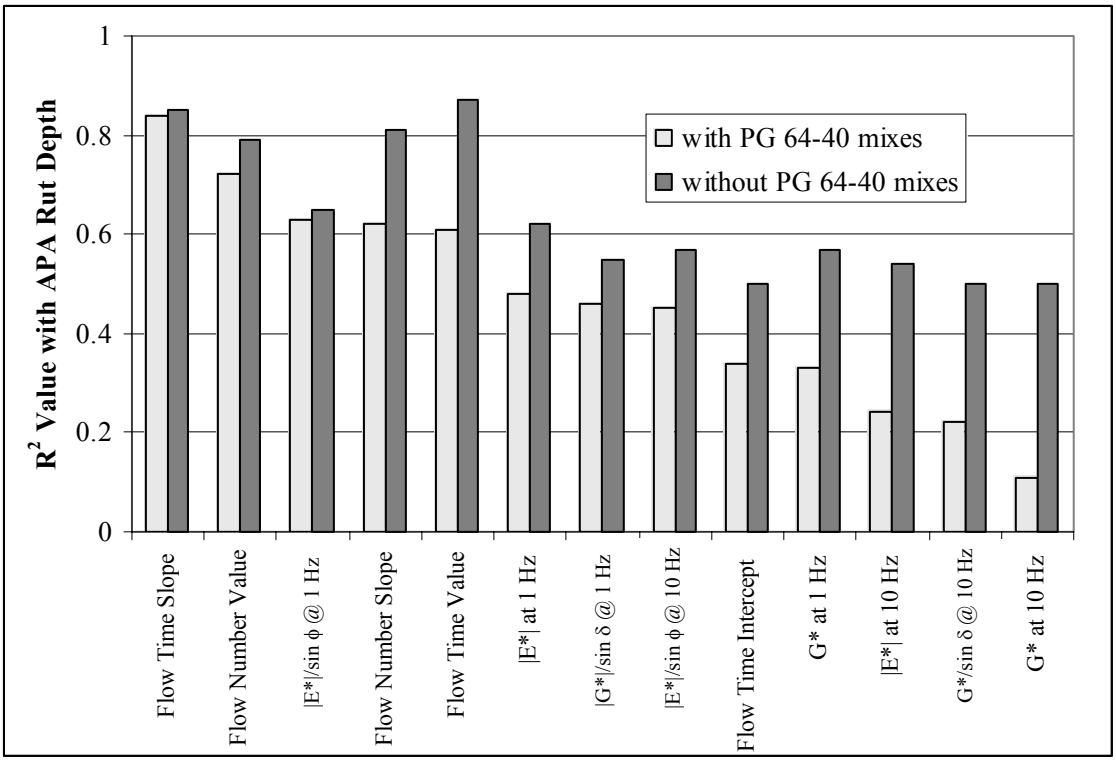

Figure 3.7 Comparison of R^2 Values with and without PG 64-40 Mixes

Table 3.28 Kendall Tau Rank Correlations with and without PG 64-40 Mixes

Parameter	Kendall Tau coefficient of Rank Correlation for APA Rut Depth versus other Test Parameters	
	with PG 64-40 mixes	without PG 64-40 mixes
Flow Time	0.79	0.82
Flow Time Slope m	0.76	0.78
Flow Number	0.70	0.78
Flow Number Slope b	0.64	0.69
|E*|/sin ϕ at 1 Hz	0.55	0.51
G*/sin δ at 1 Hz	0.49	0.60
|E*|/sin ϕ at 10 Hz	0.49	0.56
|E*| at 1 Hz	0.46	0.51
G*/sin δ at 10 Hz	0.39	0.56
|E*| at 10 Hz	0.39	0.51
Flow Time Intercept a	0.36	0.42
G* at 1 Hz	0.33	0.51
G* at 10 Hz	0.30	0.51

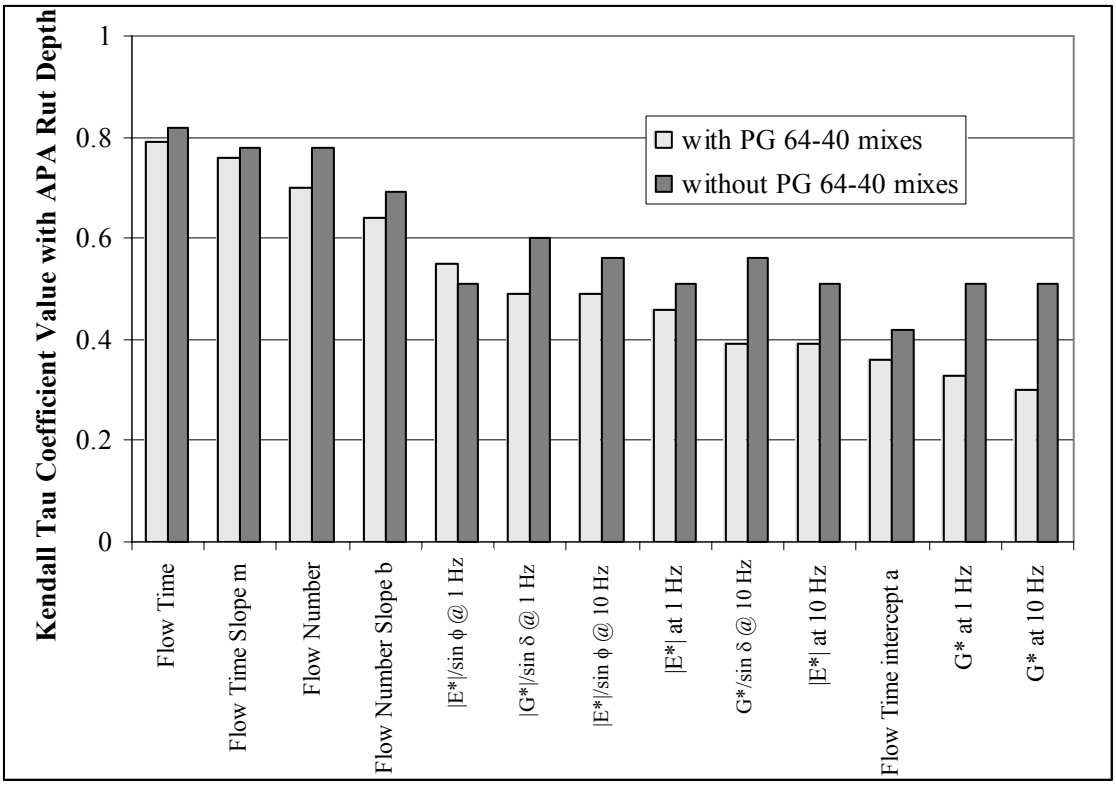

Figure 3.8 Comparison of Kendall Tau Rank Correlations with and without PG 64-40 Mixes.

Figure 3.7 demonstrates that removal of the two PG 64-40 mixes from the group of 12 mixes yields a significant increase in the R^2 values for correlation between the APA rut depth and the |E*| and |E*|/sin ϕ parameters at 10 Hz and the |G*| and |G*|/sin δ parameters at 10 Hz and 1 Hz. Further, the R^2 values for the correlation between the APA rut depth and the flow time slope, flow number value, and |E*|/sin ϕ parameters at 1Hz did not change appreciably.

This comparison, to some extent, supports the reasoning for the observations made earlier, that the |E*| and |E*|/sin ϕ parameters at 10 Hz and the |G*| and |G*|/sin ϕ parameters at 10 Hz might not account for any benefits imparted by polymer-modified binders.

Cracking Characterization of Mixtures

Cracking susceptibilities of the mixtures were ranked (from best to worst) based on the different test parameters from the dynamic modulus and the indirect tensile creep test. The rankings are shown in Table 3.29. Further, the relative elastic, plastic, viscoelastic and viscoplastic components of different mixtures are compared in Figures 3.9 and 3.10.

Table 3.29. Ranking of Mixtures for Cracking Potential

Mix Identity	Test Parameter as Basis for Ranking			
	E* sin ϕ	Compliance at 1000 sec	Viscoelastic strain at 1000 sec	Viscoplastic strain at 2000 sec
64-40RG	1	2	2	3
64-40RHY	2	1	1	1
NMVado	3	12	12	12
OK	4	7	4	7
TXBryan	5	10	10	10
NMBingham	6	11	11	11
TXWF	7	9	9	9
ROG	8	3	3	4
ARTL	9	4	6	2
ARLR	10	5	8	5
LA	11	8	7	8
AZ	12	6	5	6

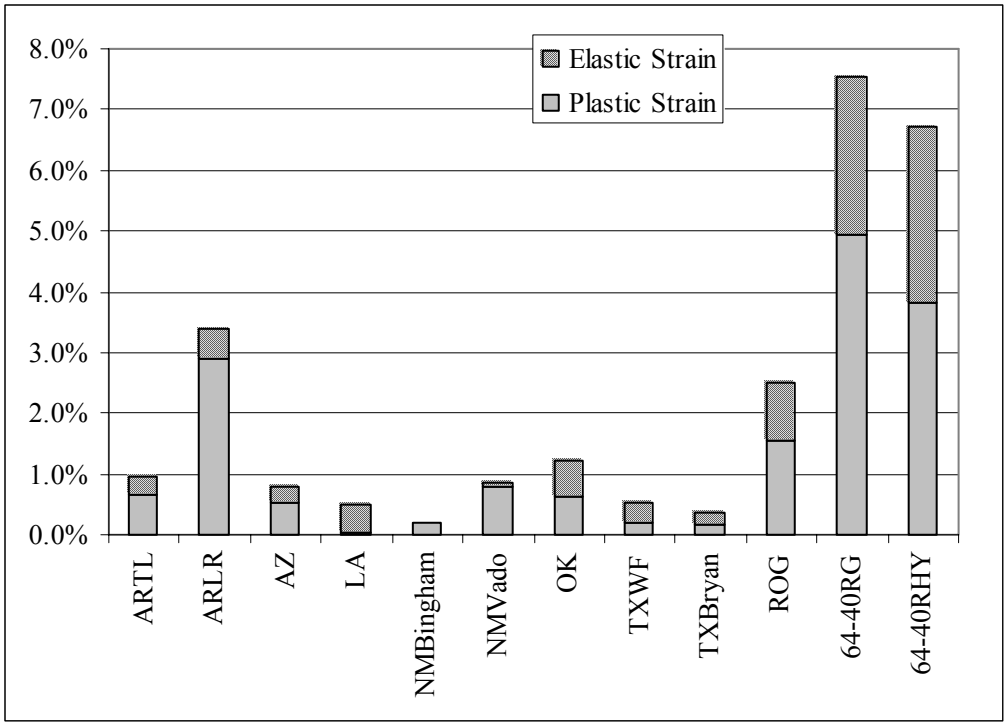

Figure 3.9. Comparison of Elastic and Plastic Strains.

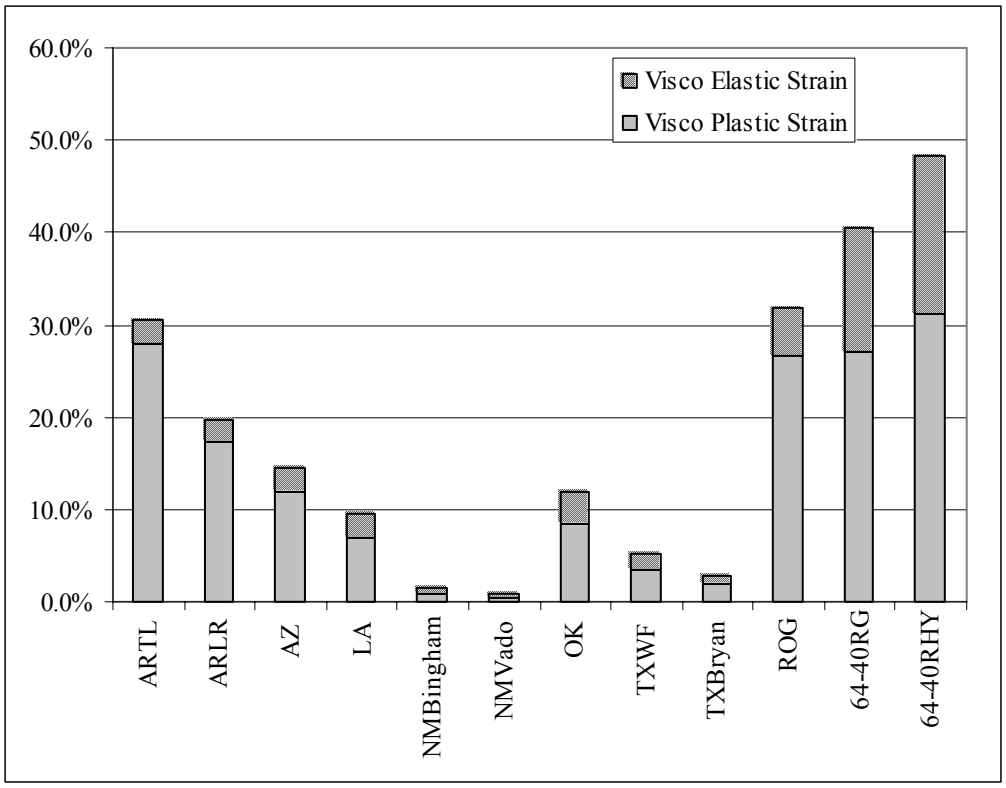

Figure 3.10 Comparison of Viscoelastic and Viscoplastic Strains.

The following observations are made from the indirect tensile creep data:

- The rankings based on the various parameters from the indirect tensile creep test are not significantly different.
- The mixtures containing PG 64-40 binder were ranked best by all the test parameters considered.
- Mixtures NMVado, NMBingham, and TXWF were characterized to be relatively very stiff by the permanent deformation tests. It could be expected that these mixtures performed poorly in terms of cracking resistance, partly due to the high PG grades (PG 82-16 to PG 70-22). Results from the indirect tensile creep tests are in line with this presumption. However, the E*sin ϕ parameter indicates that these mixtures exhibit better cracking resistance as compared to most of the other mixtures.
- The 64-40RHY mixture containing PG 64-40 binder performed relatively better than most mixes in terms of cracking resistance. However, this mixture shows different

rutting susceptibility depending on the specific test parameter used for characterizing the mix. For example, based on APA, Hamburg, flow time, and flow number, the 64-40RHY is assessed to perform relatively better than other mixes in terms of rutting resistance; whereas, the same mixture is characterized as one of the poorer performing mixes based on E* and E*/sin ϕ at 10 Hz. This reveals the necessity to select appropriate test methods that can identify mixtures that exhibit reasonable resistance to both cracking and rutting.

CHAPTER 4
CONCLUSIONS AND RECOMMENDATIONS

Nine different HMA materials and mixture designs were obtained from the six state DOTs in the south central region of the United States. Three additional mixtures were specially designed and produced in the laboratory to provide polymer-modified mixtures for this project. All mixtures were characterized using the three SPTs (dynamic modulus, flow number, and flow time), SST-FSCH, and the APA as a torture test. Selected mixtures were tested using the HWTD.

Objectives of this research included the following: evaluate applicability of current test procedures and equipment for measuring HMA mixture properties with particular emphasis on the complex modulus tests and gap-graded and polymer-modified mixtures. The findings from this work are briefly summarized below (details of these findings are provided in Chapter 3 and the appendices).

CONCLUSIONS

- Flow time slope and flow number value provided the best correlations with the APA rut depth. However, the correlation between the APA rut depth and the flow time slope was better than that between APA rut depth and flow number.
- Correlations of APA rut depth with the flow number and flow time parameters were better than the correlations of APA creep slope with the flow number and flow time parameters.
- Correlations of the APA test parameters with dynamic modulus and SST-FSCH tests were not as good as correlations of the APA test parameters with the flow time and flow number test parameters. Zhou and Scullion (2001) obtained similar results, where relatively low dynamic modulus values were observed for heavy-duty asphalt mixes in contradiction to the field performance, APA, and permanent strain test results.
- The correlations of $|E^*|/\sin \phi$ or $|G^*|/\sin \delta$ with the APA test parameters were better than correlations of $|E^*|$ and $|G^*|$ alone with these parameters. This difference could be because the phase angle captures the viscous behavior of the mix, which is also

responsible for the permanent deformation rather than the resilient modulus values alone.

- Correlations of |E*| or |G*| with the APA parameters were better at lower test frequencies than at higher frequencies. However, these values did not show strong correlations.
- The overall rut depth from the APA test at 8000 strokes correlated better with all other parameters as compared to the APA creep slope.
- Correlations of HWTD rutting with the other test parameters were similar to the correlations between the APA rut depth and those same parameters. Flow number value, flow time slope, |E*|/sin ϕ at 1 Hz, flow number slope, and flow time value were among the best five correlations both with HWTD and the APA rut depths.
- Using the Duncan Multiple Range Test, flow time slope and flow number slope parameters were able to separate the mixes into six Duncan groups of statistically equivalent values, which were much better than the flow time or flow number values.
- Based on the APA rut depth, the PG 64-40 + rhyolite mix can be placed in the second and third of the six Duncan groups in terms of ranking. The mix can therefore be said to perform better than most of the other mixes since it is in the top 33 to 50 percent of the mixtures. In contrast, the PG 64-40 + river gravel mix was ranked in the fourth of the six Duncan groups.
- Based on Duncan grouping for dynamic modulus, the PG 64-40 + rhyolite mix was placed in the fifth or sixth of six groups when |E*| values are compared at 10 Hz and in the fourth and fifth of five groups when the values are compared at 1 Hz. This means that the |E*| values placed this mix in the worst 33 percent of the mixtures. The PG 64-40 + river gravel mix was placed in the sixth of six groups and fifth of five groups when |E*| values are compared at 10 and 1 Hz, respectively. These groupings are quite contrary to those for the APA parameters.
- Results using |E*|/sin ϕ were similar to those using |E*| with the difference that there were only four different Duncan groups for |E*|/sin ϕ, and the PG 64-40 mixes were placed in the last two groups. Similarly, when using SST-FSCH results, the PG 64-40 mixes were placed into the last groups.

- Flow time slope and flow number slope categorized the PG 64-40 + rhyolite mix in the top groups similar to APA rut depth. Based on this finding and assuming that APA relates well to pavement rutting, flow number slope and flow time slope appear to relate well to predicted rutting in a pavement.
- It is possible to select mixtures that have good cracking resistance accompanied with adequate resistance to rutting, such as the 64-40RHY in this study. However, parameters such as the |E*| at 10 Hz from the dynamic modulus test may disqualify such mixes because of poor predicted rutting resistance.

RECOMMENDATIONS

The scope of this project is relatively limited; however, the findings raise a question about the ability of the dynamic modulus test (|E*|/sin ϕ at 10Hz) to properly characterize the benefits of modified asphalt binders in HMA. Flow number value and flow time slope provided better correlations with the APA torture test than dynamic modulus. The researchers recognize that the APA can, at best, simulate HMA rutting in terms of identifying rut susceptible mixes and does not provide a direct correlation to field performance.

It currently appears that the forthcoming American Association for State Highway and Transportation Officials (AASHTO) Design Guide will recommend implementation of dynamic modulus as the sole test for design of asphalt pavements. Users should understand that dynamic modulus is a stiffness test related to thickness design of asphalt pavement layers subjected to vehicular loads at highway speeds and may not always relate to HMA rutting resistance (i.e., permanent deformation), particularly when polymer-modified asphalts are used. Therefore, tests in addition to dynamic modulus should be considered to accurately assess rutting resistance of HMA paving mixtures.

REFERENCES

Barksdale, R.G., "Compressive Stress Pulse Times in Flexible Pavements for Use in Dynamic Testing," Highway Research Record 335, Highway Research Board, 1971.

Kaloush, K.E.. and Witczak, M.W., "Tertiary Flow Characteristics of Asphalt Mixtures," Journal of Association of Asphalt Paving Technologists, 2002.

Pellinen, T.K., "Asphalt Mix Master curve Construction Using Sigmoidal Fitting Function with Nonlinear Least Squares Optimization Technique," 15th ASCE Engineering Mechanics Conference, Colombia University, New York, 2002.

Shenoy, A., and Romero, P., "Standardized Procedure for Analysis of Dynamic Modulus |E*| Data to Predict Asphalt Pavement Distresses," Transportation Research Record 1789, 2002.

Williams, R.C., and Prowell, B.D., "Comparison of Wheel Tracking Test Results with WesTrack Performance," Transportation Research Record 1681, 1999.

Witczak, M.W., Kaloush, K., Pellinen, T., Basyouny, M.E., and Quintus, H.V., "Simple Performance Test for Superpave Mix Design," NCHRP Report No. 465, 2002.

Zhang, J., Cooley, Jr., L.A., and Kandhal, P.S., "Comparison of Fundamental and Simulative Test Methods for Evaluating Permanent Deformation of Hot Mix Asphalt," Transportation Research Record 1789, 2002.

Zhou, F., and Scullion, T., "Laboratory Results from Heavy Duty Asphalt Mixes," Technical Memorandum to TxDOT, 2001.

APPENDIX A

GRADATIONS OF HMA MIXES

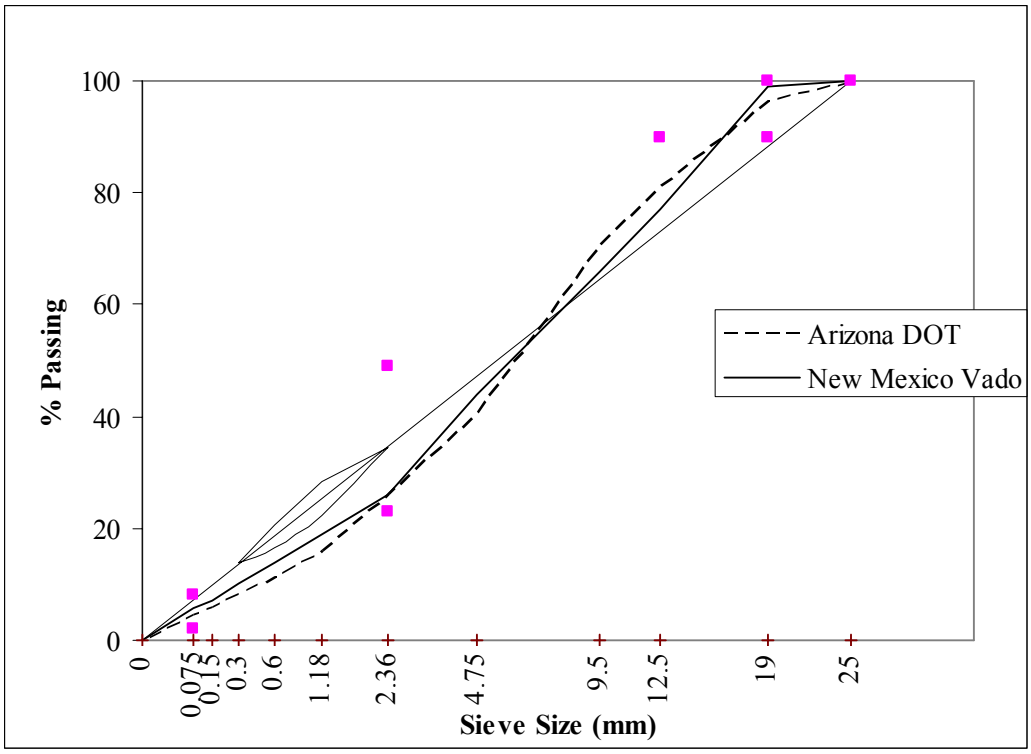

Figure A.1. Gradation of Mixes with 19-mm Maximum Nominal Aggregate Size.

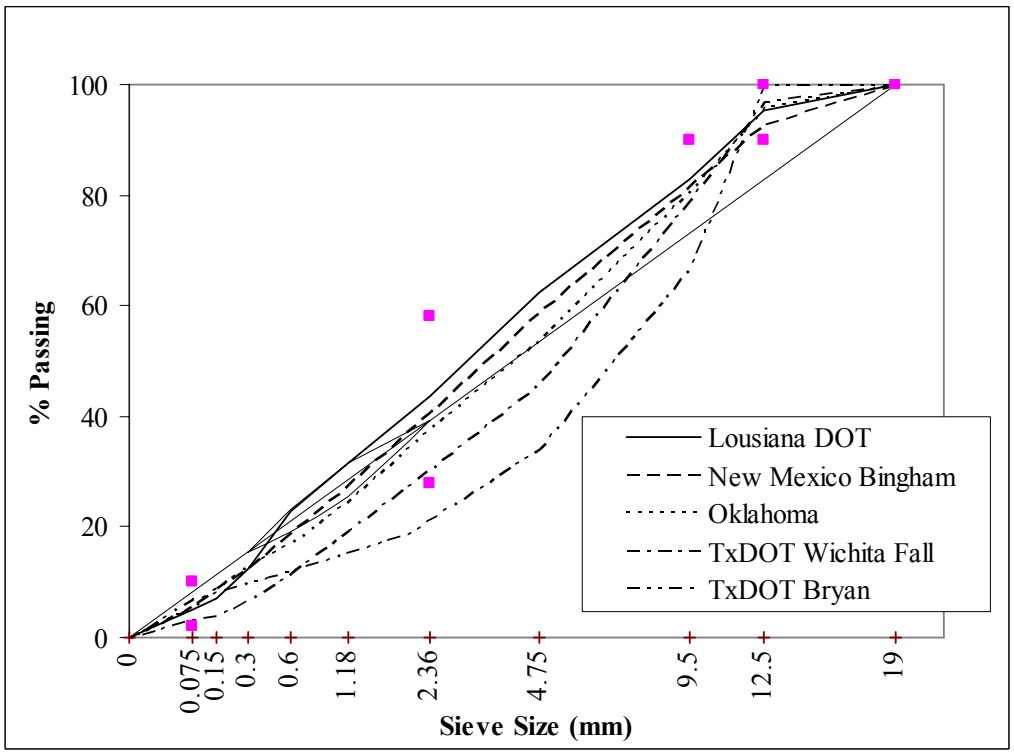

Figure A.2. Gradation of Mixes with 12.5-mm Maximum Nominal Aggregate Size.

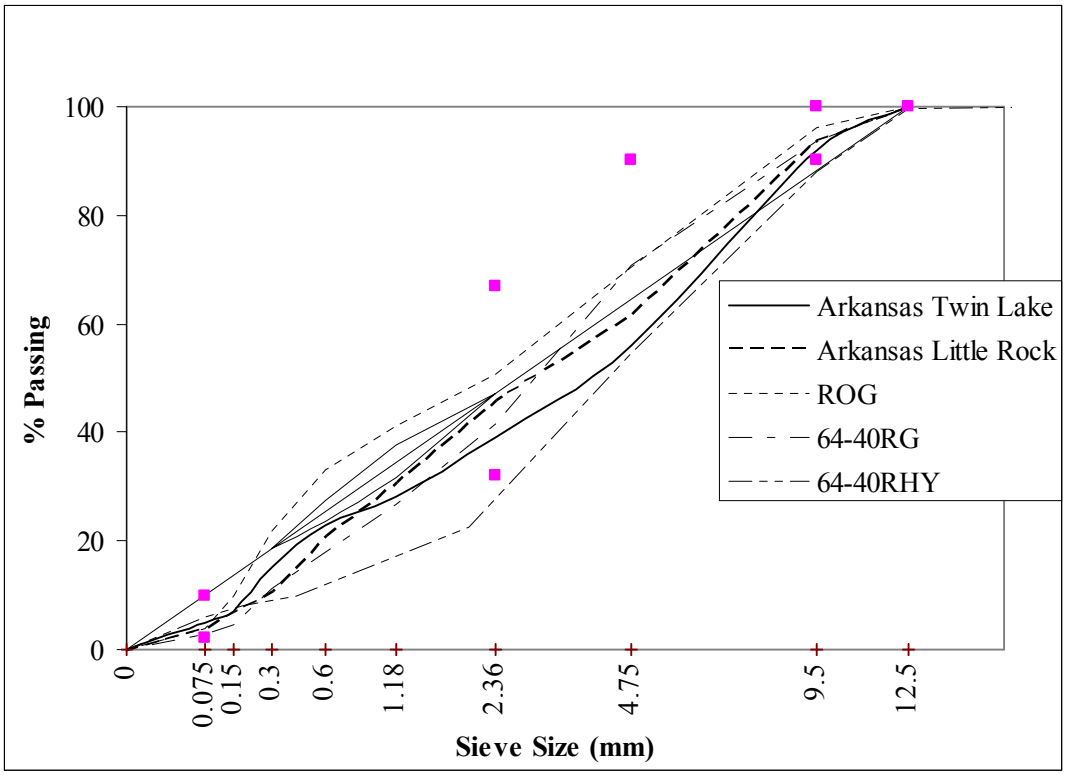

Figure A.3. Gradation of Mixes with 9.5-mm Maximum Nominal Aggregate Size.

APPENDIX B

DETERMINATION OF APA CREEP SLOPE USING BEST FIT METHOD

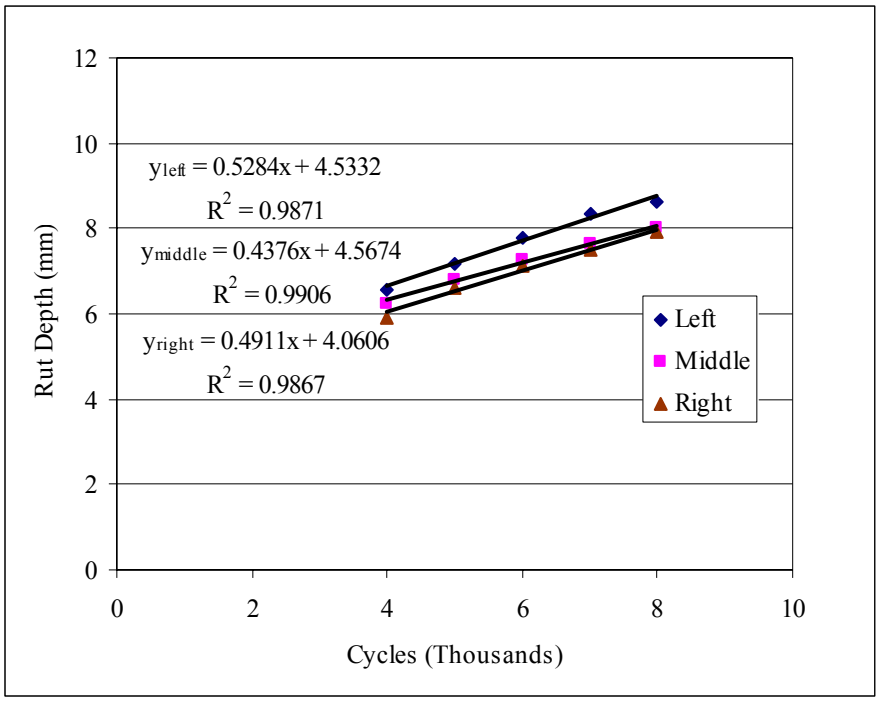

Figure B.1. APA Creep Slope Determination for ARTL.

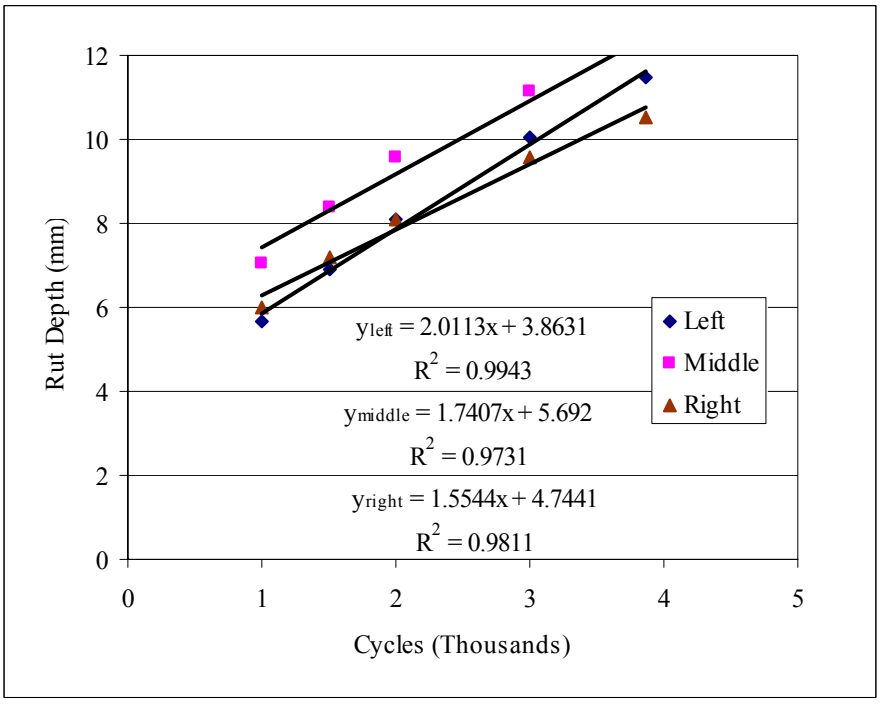

Figure B.2. APA Creep Slope Determination for ARLR.

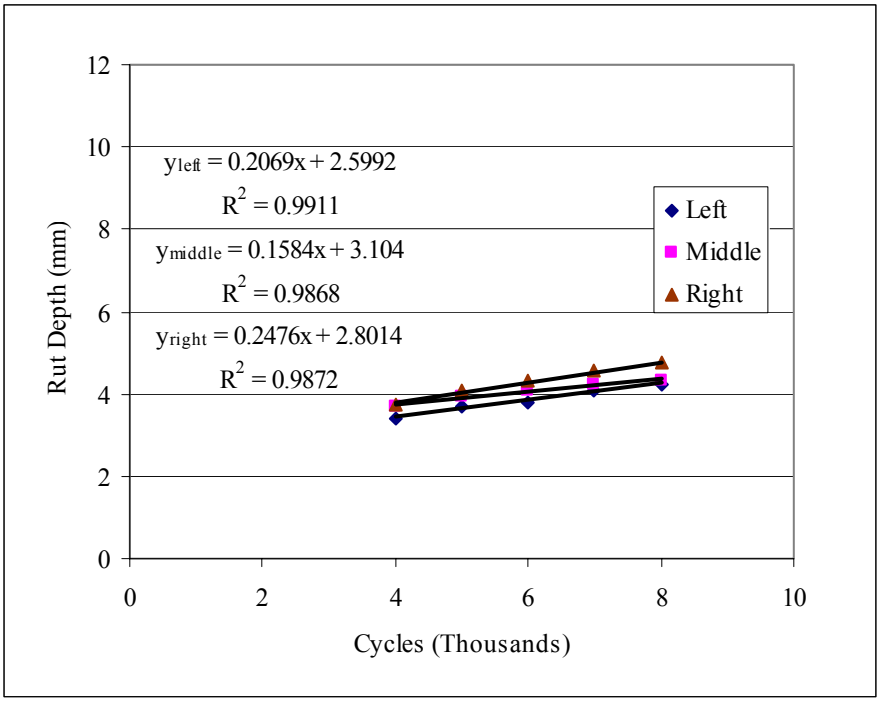

Figure B.3. APA Creep Slope Determination for AZ.

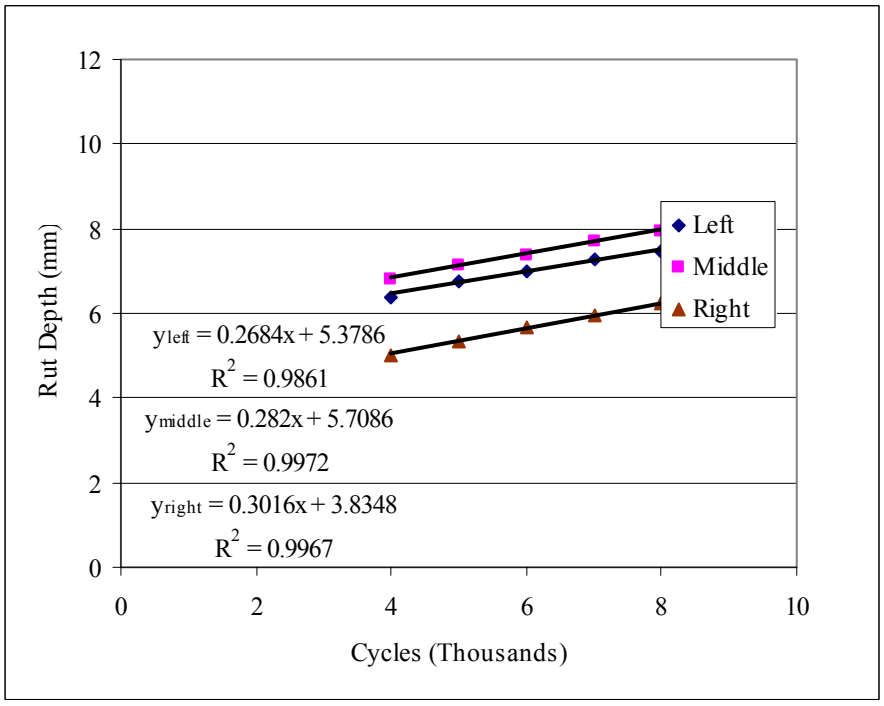

Figure B.4. APA Creep Slope Determination for LA.

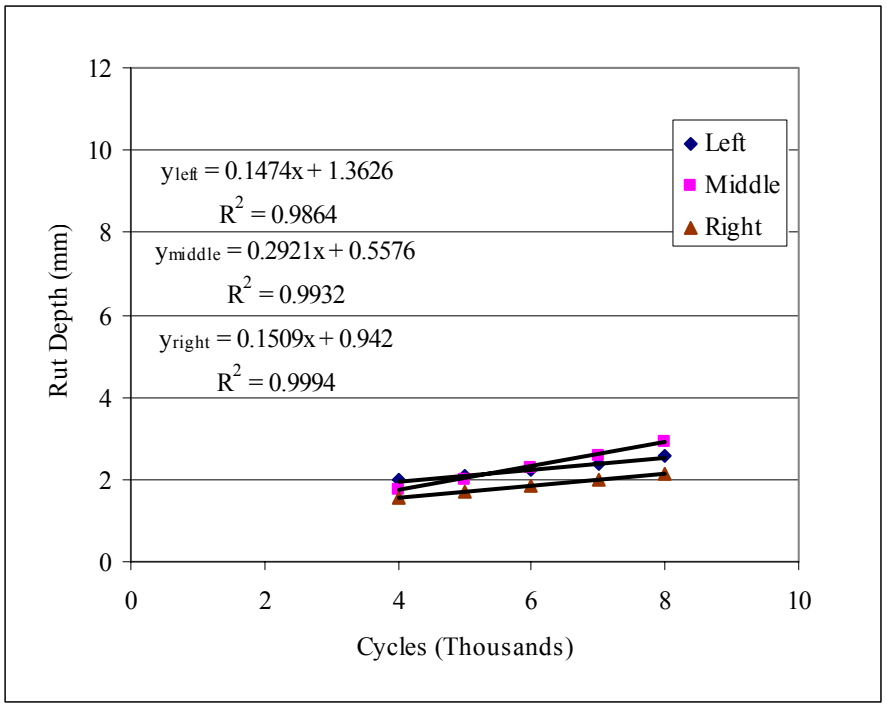

Figure B.5. APA Creep Slope Determination for NMBingham.

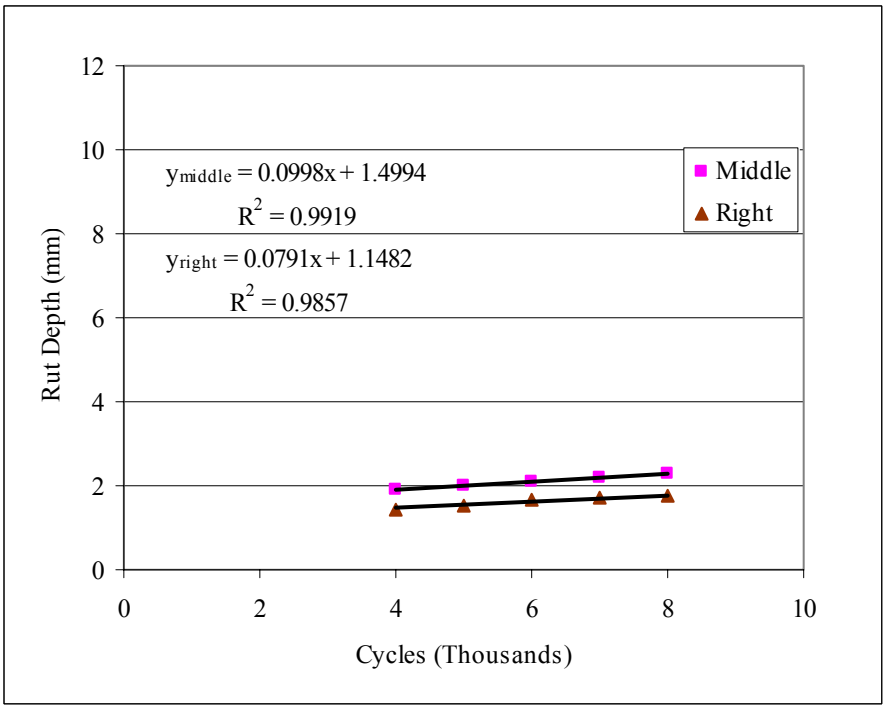

Figure B.6. APA Creep Slope Determination for NMVado.

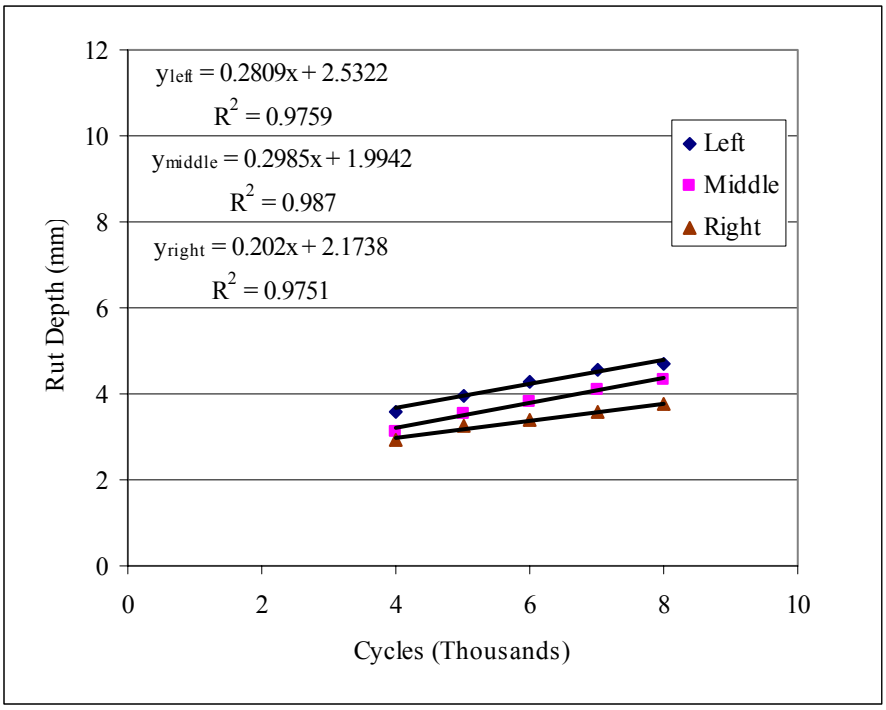

Figure B.7. APA Creep Slope Determination for OK.

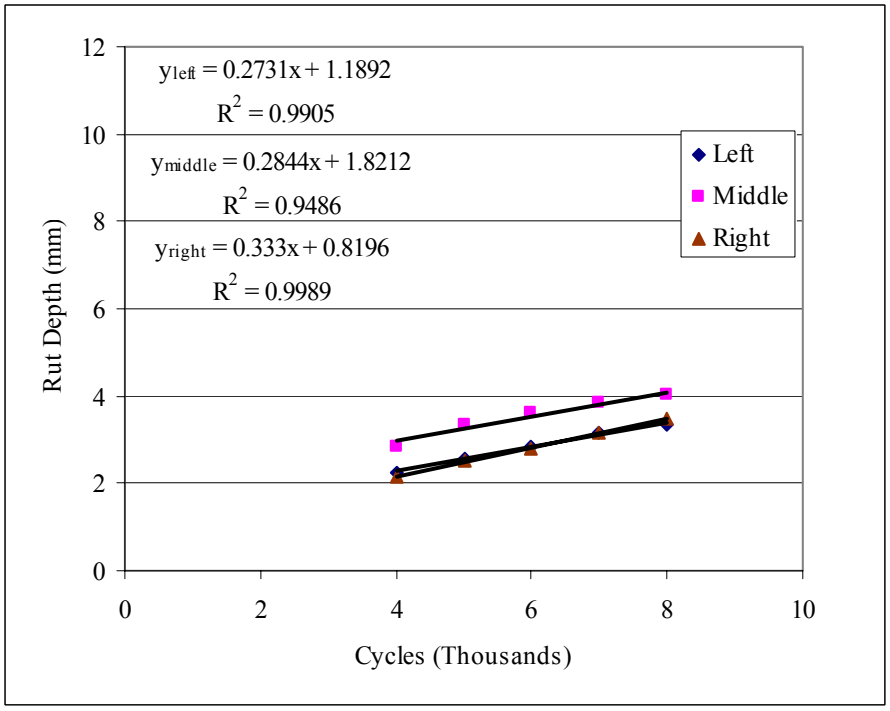

Figure B.8. APA Creep Slope Determination for TXWF.

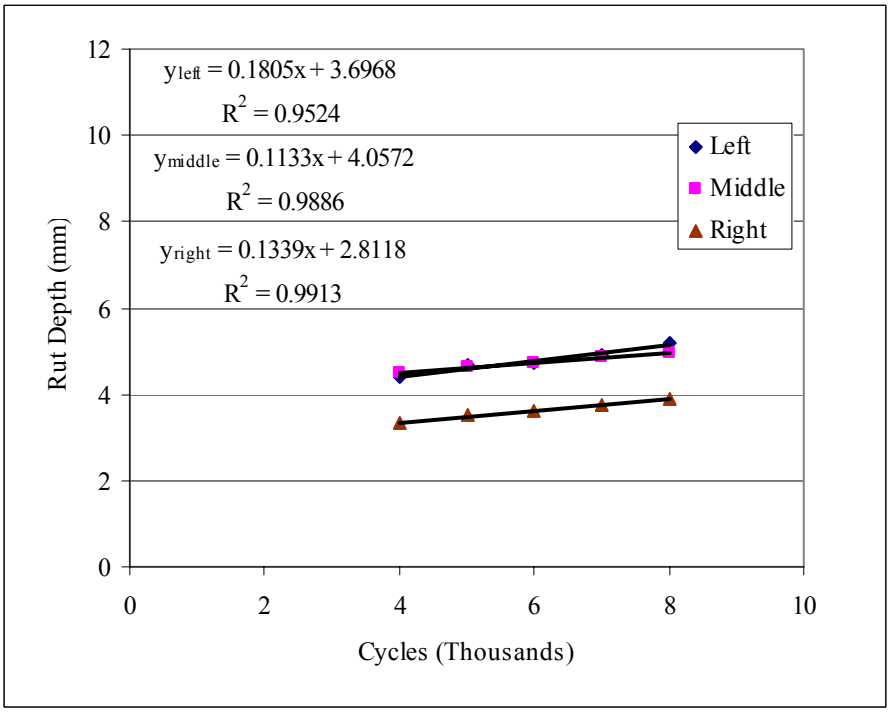

Figure B.9. APA Creep Slope Determination for TXBryan.

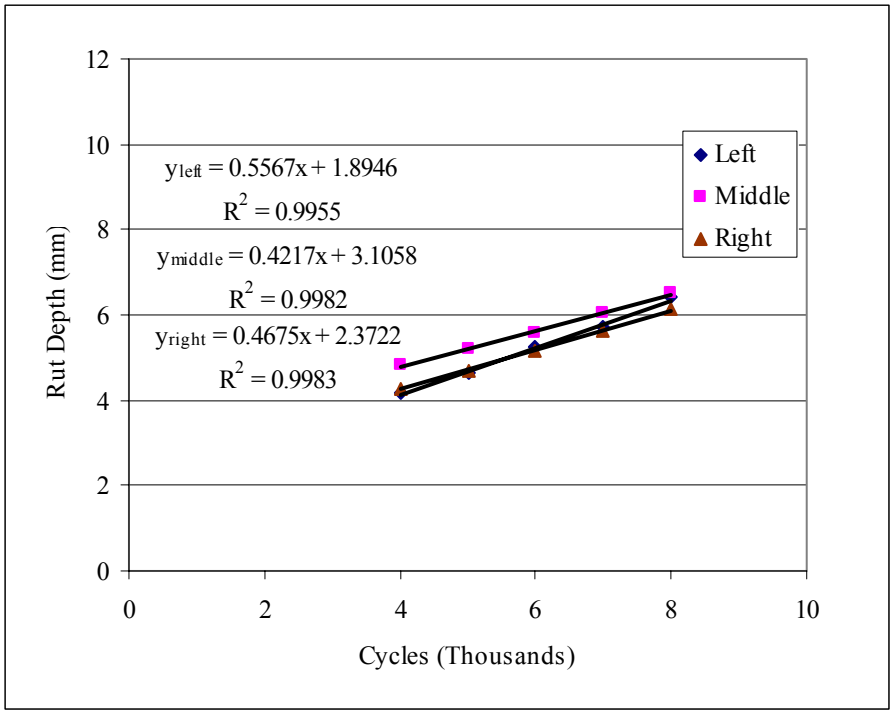

Figure B.10. APA Creep Slope Determination for 64-40RG.

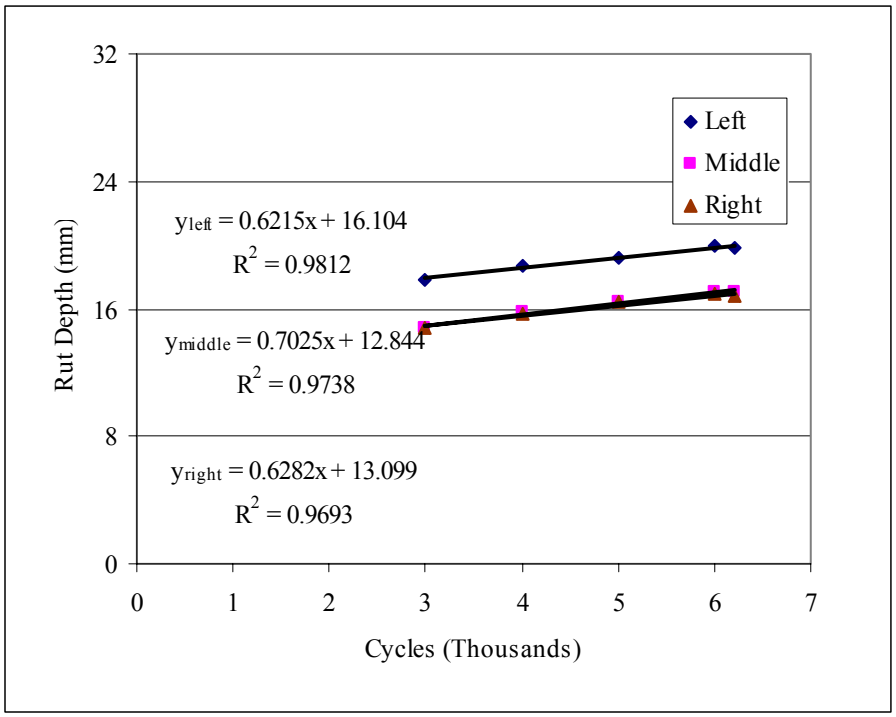

Figure B.11. APA Creep Slope Determination for ROG.

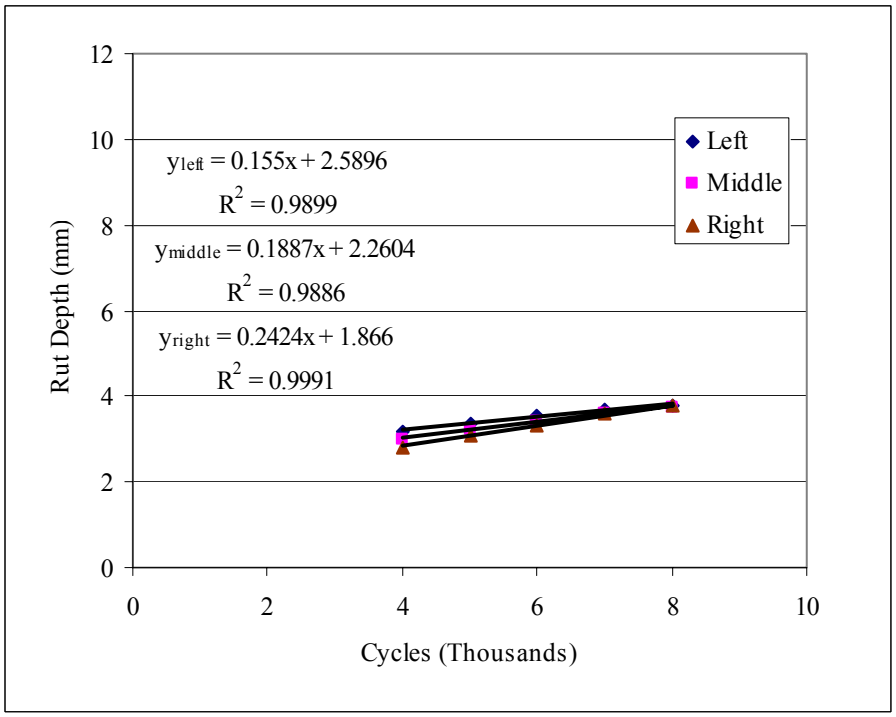

Figure B.12. APA Creep Slope Determination for 64-40RHY.

APPENDIX C

SST DATA FOR ALL TEMPERATURES AND FREQUENCIES

Table C.1. FSCH Data for ARTL.

Freq. Hz	Test at 20°C						Test at 40°C					
	|G*| (MPa)			δ (Degrees)			|G*| (MPa)			δ (Degrees)		
	#1	#2	Avg.	#1	#2	Avg.	#1	#2	Avg.	#1	#2	Avg.
10	287934	227059	257497	30.32	23.28	26.8	29865	56629	43247	58.93	50.24	54.6
5	239059	200666	219863	29.74	23.03	26.4	21620	40633	31127	56.77	52.14	54.5
2	181788	165572	173680	33.01	24.21	28.6	13988	26722	20355	54.45	53.72	54.1
1	144886	140227	142557	35.66	25.9	30.8	10407	19075	14741	53.51	54.17	53.8
0.5	110291	117549	113920	38.69	28.33	33.5	7550	14338	10944	48.77	52.94	50.9
0.2	73248	89968	81608	42.39	31.25	36.8	5770	9631	7701	52.34	52.83	52.6
0.1	52896	71216	62056	44.88	33.85	39.4	4754	7867	6311	45.86	49.34	47.6
0.05	38317	56218	47268	46.52	35.87	41.2	3848	6236	5042	34.38	48.00	41.2
0.02	25162	39714	32438	50.35	39.13	44.7	3242	5162	4202	37.91	44.95	41.4
0.01	17658	29948	23803	53.01	41.11	47.1	3533	4953	4243	35.27	40.63	38.0

Table C.2. FSCH Data for ARLR.

Freq. Hz	Test at 20°C						Test at 40°C					
	|G*| (MPa)			δ (Degrees)			|G*| (MPa)			δ (Degrees)		
	#1	#2	Avg.	#1	#2	Avg.	#1	#2	Avg.	#1	#2	Avg.
10	268908	282415	275662	28.27	28.1	28.2	29524	34174	31849	60.89	59.65	60.3
5	224572	236267	230420	28.25	28.89	28.6	20585	23005	21795	60.2	61.02	60.6
2	176265	181211	178738	31.41	32.23	31.8	12511	14112	13312	61.3	59.76	60.5
1	141022	142185	141604	33.59	36.06	34.8	8528	9913	9221	56.12	57.27	56.7
0.5	109105	108975	109040	37.01	39.66	38.3	6956	7095	7026	53.99	55.87	54.9
0.2	75008	72740	73874	41.25	44.22	42.7	5284	4840	5062	44.55	52.42	48.5
0.1	54390	51919	53155	44.75	47.1	45.9	4096	4562	4329	39.79	53.7	46.7
0.05	39306	36423	37865	46.64	49.74	48.2	3773	3400	3587	39.33	49.39	44.4
0.02	25312	23049	24181	49.41	53.14	51.3	3277	3241	3259	43.97	48.8	46.4
0.01	18244	16414	17329	52.16	56.49	54.3	3431	2929	3180	38.41	50.99	44.7

Table C.3. FSCH Data for AZ.

Freq. Hz	Test at 20°C						Test at 40°C					
	|G*| (MPa)			δ (Degrees)			|G*| (MPa)			δ (Degrees)		
	#1	#2	Avg.	#1	#2	Avg.	#1	#2	Avg.	#1	#2	Avg.
10	216007	232332	224170	27.86	31.36	29.6	36884	35757	36321	53.39	53.9	53.6
5	184308	195937	190123	26.78	30.5	28.6	27617	26433	27025	53.51	54.61	54.1
2	145513	156628	151071	28.78	30.17	29.5	18316	17191	17754	53.09	54.94	54.0
1	116912	129882	123397	31.19	30.95	31.1	14296	12039	13168	51.27	56.03	53.7
0.5	93589	105233	99411	33.16	32.38	32.8	11005	9541	10273	50.18	54.48	52.3
0.2	66762	77624	72193	36.31	34.57	35.4	8389	6973	7681	46.76	52.22	49.5
0.1	51536	61696	56616	38.9	36.02	37.5	6869	5782	6326	43.91	48.86	46.4
0.05	38800	48456	43628	41.76	37.43	39.6	5892	4799	5346	42.58	47.27	44.9
0.02	26955	34686	30821	45.58	39.08	42.3	5251	4336	4794	40.67	47.24	44.0
0.01	20112	26524	23318	48.25	39.45	43.9	5089	4432	4761	38.56	44.86	41.7

Table C.4. FSCH Data for LA.

Freq. Hz	Test at 20°C						Test at 40°C					
	|G*| (MPa)			δ (Degrees)			|G*| (MPa)			δ (Degrees)		
	#1	#2	Avg.	#1	#2	Avg.	#1	#2	Avg.	#1	#2	Avg.
10	272570	259255	265913	29.29	29.54	29.4	46393	41339	43866	56.22	51.49	53.9
5	224736	213100	218918	31	30.14	30.6	31535	29378	30457	55.83	49.11	52.5
2	169114	158865	163990	34.16	33.22	33.7	20154	20123	20139	52.37	47.55	50.0
1	132332	126383	129358	36.66	35.06	35.9	14141	15308	14725	50.69	44.48	47.6
0.5	103077	99185	101131	39.82	37.45	38.6	10929	12048	11489	49.93	41.33	45.6
0.2	72046	71321	71684	42.94	40.07	41.5	7726	9154	8440	41.34	39.63	40.5
0.1	55088	55122	55105	44.94	41.31	43.1	6110	7939	7025	35.59	35.72	35.7
0.05	42266	43082	42674	45.64	42.49	44.1	5497	6826	6162	34.62	33.91	34.3
0.02	29989	31625	30807	46.72	43.14	44.9	4227	6137	5182	33.06	37.46	35.3
0.01	23588	24627	24108	46.44	43.90	45.2	4069	5334	4702	33.2	39.17	36.2

Table C.5. FSCH Data for NMBingham.

Freq. Hz	Test at 20°C						Test at 40°C					
	|G*| (MPa)			δ (Degrees)			|G*| (MPa)			δ (Degrees)		
	#1	#2	Avg.	#1	#2	Avg.	#1	#2	Avg.	#1	#2	Avg.
10	273758	379079	326419	30.41	21.96	26.2	72198	54706	63452	36.99	40.44	38.7
5	215222	309136	262179	29.55	23.66	26.6	58664	47077	52871	36.55	37.03	36.8
2	187310	244326	215818	26.99	24.42	25.7	42895	35636	39266	37.6	32.93	35.3
1	164551	206501	185526	27.43	25.44	26.4	34118	33910	34014	34.31	32.1	33.2
0.5	142697	174729	158713	27.62	26.26	26.9	28468	27658	28063	32.35	34.42	33.4
0.2	115700	138902	127301	29.21	27.27	28.2	23349	24310	23830	30.8	32.09	31.4
0.1	96398	115476	105937	29.94	28.06	29.0	19537	21236	20387	30.94	32.96	32.0
0.05	79981	96510	88246	31.66	28.6	30.1	16794	18378	17586	30.59	33.79	32.2
0.02	62393	75910	69152	34.07	30.41	32.2	14118	16227	15173	30.14	35.2	32.7
0.01	51185	62564	56875	35.85	31.35	33.6	12124	14907	13516	32.22	37.18	34.7

Table C.6. FSCH Data for NMVado.

Freq. Hz	Test at 20°C						Test at 40°C					
	|G*| (MPa)			δ (Degrees)			|G*| (MPa)			δ (Degrees)		
	#1	#2	Avg.	#1	#2	Avg.	#1	#2	Avg.	#1	#2	Avg.
10	328813	273245	301029	17.97	14.60	16.3	151066	110063	130565	27.23	25.33	26.3
5	313213	253672	283443	15.46	13.27	14.4	127054	94732	110893	26.93	25.46	26.2
2	284647	229052	256850	14.58	13.49	14.0	102809	75898	89354	26.32	25.98	26.2
1	264239	210958	237599	14.57	13.99	14.3	86288	63868	75078	27.37	27.57	27.5
0.5	243885	193745	218815	14.87	14.95	14.9	72738	53108	62923	28.28	28.42	28.4
0.2	215360	172540	193950	15.87	15.79	15.8	56443	41113	48778	28.85	30.71	29.8
0.1	196462	158284	177373	16.85	16.99	16.9	46783	33572	40178	30.41	31.04	30.7
0.05	176874	144311	160593	18.25	18.34	18.3	38694	27322	33008	32.33	33.43	32.9
0.02	153572	126152	139862	21.4	20.09	20.7	29926	20360	25143	34.47	36.01	35.2
0.01	134771	114222	124497	25.01	22.19	23.6	24349	16123	20236	36.6	38.22	37.4

Table C.7. FSCH Data for OK.

Freq. Hz	Test at 20°C						Test at 40°C					
	|G*| (MPa)			δ (Degrees)			|G*| (MPa)			δ (Degrees)		
	#1	#2	Avg.	#1	#2	Avg.	#1	#2	Avg.	#1	#2	Avg.
10	206533	228349	217441	32.41	29.91	31.2	49815	56280	53048	41.73	41.99	41.9
5	169299	190136	179718	31.28	29.09	30.2	39345	41870	40608	39.94	39.17	39.6
2	126994	148697	137846	32.01	29.93	31.0	28962	31139	30051	38.42	36.73	37.6
1	101887	121772	111830	32.79	31.19	32.0	22695	24005	23350	36.53	35.24	35.9
0.5	81609	98138	89874	33.48	32.03	32.8	17397	20988	19193	34.97	32.71	33.8
0.2	60617	74135	67376	33.32	32.78	33.1	15375	16266	15821	29.23	30.05	29.6
0.1	48882	59881	54382	33.17	32.94	33.1	12983	13431	13207	27.65	28.58	28.1
0.05	39366	49097	44232	33.38	33.64	33.5	11652	11732	11692	27.43	28.4	27.9
0.02	30314	37966	34140	33.57	34.36	34.0	10223	9644	9934	25.49	27.9	26.7
0.01	24522	31720	28121	35.61	35.78	35.7	9016	8877	8947	26.34	28.7	27.5

Table C.8. FSCH Data for TXWF.

Freq. Hz	Test at 20°C						Test at 40°C					
	|G*| (MPa)			δ (Degrees)			|G*| (MPa)			δ (Degrees)		
	#1	#2	Avg.	#1	#2	Avg.	#1	#2	Avg.	#1	#2	Avg.
10	176216	243264	209740	26.09	27.4	26.7	51645	44354	48000	43.6	45.36	44.5
5	150490	202942	176716	24.8	26.27	25.5	40027	34444	37236	41.86	44.45	43.2
2	125621	162840	144231	24.25	26.83	25.5	27693	23191	25442	44.7	46.14	45.4
1	108360	134927	121644	24.8	27.74	26.3	19880	17087	18484	42.81	45.26	44.0
0.5	91715	111269	101492	25.77	28.85	27.3	15920	13027	14474	44.8	45.51	45.2
0.2	73678	85788	79733	27.99	30.74	29.4	11415	9891	10653	42.86	44.07	43.5
0.1	62400	69936	66168	29.79	31.81	30.8	8811	8020	8416	42.39	42.67	42.5
0.05	52126	57732	54929	31.33	33.74	32.5	7127	6652	6890	41.64	41.98	41.8
0.02	40805	44378	42592	34.61	36.53	35.6	5791	5275	5533	41.45	43.23	42.3
0.01	34038	36403	35221	37.84	38.94	38.4	5209	4693	4951	42.43	43.81	43.1

Table C.9. FSCH Data for TXBryan.

Freq. Hz	Test at 20°C						Test at 40°C					
	|G*| (MPa)			δ (Degrees)			|G*| (MPa)			δ (Degrees)		
	#1	#2	Avg.	#1	#2	Avg.	#1	#2	Avg.	#1	#2	Avg.
10	356004	123570	239787	22.32	27.69	25.0	67367	65693	66530	46.83	53.01	49.9
5	299804	99263	199534	24.11	29.44	26.8	48408	45195	46802	47.21	52.74	50.0
2	243717	77018	160368	26.06	32.54	29.3	32461	29462	30962	45.69	49.65	47.7
1	202166	61566	131866	28.55	33.13	30.8	24934	22102	23518	43.33	46.94	45.1
0.5	165982	50406	108194	30.85	34.20	32.5	19097	17528	18313	39.55	44.16	41.9
0.2	126340	39342	82841	33.63	34.66	34.1	14650	12381	13516	37.13	37.15	37.1
0.1	101296	32207	66752	35.55	35.59	35.6	11621	10984	11303	36.03	34.61	35.3
0.05	81383	27518	54451	36.75	35.69	36.2	9999	9236	9618	32.09	31.99	32.0
0.02	61235	22872	42054	38.01	38.04	38.0	8854	8197	8526	32.88	34.08	33.5
0.01	49557	19754	34656	38.95	40.62	39.8	7836	7468	7652	32.16	33.92	33.0

Table C.10. FSCH Data for 64-22ROG.

Freq. Hz	Test at 20°C						Test at 40°C					
	|G*| (MPa)			δ (Degrees)			|G*| (MPa)			δ (Degrees)		
	#1	#2	Avg.	#1	#2	Avg.	#1	#2	Avg.	#1	#2	
10	252285	246605	249445	26.62	31.2	28.9	45657	43436	44547	44.03	45.78	44.9
5	207808	201048	204428	27.79	30.5	29.1	35023	33533	34278	42.98	45.46	44.2
2	162613	157045	159829	29.63	30.94	30.3	24082	23419	23751	45.83	46.83	46.3
1	131895	125295	128595	31.04	32.62	31.8	17410	17674	17542	41.79	45.24	43.5
0.5	106392	100799	103596	32.71	33.64	33.2	13464	13380	13422	43.78	45.94	44.9
0.2	79072	73495	76284	34.78	34.81	34.8	10158	10607	10383	41.93	43.66	42.8
0.1	62421	57871	60146	36.62	36.39	36.5	8395	8359	8377	41.69	41.64	41.7
0.05	49603	45431	47517	37.4	38.25	37.8	6880	7139	7010	39.19	40.25	39.7
0.02	36083	32890	34487	40.12	40.14	40.1	5790	6267	6029	37.6	37.75	37.7
0.01	28313	25892	27103	41.48	42.2	41.8	4992	5638	5315	41.78	36.33	39.1

Table C.11. FSCH Data for 64-40RG.

Freq. Hz	Test at 20°C						Test at 40°C					
	|G*| (MPa)			δ (Degrees)			|G*| (MPa)			δ (Degrees)		
	#1	#2	Avg.	#1	#2	Avg.	#1	#2	Avg.	#1	#2	Avg.
10	69840	55079	62460	40.56	42.6	41.6	35757	15221	25489	53.9	39.38	46.6
5	53863	41418	47641	38.17	42.1	40.1	26433	12880	19657	54.61	34.97	44.8
2	38532	29230	33881	35.96	41.04	38.5	17191	10533	13862	54.94	28.3	41.6
1	30658	23132	26895	34.85	40.63	37.7	12039	8999	10519	56.03	31.83	43.9
0.5	25149	17964	21557	33.52	38.61	36.1	9541	7791	8666	54.48	26.95	40.7
0.2	19662	13566	16614	31.46	35.92	33.7	6973	7002	6988	52.22	24.61	38.4
0.1	16204	11069	13637	31.28	36.09	33.7	5782	6687	6235	48.86	23.39	36.1
0.05	13789	9358	11574	30.03	35.95	33.0	4799	6221	5510	47.27	19.27	33.3
0.02	11515	7561	9538	31.74	37.65	34.7	4336	5442	4889	47.24	22.82	35.0
0.01	10127	6817	8472	31.47	39.96	35.7	4432	5208	4820	44.86	22.59	33.7

Table C.12. FSCH Data for 64-40RHY.

Freq. Hz	Test at 20°C						Test at 40°C					
	|G*| (MPa)			δ (Degrees)			|G*| (MPa)			δ (Degrees)		
	#1	#2	Avg.	#1	#2	Avg.	#1	#2	Avg.	#1	#2	Avg.
10	50195	73960	62078	43.17	40.04	41.6	8181	15276	11729	49.54	31.81	40.7
5	37561	57974	47768	41.66	38.31	40.0	6444	13832	10138	46.51	27.11	36.8
2	26719	41241	33980	40.12	37.46	38.8	4659	11827	8243	44.63	23.11	33.9
1	21290	32699	26995	39.4	36.12	37.8	4227	11145	7686	47.93	21.64	34.8
0.5	16880	26461	21671	39.16	34.44	36.8	3827	10317	7072	45.43	20.89	33.2
0.2	12407	19825	16116	36.53	32.93	34.7	3327	9585	6456	45.43	20.64	33.0
0.1	10402	16225	13314	35.69	33.06	34.4	3097	8983	6040	45.87	19.89	32.9
0.05	8510	14156	11333	33.34	31.96	32.7	2957	8676	5817	38.45	19.21	28.8
0.02	6892	11702	9297	32.83	32.71	32.8	2912	8039	5476	42.63	19.76	31.2
0.01	5696	9843	7770	31.83	34.16	33.0	3303	7757	5530	45.74	20.59	33.2

APPENDIX D

DYNAMIC MODULUS DATA
FOR ALL
TEMPERATURES AND FREQUENCIES

Table D.1. Dynamic Modulus Data for ARTL.

Temp. (°C)	Freq. (Hz)	ARTL #2			ARTL #3		
		|E*| (MPa)	ϕ (Degrees)	|E*|/sin ϕ (MPa)	|E*| (MPa)	ϕ (Degrees)	|E*|/sin ϕ (MPa)
-10.0	25	19062	2.11	517734	27457	1.65	953568
-10.0	10	18339	4.40	239041	25779	4.30	343818
-10.0	5	17652	5.52	183506	24485	5.29	265573
-10.0	1	15899	7.58	120529	21968	7.51	168081
-10.0	0.5	15006	8.53	101168	20596	8.48	139668
-10.0	0.1	12879	10.84	68481	17197	10.91	90861
4.4	25	16417	5.45	172852	20639	4.93	240160
4.4	10	15334	7.78	113275	18613	7.80	137147
4.4	5	14518	9.25	90318	17554	8.88	113717
4.4	1	12440	11.34	63266	14749	11.85	71824
4.4	0.5	11786	12.20	55772	13605	13.26	59315
4.4	0.1	9379	15.64	34790	11287	16.03	40874
21.1	25	9987	12.10	47644	11111	12.53	51214
21.1	10	8519	17.53	28283	9523	16.09	34361
21.1	5	7640	18.24	24409	8590	18.13	27605
21.1	1	5462	23.57	13659	6289	23.67	15665
21.1	0.5	4586	25.91	10495	5407	26.39	12165
21.1	0.1	3042	30.55	5985	3356	31.98	6337
37.8	25	3611	26.67	8045	3843	28.65	8015
37.8	10	2451	24.72	5861	2672	26.44	6001
37.8	5	1846	29.22	3782	1966	31.40	3773
37.8	1	1020	35.11	1773	996	38.64	1595
37.8	0.5	804	34.96	1403	761	39.19	1204
37.8	0.1	482	31.93	911	399	35.75	683
54.4	25	1777	34.54	3134	1459	40.34	2254
54.4	10	1323	28.72	2753	848	35.09	1475
54.4	5	917	26.78	2035	560	33.16	1024
54.4	1	453	31.13	876	263	39.51	413
54.4	0.5	363	31.14	702	205	34.39	363
54.4	0.1	245	26.42	551	136	28.13	288

Table D.2. Dynamic Modulus Data for ARLR.

Temp. (°C)	Freq. (Hz)	ARLR #1			ARLR #2		
		|E*| (MPa)	ϕ (Degrees)	|E*|/sin ϕ (MPa)	|E*| (MPa)	ϕ (Degrees)	|E*|/sin ϕ (MPa)
-10.0	25	22110	2.15	589352	25581	1.72	852269
-10.0	10	21073	4.60	262759	24269	4.37	318504
-10.0	5	20290	5.77	201820	23501	5.59	241261
-10.0	1	18181	7.66	136397	21207	7.57	160979
-10.0	0.5	17228	8.42	117655	20203	8.52	136364
-10.0	0.1	14733	10.82	78482	17211	10.87	91266
4.4	25	15874	5.12	177876	18740	5.63	191022
4.4	10	15077	8.09	107135	17170	7.64	129148
4.4	5	14285	9.69	84869	16002	9.26	99444
4.4	1	11964	12.60	54845	13421	11.92	64978
4.4	0.5	10977	14.40	44139	12269	13.10	54132
4.4	0.1	8509	18.69	26553	9533	16.76	33059
21.1	25	10775	13.33	46734	11848	12.95	52869
21.1	10	8858	19.52	26510	9686	16.29	34531
21.1	5	7761	20.35	22318	8548	18.38	27109
21.1	1	5375	27.55	11621	6148	23.91	15169
21.1	0.5	4460	31.06	8644	5107	26.57	11418
21.1	0.1	2716	36.45	4571	3274	32.39	6112
37.8	25	1866	42.54	2760	2735	37.98	4444
37.8	10	1136	37.52	1865	1763	33.05	3233
37.8	5	711	36.53	1194	1136	32.70	2103
37.8	1	334	36.90	556	515	40.29	796
37.8	0.5	254	34.42	449	384	38.43	618
37.8	0.1	151	25.63	349	218	31.04	423
54.4	25	573	33.30	1044	649	44.17	931
54.4	10	390	32.09	734	480	33.73	864
54.4	5	251	30.39	496	290	28.00	618
54.4	1	135	29.51	274	147	28.15	312
54.4	0.5	114	28.50	239	122	26.80	271
54.4	0.1	90	20.67	255	89	19.83	262

Table D.3. Dynamic Modulus Data for AZ.

Temp. (°C)	Freq. (Hz)	AZ #11			AZ #1		
		|E*| (MPa)	ϕ (Degrees)	|E*|/sin ϕ (MPa)	|E*| (MPa)	ϕ (Degrees)	|E*|/sin ϕ (MPa)
-10.0	25	24502	3.46	405987	22791	3.54	369113
-10.0	10	23274	6.05	220824	21833	6.12	204791
-10.0	5	22108	7.26	174944	20780	7.36	162213
-10.0	1	19317	9.31	119406	18190	9.42	111138
-10.0	0.5	18034	10.27	101151	17017	10.25	95631
-10.0	0.1	15115	13.05	66939	14247	13.03	63190
4.4	25	21404	6.22	197552	20038	6.08	189186
4.4	10	19312	8.38	132512	18389	8.48	124701
4.4	5	17963	10.44	99130	17048	10.10	97213
4.4	1	14950	13.39	64557	14281	13.11	62961
4.4	0.5	13824	14.51	55175	13141	14.44	52698
4.4	0.1	10524	18.44	33271	10203	18.12	32806
21.1	25	13604	17.55	45115	12634	12.79	57070
21.1	10	11445	20.07	33351	10877	16.75	37742
21.1	5	10070	21.09	27985	9608	18.37	30487
21.1	1	7136	25.71	16449	6961	23.38	17542
21.1	0.5	6068	27.95	12946	5924	25.69	13665
21.1	0.1	3873	32.11	7286	3931	30.03	7855
37.8	25	4526	26.40	10179	4549	26.02	10370
37.8	10	3434	26.53	7688	3106	26.15	7048
37.8	5	2477	27.72	5325	2458	32.48	4577
37.8	1	1312	36.08	2228	1344	36.42	2264
37.8	0.5	1025	35.54	1763	1043	37.02	1732
37.8	0.1	618	31.96	1168	583	34.93	1018
54.4	25	1205	33.56	2180	1461	37.06	2424
54.4	10	826	27.45	1792	913	30.52	1798
54.4	5	582	23.88	1438	617	26.48	1384
54.4	1	333	30.86	649	347	33.91	622
54.4	0.5	276	28.98	570	276	32.02	521
54.4	0.1	215	25.14	506	196	28.05	417

Table D.4. Dynamic Modulus Data for LA.

Temp. (°C)	Freq. (Hz)	LA#1			LA#2		
		|E*| (MPa)	ϕ (Degrees)	|E*|/sin ϕ (MPa)	|E*| (MPa)	ϕ (Degrees)	|E*|/sin ϕ (MPa)
-10.0	25	19560	0.71	1578491	27220	2.66	586517
-10.0	10	19379	3.20	347165	24955	4.97	288045
-10.0	5	18945	4.45	244171	23596	6.04	224247
-10.0	1	17478	6.01	166929	20907	8.07	148926
-10.0	0.5	16700	6.82	140632	19476	8.87	126310
-10.0	0.1	14734	8.94	94815	16204	11.30	82695
4.4	25	16648	3.37	283203	24183	4.23	327864
4.4	10	16166	6.30	147322	21440	6.62	185974
4.4	5	15376	7.32	120677	19914	8.51	134573
4.4	1	13423	9.70	79664	16886	11.18	87090
4.4	0.5	12519	10.95	65905	15414	12.43	71613
4.4	0.1	10303	14.03	42501	11960	15.70	44198
21.1	25	12597	12.58	57838	13658	10.10	77884
21.1	10	10451	16.41	36992	11476	14.68	45282
21.1	5	9223	17.87	30057	10293	15.40	38760
21.1	1	6938	22.59	18061	7942	20.34	22850
21.1	0.5	6075	24.93	14412	6927	22.56	18057
21.1	0.1	4032	30.24	8005	4787	28.28	10104
37.8	25	3025	27.54	6542	4340	24.33	10534
37.8	10	2038	30.90	3968	2951	28.96	6095
37.8	5	1525	38.49	2449	2198	38.72	3513
37.8	1	757	39.58	1188	1178	39.90	1836
37.8	0.5	607	39.94	946	912	41.05	1388
37.8	0.1	365	35.74	625	502	38.24	812
54.4	25	1132	34.73	1986	1259	35.65	2160
54.4	10	712	30.50	1402	794	35.50	1367
54.4	5	485	35.30	840	519	33.86	932
54.4	1	239	35.01	417	272	32.09	511
54.4	0.5	193	34.18	343	222	31.16	428
54.4	0.1	127	28.09	269	155	25.04	367

Table D.5. Dynamic Modulus Data for NMBingham.

Temp. (°C)	Freq. (Hz)	NMBingham #4			NMBingham #5		
		|E*| (MPa)	ϕ (Degrees)	|E*|/sin ϕ (MPa)	|E*| (MPa)	ϕ (Degrees)	|E*|/sin ϕ (MPa)
-10.0	25	22608	3.10	418064	26368	1.15	1313791
-10.0	10	20176	5.99	193339	25720	3.61	408488
-10.0	5	18637	7.13	150153	24897	4.43	322330
-10.0	1	16369	8.79	107115	22586	5.55	233536
-10.0	0.5	15234	9.65	90879	21681	5.99	207765
-10.0	0.1	12613	11.97	60815	19121	7.62	144196
4.4	25	17922	4.86	211538	19960	3.84	298040
4.4	10	16342	7.56	124215	19038	6.03	181231
4.4	5	15227	9.01	97228	18132	6.95	149845
4.4	1	12920	10.82	68825	15873	8.55	106762
4.4	0.5	11967	11.72	58912	14797	9.48	89838
4.4	0.1	9582	14.22	39005	12359	11.77	60589
21.1	25	12556	8.23	87715	14886	9.80	87456
21.1	10	11088	12.67	50551	13427	11.15	69434
21.1	5	10227	12.95	45635	12555	13.11	55351
21.1	1	8105	16.06	29297	9946	16.05	35974
21.1	0.5	7282	17.11	24752	8983	16.99	30744
21.1	0.1	5452	20.29	15722	6770	19.98	19813
37.8	25	3568	19.83	10517	5070	20.71	14338
37.8	10	2709	21.26	7472	3639	22.71	9426
37.8	5	2314	27.27	5050	3056	31.30	5882
37.8	1	1490	29.69	3009	1906	32.24	3573
37.8	0.5	1264	30.80	2469	1593	34.22	2832
37.8	0.1	874	33.08	1601	1014	34.96	1770
54.4	25	2048	23.61	5112	2340	24.13	5725
54.4	10	1518	22.93	3896	1771	20.82	4982
54.4	5	1255	29.12	2579	1399	22.71	3624
54.4	1	769	30.54	1512	894	29.61	1810
54.4	0.5	642	31.77	1219	738	30.97	1434
54.4	0.1	436	31.37	837	500	31.17	966

Table D.6. Dynamic Modulus Data for NMVado.

Temp. (°C)	Freq. (Hz)	NMVado #1			NMVado #6		
		|E*| (MPa)	ϕ (Degrees)	|E*|/sin ϕ (MPa)	|E*| (MPa)	ϕ (Degrees)	|E*|/sin ϕ (MPa)
-10.0	25	20892	3.13	382619	17369	1.42	700892
-10.0	10	19786	5.43	209084	16841	3.86	250164
-10.0	5	19011	6.40	170552	16362	4.74	198006
-10.0	1	17396	7.58	131879	15047	6.04	143001
-10.0	0.5	16621	7.74	123413	14418	6.57	126009
-10.0	0.1	15389	7.98	110851	12882	7.90	93722
4.4	25	19785	2.06	550403	16164	3.86	240111
4.4	10	18453	4.31	245537	15393	6.17	143219
4.4	5	17671	5.30	191309	14865	6.93	123198
4.4	1	16026	6.54	140707	13280	8.27	92327
4.4	0.5	15224	6.81	128391	12714	9.04	80918
4.4	0.1	13248	8.11	93909	11053	10.22	62293
21.1	25	13858	6.40	124320	12175	5.37	130091
21.1	10	12512	8.28	86882	11100	8.21	77729
21.1	5	11748	9.79	69091	10480	9.23	65339
21.1	1	9988	12.14	47492	8835	10.80	47151
21.1	0.5	9233	12.98	41105	8187	12.15	38900
21.1	0.1	7327	15.47	27471	6633	14.75	26052
37.8	25	3789	15.68	14020	4409	16.78	15271
37.8	10	2913	16.84	10056	3539	20.87	9935
37.8	5	2497	25.06	5895	3008	23.46	7555
37.8	1	1717	26.15	3895	2028	27.72	4361
37.8	0.5	1484	27.52	3211	1736	29.50	3526
37.8	0.1	996	29.44	2027	1168	32.07	2200
54.4	25	2166	20.02	6328	2779	23.89	6863
54.4	10	1625	19.31	4915	1978	22.55	5159
54.4	5	1341	25.61	3102	1622	27.23	3544
54.4	1	854	28.45	1792	992	32.06	1869
54.4	0.5	712	30.03	1422	828	33.53	1499
54.4	0.1	475	31.11	920	539	34.94	941

Table D.7. Dynamic Modulus Data for OK.

Temp. (°C)	Freq. (Hz)	OK #1			OK #2		
		|E*| (MPa)	ϕ (Degrees)	|E*|/sin ϕ (MPa)	|E*| (MPa)	ϕ (Degrees)	|E*|/sin ϕ(MPa)
-10.0	25	36248	1.29	1610112	12776	6.32	116063
-10.0	10	34070	4.22	462991	11956	9.31	73906
-10.0	5	32070	6.58	279862	11290	10.90	59706
-10.0	1	28251	8.90	182605	9531	14.06	39233
-10.0	0.5	26364	10.57	143723	8802	15.60	32729
-10.0	0.1	21256	13.85	88796	7076	19.23	21484
4.4	25	14391	5.73	144138	13391	6.95	110662
4.4	10	13259	8.78	86866	12276	10.26	68920
4.4	5	12321	10.31	68842	11282	11.83	55029
4.4	1	10162	13.62	43155	9140	15.44	34329
4.4	0.5	9254	15.09	35546	8223	17.21	27794
4.4	0.1	7168	18.98	22038	6089	21.28	16777
21.1	25	8287	13.27	36103	8074	13.64	34239
21.1	10	6891	17.41	23031	6952	18.47	21944
21.1	5	6067	18.17	19455	6100	19.20	18549
21.1	1	4385	23.80	10865	4384	24.61	10526
21.1	0.5	3782	26.22	8561	3751	27.39	8154
21.1	0.1	2552	30.37	5047	2428	31.72	4618
37.8	25	1828	25.96	4176	1638	27.77	3515
37.8	10	1284	28.97	2651	1076	29.45	2189
37.8	5	960	31.99	1811	809	31.29	1557
37.8	1	520	33.57	941	457	31.40	876
37.8	0.5	426	34.41	754	366	33.78	658
37.8	0.1	277	31.97	523	235	30.26	466
54.4	25	1193	110.35	1273	627	104.58	648
54.4	10	629	33.47	1140	406	28.31	855
54.4	5	441	33.82	793	288	24.78	686
54.4	1	228	32.27	427	181	26.09	411
54.4	0.5	190	32.33	355	154	25.19	363
54.4	0.1	131	28.80	272	118	20.75	332

Table D.8. Dynamic Modulus Data for TXWF.

Temp. (°C)	Freq. Hz	TXWF #3			TXWF #2		
		|E*| (MPa)	ϕ (Degrees)	|E*|/sin ϕ (MPa)	|E*| (MPa)	ϕ (Degrees)	|E*|/sin ϕ (MPa)
-10.0	25	21946	3.13	401933	23373	2.48	540154
-10.0	10	20698	6.13	193827	21860	4.78	262331
-10.0	5	19685	7.01	161298	20874	6.28	190827
-10.0	1	17284	9.07	109644	18551	8.22	129753
-10.0	0.5	16297	9.62	97518	17415	8.89	112688
-10.0	0.1	13676	12.02	65668	14662	10.97	77049
4.4	25	23364	4.25	315268	18172	4.42	235799
4.4	10	21376	7.06	173919	16894	7.39	131342
4.4	5	20077	8.01	144082	15975	8.77	104778
4.4	1	17139	9.81	100594	13756	10.54	75204
4.4	0.5	15829	10.68	85412	12841	11.50	64407
4.4	0.1	12743	13.06	56392	10601	13.96	43944
21.1	25	14474	9.70	85906	11485	10.45	63320
21.1	10	12635	12.37	58980	9583	14.61	37991
21.1	5	11428	14.32	46206	8692	15.72	32080
21.1	1	8964	17.04	30591	6598	19.34	19922
21.1	0.5	7946	18.51	25029	5784	20.90	16215
21.1	0.1	5782	21.84	15542	3994	24.40	9668
37.8	25	5088	18.78	15805	3183	21.35	8743
37.8	10	3878	19.83	11433	2376	22.79	6134
37.8	5	3107	28.21	6573	1879	30.67	3684
37.8	1	1968	29.04	4053	1140	32.74	2108
37.8	0.5	1644	30.82	3208	920	35.59	1580
37.8	0.1	1072	32.39	2000	597	35.77	1021
54.4	25	1553	23.99	3819	1396	25.23	3275
54.4	10	1120	21.64	3037	1035	26.40	2327
54.4	5	888	26.07	2022	763	27.52	1651
54.4	1	544	28.04	1158	430	32.54	799
54.4	0.5	465	29.05	957	359	34.33	636
54.4	0.1	328	29.16	673	244	33.20	446

Table D.9. Dynamic Modulus Data for TXBryan.

Temp. (°C)	Freq. (Hz)	TXBryan #1			TXBryan #2		
		|E*| (MPa)	ϕ (Degrees)	|E*|/sin ϕ (MPa)	|E*| (MPa)	ϕ (Degrees)	|E*|/sin ϕ (MPa)
-10.0	25	23941	0.77	1781484	22471	0.19	6776354
-10.0	10	23487	3.25	414284	22076	2.75	460128
-10.0	5	22886	4.04	324845	21588	3.69	335439
-10.0	1	21362	5.62	218131	20131	5.19	222541
-10.0	0.5	20587	6.27	188502	19467	5.66	197387
-10.0	0.1	18754	7.89	136617	17649	7.37	137583
4.4	25	22750	1.27	1026432	19072	1.83	597224
4.4	10	21679	3.90	318743	18712	4.47	240088
4.4	5	20768	5.04	236395	17969	5.14	200566
4.4	1	18900	6.76	160559	16242	7.09	131594
4.4	0.5	17996	7.67	134833	15250	7.81	112225
4.4	0.1	15465	9.87	90218	13378	10.45	73755
21.1	25	17450	5.51	181730	17180	5.94	166007
21.1	10	15339	8.72	101174	15480	9.25	96305
21.1	5	14450	9.48	87736	14521	10.89	76862
21.1	1	12020	14.15	49169	11915	14.61	47238
21.1	0.5	11011	16.29	39256	10674	16.32	37985
21.1	0.1	8408	20.85	23624	7895	21.92	21148
37.8	25	5572	23.68	13875	6355	22.26	16775
37.8	10	4071	27.37	8854	4991	26.76	11084
37.8	5	3223	33.34	5864	4063	31.06	7875
37.8	1	1844	34.05	3294	2400	36.75	4011
37.8	0.5	1424	34.57	2509	1869	39.44	2942
37.8	0.1	898	31.78	1705	1067	40.35	1648
54.4	25	1809	31.47	3466	2091	32.02	3944
54.4	10	1145	28.23	2421	1312	31.42	2517
54.4	5	872	33.21	1591	965	33.65	1742
54.4	1	528	29.29	1079	503	33.95	900
54.4	0.5	452	28.94	933	419	33.79	753
54.4	0.1	341	26.33	769	295	30.23	586

Table D.10. Dynamic Modulus Data for ROG.

Temp. (°C)	Freq. (Hz)	1819 ROG #12			1819 ROG #13		
		|E*| (MPa)	ϕ (Degrees)	|E*|/sin ϕ (MPa)	|E*| (MPa)	ϕ (Degrees)	|E*|/sin ϕ (MPa)
-10.0	25	21579	4.84	255756	17855	4.00	255962
-10.0	10	19997	7.51	153000	17078	6.47	151558
-10.0	5	18780	8.86	121932	16277	7.85	119175
-10.0	1	16062	11.15	83060	14154	10.33	78933
-10.0	0.5	14978	12.30	70309	13169	11.28	67325
-10.0	0.1	12190	15.02	47037	10864	14.06	44719
4.4	25	16381	7.54	124838	16211	6.80	136913
4.4	10	14533	10.10	82872	14501	9.69	86153
4.4	5	13428	11.55	67065	13359	11.38	67704
4.4	1	10760	15.07	41385	10948	14.44	43903
4.4	0.5	9614	16.21	34439	9990	15.81	36668
4.4	0.1	7293	19.83	21499	7549	19.39	22738
21.1	25	9836	15.47	36876	9198	12.98	40951
21.1	10	8257	19.81	24364	7711	18.09	24833
21.1	5	7085	20.64	20100	6917	19.18	21054
21.1	1	5002	24.85	11903	5004	23.74	12430
21.1	0.5	4229	27.01	9312	4253	25.71	9804
21.1	0.1	2746	30.50	5410	2783	30.23	5528
37.8	25	3007	26.39	6765	3540	25.72	8157
37.8	10	2022	25.72	4659	2483	24.89	5900
37.8	5	1577	30.50	3107	1889	29.08	3887
37.8	1	864	35.61	1484	1082	35.91	1845
37.8	0.5	694	36.98	1154	877	37.04	1456
37.8	0.1	412	35.88	703	523	35.63	898
54.4	25	873	35.45	1505	1117	31.93	2112
54.4	10	591	30.07	1180	786	26.32	1773
54.4	5	422	30.06	842	616	23.13	1568
54.4	1	231	33.33	420	323	31.78	613
54.4	0.5	187	32.78	345	260	31.30	500
54.4	0.1	135	30.31	267	204	29.42	415

Table D.11. Dynamic Modulus Data for 64-40RG.

Temp. (°C)	Freq. (Hz)	64-40RG #2			64-40RG #3		
		|E*| (MPa)	ϕ (Degrees)	|E*|/sin ϕ (MPa)	|E*| (MPa)	ϕ (Degrees)	|E*|/sin ϕ (MPa)
-10.0	25	10549	14.73	41488	14819	13.11	65333
-10.0	10	8631	18.09	27796	12425	16.77	43063
-10.0	5	7464	20.44	21373	10800	18.66	33755
-10.0	1	5264	25.04	12437	7643	23.75	18977
-10.0	0.5	4405	27.07	9680	6423	26.50	14395
-10.0	0.1	2901	30.79	5667	4011	31.36	7707
4.4	25	6452	20.00	18864	10562	17.20	35718
4.4	10	5024	23.58	12559	8438	21.37	23157
4.4	5	4174	25.39	9735	7099	23.94	17495
4.4	1	2690	29.72	5426	4706	28.72	9793
4.4	0.5	2164	31.89	4096	3902	30.77	7627
4.4	0.1	1327	33.18	2425	2418	32.38	4515
21.1	25	2298	24.43	5556	3679	22.73	9521
21.1	10	1626	27.53	3518	2752	27.63	5934
21.1	5	1282	33.37	2331	2157	32.68	3995
21.1	1	745	31.45	1428	1270	31.40	2438
21.1	0.5	584	31.31	1124	1012	31.84	1918
21.1	0.1	393	28.66	819	648	29.48	1317
37.8	25	737	30.03	1473	966	31.53	1847
37.8	10	473	22.40	1241	632	24.28	1537
37.8	5	360	19.68	1069	475	22.45	1244
37.8	1	247	20.82	695	296	26.47	664
37.8	0.5	223	20.81	628	256	26.05	583
37.8	0.1	188	18.60	589	198	23.58	495
54.4	25	287	18.04	927	339	26.16	769
54.4	10	211	14.01	872	231	18.48	729
54.4	5	187	11.52	936	195	16.31	694
54.4	1	152	12.96	678	145	18.36	460
54.4	0.5	142	13.68	600	137	18.20	439
54.4	0.1	131	11.71	645	124	16.25	443

Table D.12. Dynamic Modulus Data for 64-40RHY.

Temp. (°C)	Freq. (Hz)	64-40RHY #0			64-40RHY #14		
		|E*| (MPa)	ϕ (Degrees)	|E*|/sin ϕ (MPa)	|E*| (MPa)	ϕ (Degrees)	|E*|/sin ϕ (MPa)
-10.0	25	11932	10.91	63043	10610	10.46	58442
-10.0	10	10032	14.19	40924	9240	13.81	38709
-10.0	5	8977	16.05	32469	8315	15.77	30595
-10.0	1	6796	19.98	19889	6265	20.27	18084
-10.0	0.5	5928	21.87	15914	5438	22.35	14301
-10.0	0.1	4108	24.95	9739	3715	26.39	8358
4.4	25	8440	14.86	32910	7598	16.77	26333
4.4	10	6912	18.32	21990	6101	20.87	17126
4.4	5	6079	19.81	17937	5239	21.76	14132
4.4	1	4245	23.97	10449	3585	25.95	8193
4.4	0.5	3546	25.79	8150	2997	27.89	6407
4.4	0.1	2386	27.30	5202	1955	29.60	3958
21.1	25	3784	21.52	10316	4055	21.37	11128
21.1	10	2683	24.09	6573	2915	27.10	6399
21.1	5	2189	30.06	4370	2185	33.17	3994
21.1	1	1340	28.60	2799	1293	32.65	2397
21.1	0.5	1047	29.32	2138	1011	33.65	1825
21.1	0.1	699	27.16	1531	685	31.31	1318
37.8	25	1188	28.81	2465	1260	28.45	2645
37.8	10	806	23.70	2005	830	25.75	1910
37.8	5	629	20.80	1771	670	21.96	1792
37.8	1	396	21.71	1071	389	24.98	921
37.8	0.5	343	22.12	911	337	24.35	817
37.8	0.1	266	20.23	769	265	22.95	680
54.4	25	685	23.38	1726	750	109.69	797
54.4	10	507	17.64	1673	405	18.90	1250
54.4	5	423	15.22	1611	321	18.06	1035
54.4	1	311	21.59	845	218	20.32	628
54.4	0.5	274	19.17	834	198	20.66	561
54.4	0.1	236	16.75	819	172	19.01	528

APPENDIX E

RATE OF CHANGE OF COMPLIANCE VERSUS TIME
FOR
FLOW TIME TEST

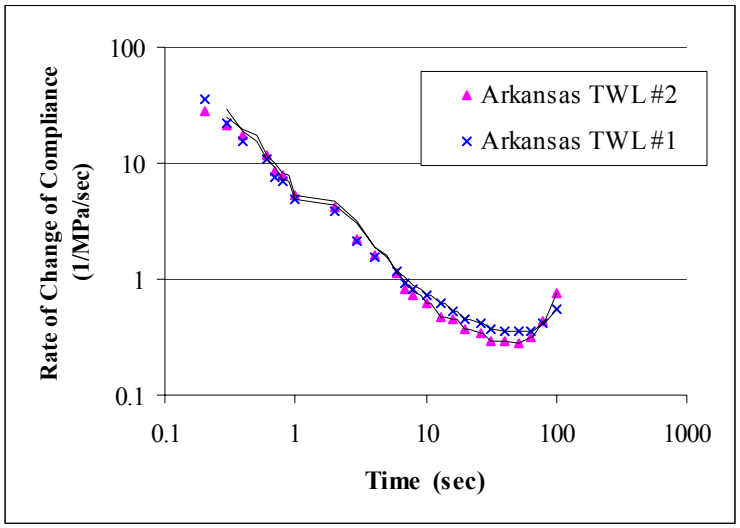

Figure E.1. Rate of Change of Creep Compliance versus Flow Time for ARTL.

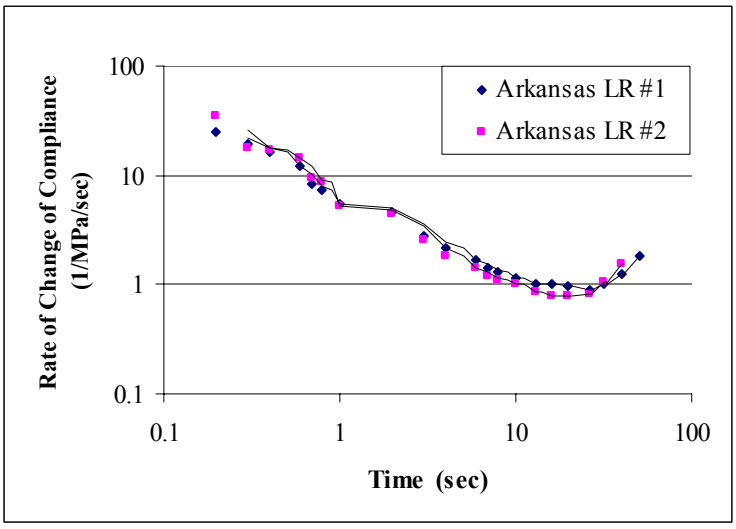

Figure E.2. Rate of Change of Creep Compliance versus Flow Time for ARLR.

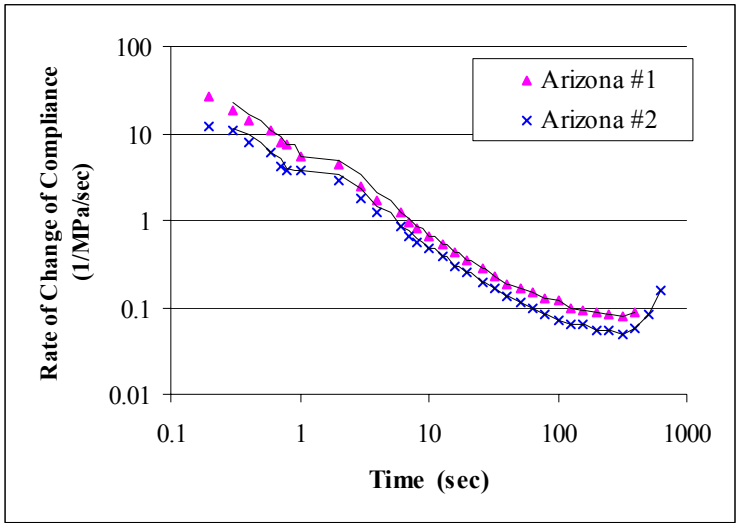

Figure E.3. Rate of Change of Creep Compliance versus Flow Time for AZ.

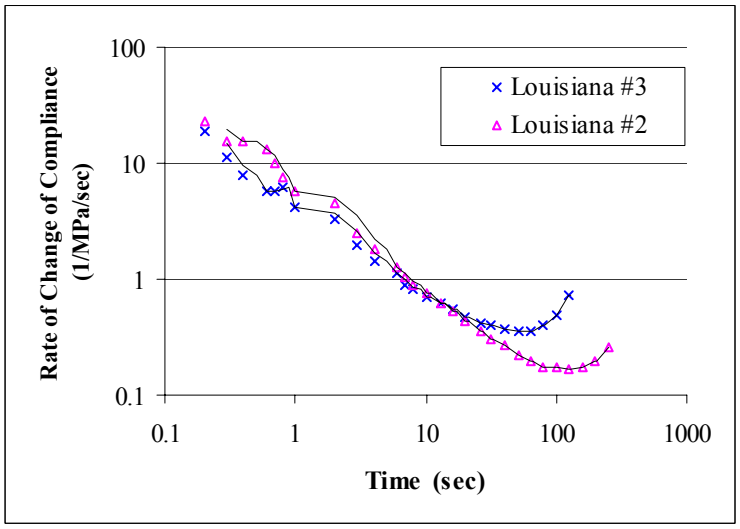

Figure E.4. Rate of Change of Creep Compliance versus Flow Time for LA.

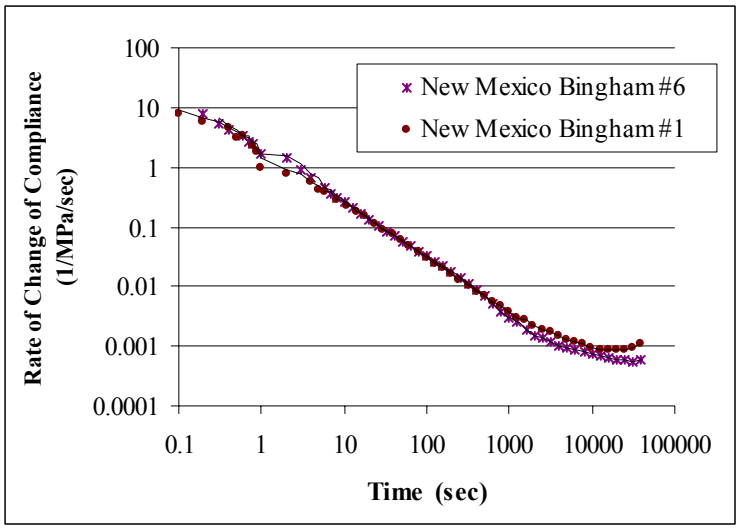

Figure E.5. Rate of Change of Creep Compliance versus Flow Time for NMBingham.

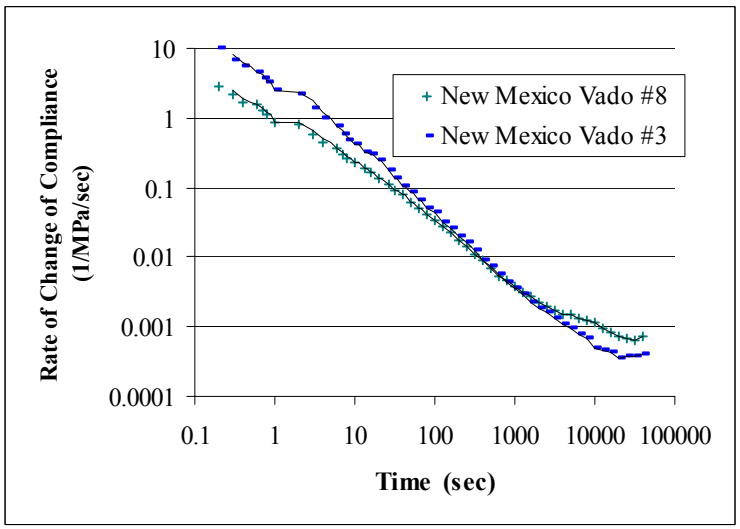

Figure E.6. Rate of Change of Creep Compliance versus Flow Time for NMVado.

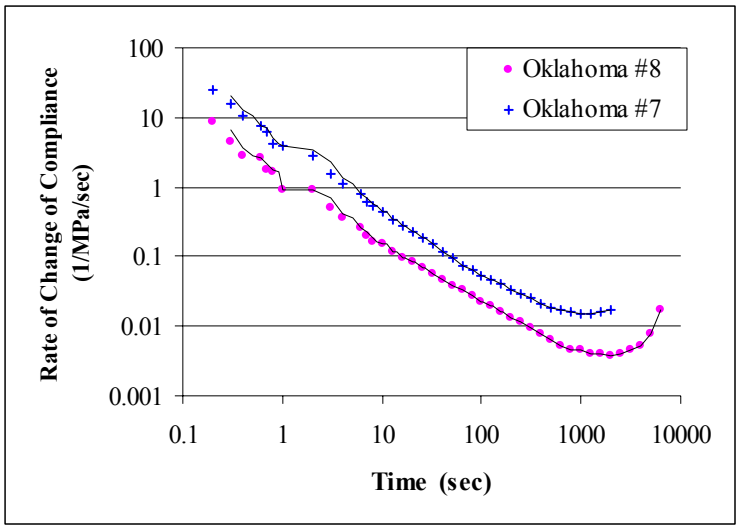

Figure E.7. Rate of Change of Creep Compliance versus Flow Time for OK.

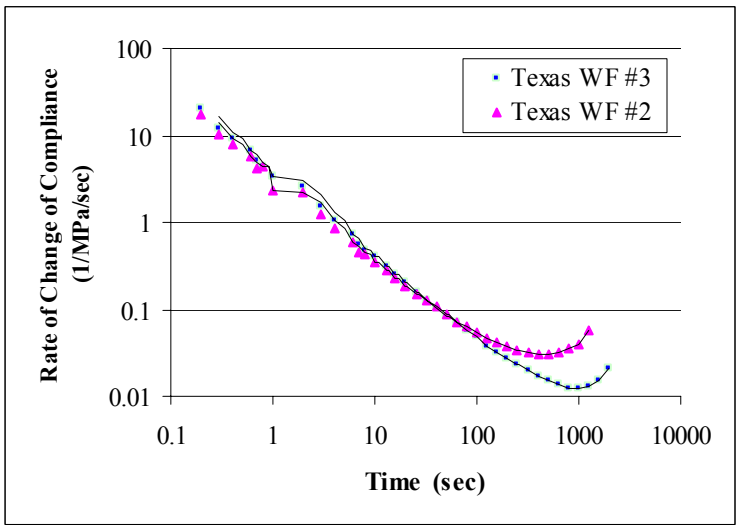

Figure E.8. Rate of Change of Creep Compliance versus Flow Time for TXWF.

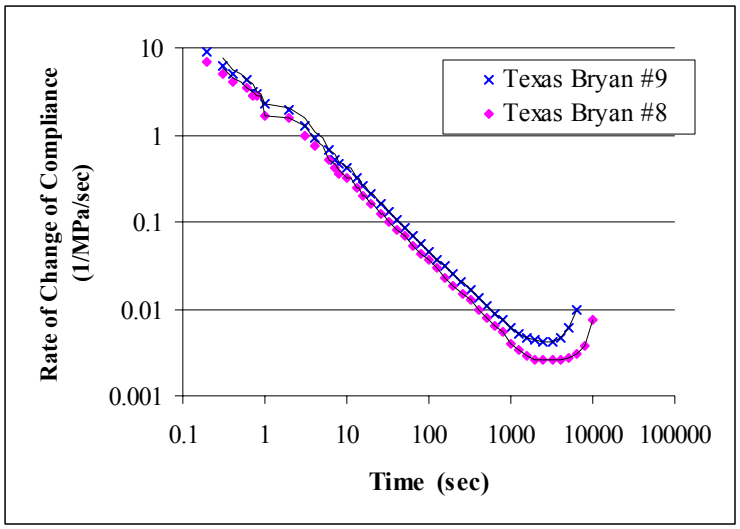

Figure E.9. Rate of Change of Creep Compliance versus Flow Time for TXBryan.

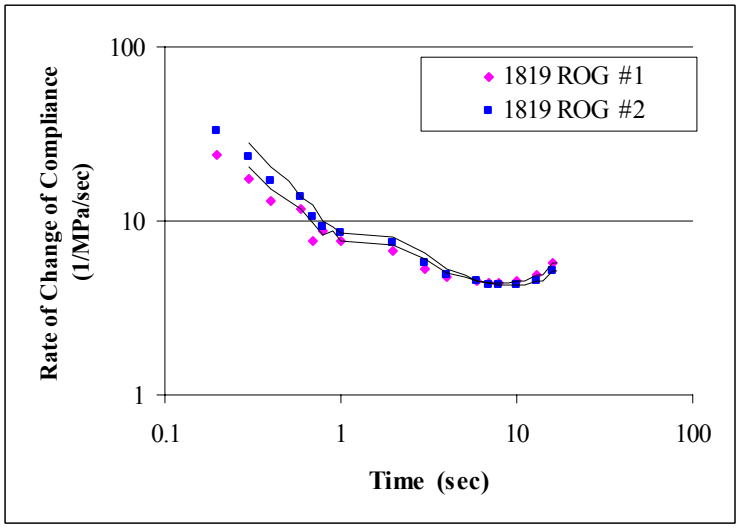

Figure E.10. Rate of Change of Creep Compliance versus Flow Time for ROG.

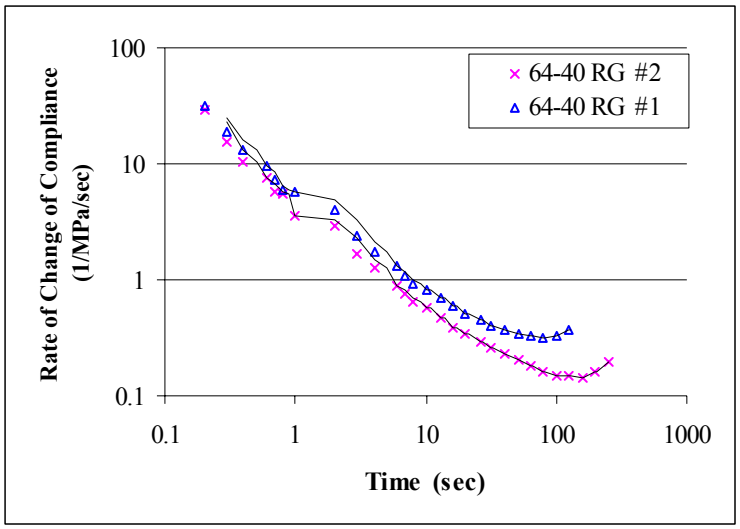

Figure E.11. Rate of Change of Creep Compliance versus Flow Time for 64-40RG.

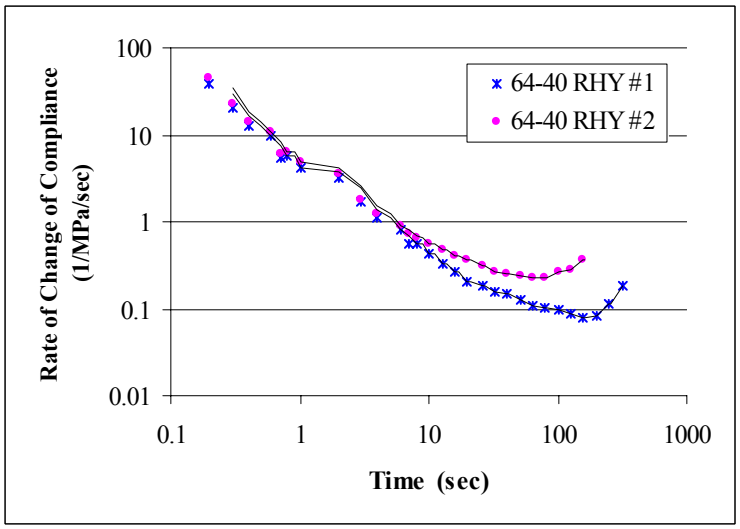

Figure E.12. Rate of Change of Creep Compliance versus Flow Time for 64-40RHY.

APPENDIX F

STATISTICAL GROUPINGS OF DIFFERENT TEST RESULTS

All groupings were generated using the Duncan method with a significance level of $\alpha = 0.05$.

Table F.1. Grouping of Data Based on APA Rut Depth.

	Sum of Squares	df	Mean Square	F	Sig.
Between Groups	1082.26028	11	98.387298	157.2428	6.29642E-19
Within Groups	14.3911672	23	0.6257029		
Total	1096.65144	34			

Mix Type	N	1	2	3	4	5	6
NMVado	2	2.0					
NMBingham	3	2.6	2.6				
TXWF	3		3.6	3.6			
64-40RHY	3		3.8	3.8			
OK	3			4.3			
AZ	3			4.4			
TXBryan	3			4.7			
64-40RG	3				6.4		
LA	3				7.2	7.2	
ARTL	3					8.2	
ARLR	3						18.7
ROG	3						19.0
Sig.		0.433	0.090	0.159	0.203	0.156	0.594

Uses Harmonic Mean Sample Size = 2.880.

The group sizes are unequal. The harmonic mean of the group sizes is used. Type I error levels are not guaranteed.

Table F.2. Grouping of Data Based on APA Creep Slope.

	Sum of Squares	df	Mean Square	F	Sig.
Between Groups	5.66186381	11	0.51471489	62.4379451	1.89701E-14
Within Groups	0.189603333	23	0.00824362		
Total	5.851467143	34			

Mix Type	N	1	2	3	4
NMVado	2	0.090			
TXBryan	3	0.149	0.149		
64-40RHY	3	0.197	0.197		
NMBingham	3	0.198	0.198		
AZ	3	0.206	0.206		
OK	3	0.265	0.265		
LA	3		0.285		
TXWF	3		0.299		
64-40RG	3			0.483	
ARTL	3			0.483	
ROG	3			0.646	
ARLR	3				1.637
Sig.		0.0507	0.0945	0.0514	1.0000

Uses Harmonic Mean Sample Size = 2.880.

The group sizes are unequal. The harmonic mean of the group sizes is used. Type I error levels are not guaranteed.

Tabel F.3. Grouping of Data Based on |E*| at 10 Hz, 54.4°C.

	Sum of Squares	df	Mean Square	F	Sig.
Between Groups	5257501.33	11.00	477954.67	20.11	4.781E-06
Within Groups	285154.00	12.00	23762.83		
Total	5542655.33	23.00			

Mix Type	N	1	2	3	4	5	6
64-40RG	2.00	221.00					
ARLR	2.00	435.00	435.00				
64-40RHY	2.00	456.00	456.00				
OK	2.00	517.50	517.50	517.50			
ROG	2.00		688.50	688.50			
LA	2.00		753.00	753.00	753.00		
AZ	2.00			869.50	869.50	869.50	
TXWF	2.00				1077.50	1077.50	
ARTL	2.00				1085.50	1085.50	
TXBryan	2.00					1228.50	
NMBingham	2.00						1644.50
NMVado	2.00						1801.50
Sig.		0.10	0.08	0.06	0.07	0.05	0.33

Table F.4. Grouping of Data Based on |E*| at 1 Hz, 54.4°C.

	Sum of Squares	df	Mean Square	F	Sig.
Between Groups	1417525.578	11	128865.962	29.2678851	5.906E-07
Within Groups	52835.78	12	4402.98167		
Total	1470361.358	23			

Mix Type	N	1	2	3	4	5
ARLR	2	141.00				
64-40RG	2	148.50				
OK	2	204.25	204.25			
LA	2	255.35	255.35			
64-40RHY	2	264.50	264.50			
ROG	2	277.00	277.00			
AZ	2		340.00	340.00		
ARTL	2		358.00	358.00		
TXWF	2			487.05	487.05	
TXBryan	2				515.40	
NMBingham	2					831.40
NMVado	2					923.05
Sig.		0.09	0.06	0.06	0.68	0.19

Table F.5. Grouping of Data Based on |E*| /sin ϕ at 10 Hz, 54.4°C.

	Sum of Squares	df	Mean Square	F	Sig.
Between Groups	41125281.27	11	3738661.93	22.2353258	2.749E-06
Within Groups	2017687.689	12	168140.641		
Total	43142968.96	23			

Mix Type	N	1	2	3	4
ARLR	2	799.27			
64-40RG	2	800.17			
OK	2	997.70			
LA	2	1384.34	1384.34		
64-40RHY	2	1461.70	1461.70		
ROG	2	1476.12	1476.12		
AZ	2	1794.84	1794.84	1794.84	
ARTL	2		2114.17	2114.17	
TXBryan	2			2468.92	
TXWF	2			2682.20	
NMBingham	2				4438.63
NMVado	2				5036.86
Sig.		0.05	0.13	0.07	0.17

Table F.6. Grouping of Data Based on |E*| /sin ϕ at 1 Hz, 54.4°C.

	Sum of Squares	df	Mean Square	F	Sig.
Between Groups	5149234.729	11	468112.248	18.336449	7.9317E-06
Within Groups	306348.682	12	25529.0568		
Total	5455583.411	23			

Mix Type	N	1	2	3	4
ARLR	2	292.83			
OK	2	418.75	418.75		
LA	2	463.99	463.99		
ROG	2	516.86	516.86		
64-40RG	2	569.04	569.04		
AZ	2	635.59	635.59	635.59	
ARTL	2	644.81	644.81	644.81	
64-40RHY	2		736.48	736.48	
TXWF	2			978.47	
TXBryan	2			989.77	
NMBingham	2				1661.18
NMVado	2				1830.82
Sig.		0.07	0.10	0.07	0.31

Table F.7. Grouping of Data Based on |G*| at 10 Hz, 40°C.

	Sum of Squares	df	Mean Square	F	Sig.
Between Groups	19306049938	11	1755095449	12.6618096	5.7347E-05
Within Groups	1663359829	12	138613319		
Total	20969409767	23			

Mix Type	N	1	2	3	4	5
64-40RHY	2	11728.50				
64-40RG	2	25489.00	25489.00			
ARLR	2	31849.00	31849.00			
AZ	2	36320.50	36320.50	36320.50		
ARTL	2		43247.00	43247.00	43247.00	
LA	2		43866.00	43866.00	43866.00	
ROG	2		44546.50	44546.50	44546.50	
TXWF	2		47999.50	47999.50	47999.50	
OK	2		53047.50	53047.50	53047.50	
NMBingham	2			63452.00	63452.00	
TXBryan	2				66530.00	
NMVado	2					130564.50
Sig.		0.08	0.06	0.06	0.10	1.00

Table F.8. Grouping of Data Based on |G*| at 1 Hz, 40°C.

	Sum of Squares	df	Mean Square	F	Sig.
Between Groups	7362632854	11	669330259	24.3055768	1.6758E-06
Within Groups	330457622	12	27538135.2		
Total	7693090476	23			

Mix Type	N	1	2	3	4
64-40RHY	2	7686.00			
ARLR	2	9220.50			
64-40RG	2	10519.00			
AZ	2	13167.50	13167.50		
LA	2	14724.50	14724.50		
ARTL	2	14741.00	14741.00		
ROG	2	17542.00	17542.00		
TXWF	2	18483.50	18483.50		
OK	2		23350.00	23350.00	
TXBryan	2		23518.00	23518.00	
NMBingham	2			34014.00	
NMVado	2				75078.00
Sig.		0.09	0.10	0.08	1.00

Table F.9. Grouping of Data Based on |G*| /sin δ at 10 Hz, 40°C.

	Sum of Squares	df	Mean Square	F	Sig.
Between Groups	1.13453E+11	11	1.0314E+10	26.7576588	9.7857E-07
Within Groups	4625485897	12	385457158		
Total	1.18079E+11	23			

Mix Type	N	1	2	3	4	5
64-40RHY	2	19866.65				
64-40RG	2	34122.36	34122.36			
ARLR	2	36696.78	36696.78			
AZ	2	45101.71	45101.71	45101.71		
ARTL	2	54266.38	54266.38	54266.38		
LA	2	54322.67	54322.67	54322.67		
ROG	2	63149.28	63149.28	63149.28	63149.28	
TXWF	2		68612.36	68612.36	68612.36	
OK	2		79482.66	79482.66	79482.66	
TXBryan	2			87307.23	87307.23	
NMBingham	2				102166.5	
NMVado	2					293705.53
Sig.		0.07	0.06	0.08	0.09	1.00

Table F.10. Grouping of Data Based on |G*| /sin δ at 1 Hz, 40°C.

	Sum of Squares	df	Mean Square	F	Sig.
Between Groups	38555077245	11	3505007022	25.4303765	1.3015E-06
Within Groups	1653930850	12	137827571		
Total	40209008095	23			

Mix Type	N	1	2	3
ARLR	2	11028.05		
64-40RG	2	15789.73		
AZ	2	16421.16		
64-40RHY	2	17958.03		
ARTL	2	18236.02		
LA	2	20062.19		
ROG	2	25508.06		
TXWF	2	26654.79		
TXBryan	2	33293.30		
OK	2	39865.09	39865.09	
NMBingham	2		62170.52	
NMVado	2			162842.36
Sig.		0.05	0.08	1.00

Table F.11. Grouping of Data Based on Flow Number.

	Sum of Squares	df	Mean Square	F	Sig.
Between Groups	668296516.5	11	60754228.77	26.1882056	1.1041E-06
Within Groups	27838896.5	12	2319908.042		
Total	696135413	23			

Mix Type	N	1	2	3
ARLR	2	169		
64-40RG	2	197		
ROG	2	202		
ARTL	2	218		
LA	2	428		
AZ	2	534		
64-40RHY	2	1617		
TXWF	2	3159	3159	
OK	2	3559	3559	
TXBryan	2		5807	
NMBingham	2			15000.5
NMVado	2			15001
Sig.		0.07	0.12	1.00

Table F.12. Grouping of Data Based on Flow Number Slope.

	Sum of Squares	df	Mean Square	F	Sig.
Between Groups	0.235628605	11	0.021420782	10.7679165	0.00013238
Within Groups	0.023871785	12	0.001989315		
Total	0.25950039	23			

Mix Type	N	1	2	3	4	5	6
64-40RHY	2	0.218					
NMBingham	2	0.293	0.293				
OK	2	0.312	0.312	0.312			
NMVado	2	0.315	0.315	0.315			
TXBryan	2		0.356	0.356	0.356		
64-40RG	2		0.373	0.373	0.373		
TXWF	2			0.401	0.401		
LA	2				0.433		
ARTL	2				0.434		
AZ	2				0.445	0.445	
ARLR	2					0.542	0.542
ROG	2						0.579
Sig.		0.068	0.128	0.094	0.094	0.050	0.426

Table F.13. Grouping of Data Based on Flow Time.

	Sum of Squares	df	Mean Square	F	Sig.
Between Groups	2344140854	11	213103714	50.2505531	2.6731E-08
Within Groups	50889879	12	4240823.25		
Total	2395030733	23			

Mix Type	N	1	2
ROG	2	8	
ARLR	2	22	
ARTL	2	47.5	
LA	2	90.5	
64-40RG	2	110	
64-40RHY	2	113	
AZ	2	297.5	
TXWF	2	743	
OK	2	1536.5	
TXBryan	2	2966	
NMBingham	2		25697.5
NMVado	2		28263.5
Sig.		0.22	0.24

Table F.14. Grouping of Data Based on Flow Time Intercept.

	Sum of Squares	df	Mean Square	F	Sig.
Between Groups	0.000114689	11	1.04263E-05	1.04422674	0.46795633
Within Groups	0.000119816	12	9.9847E-06		
Total	0.000234506	23			

Mix Type	N	1
OK	2	0.007465
TXBryan	2	0.00765
NMBingham	2	0.00785
NMVado	2	0.00875
TXWF	2	0.0092
64-40RG	2	0.01095
LA	2	0.0111
ROG	2	0.01175
AZ	2	0.01185
ARLR	2	0.01295
64-40RHY	2	0.01345
ARTL	2	0.0136
Sig.		0.1091309

Table F.15. Grouping of Data Based on Flow Time Slope.

	Sum of Squares	df	Mean Square	F	Sig.
Between Groups	0.356144315	11	0.032376756	17.4244425	1.0467E-05
Within Groups	0.022297475	12	0.001858123		
Total	0.37844179	23			

Mix Type	N	1	2	3	4	5	6
NMBingham	2	0.152					
NMVado	2	0.159	0.159				
TXBryan	2	0.185	0.185				
TXWF	2	0.203	0.203	0.203			
OK	2	0.207	0.207	0.207			
64-40RHY	2	0.211	0.211	0.211			
AZ	2	0.232	0.232	0.232	0.232		
ARTL	2		0.263	0.263	0.263	0.263	
64-40RG	2			0.303	0.303	0.303	
LA	2				0.314	0.314	
ARLR	2					0.351	
ROG	2						0.619
Sig.		0.123	0.052	0.056	0.102	0.082	1.000

APPENDIX G

CORRELATIONS OF DIFFERENT TEST PARAMETERS WITH APA RUT DEPTH

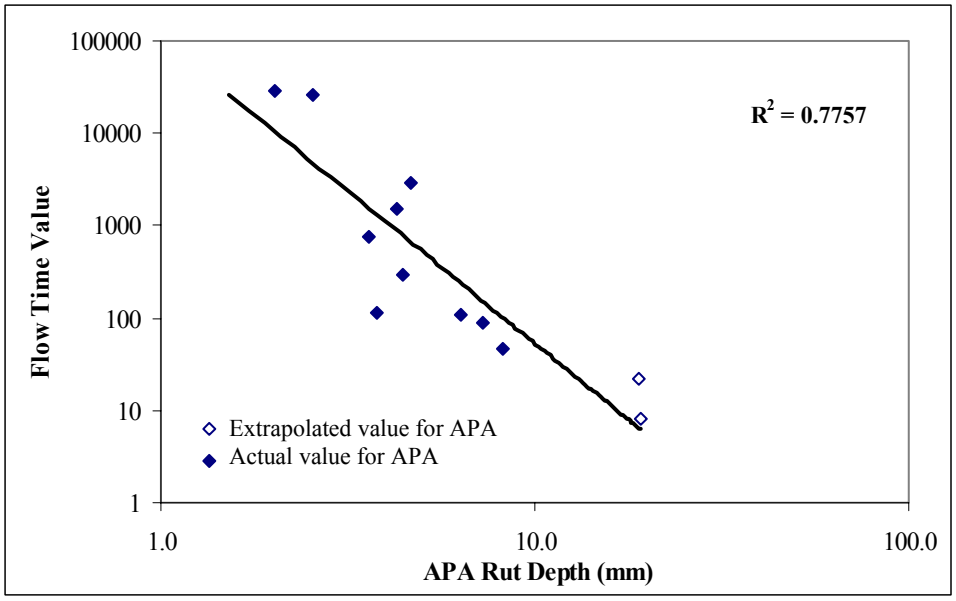

Figure G.1. APA Rut Depth versus Flow Time Value.

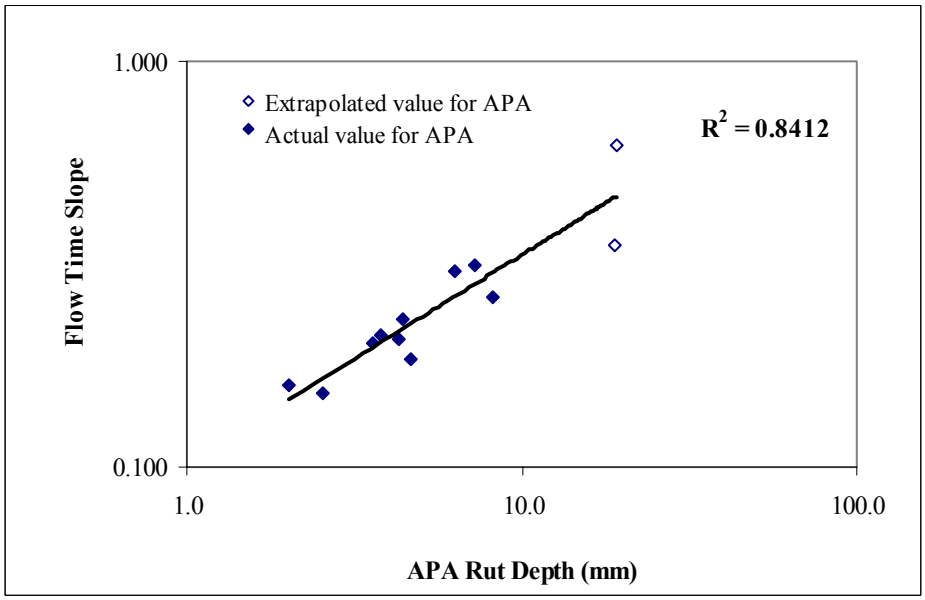

Figure G.2. APA Rut Depth versus Flow Time Slope.

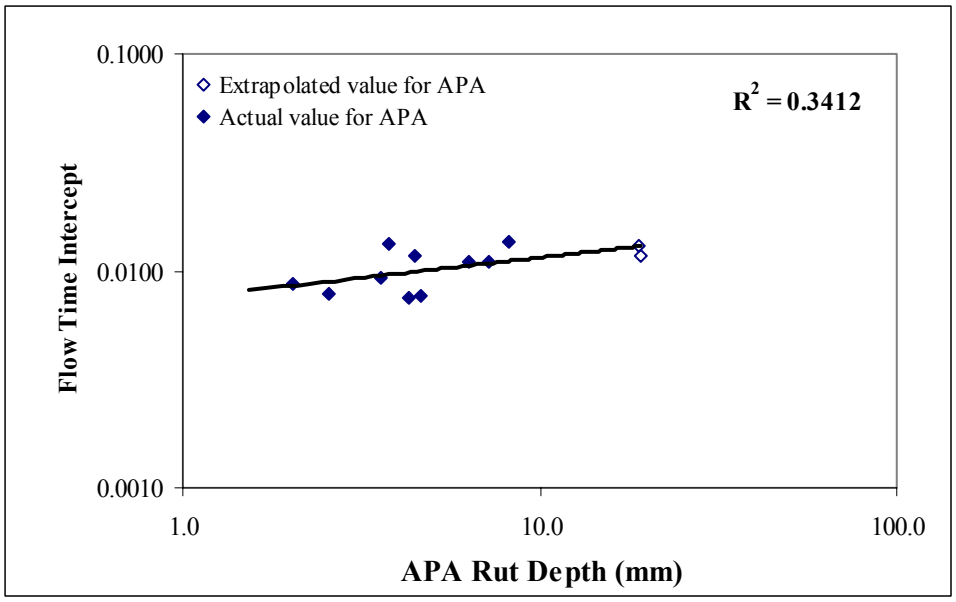

Figure G.3. APA Rut Depth versus Flow Time Intercept.

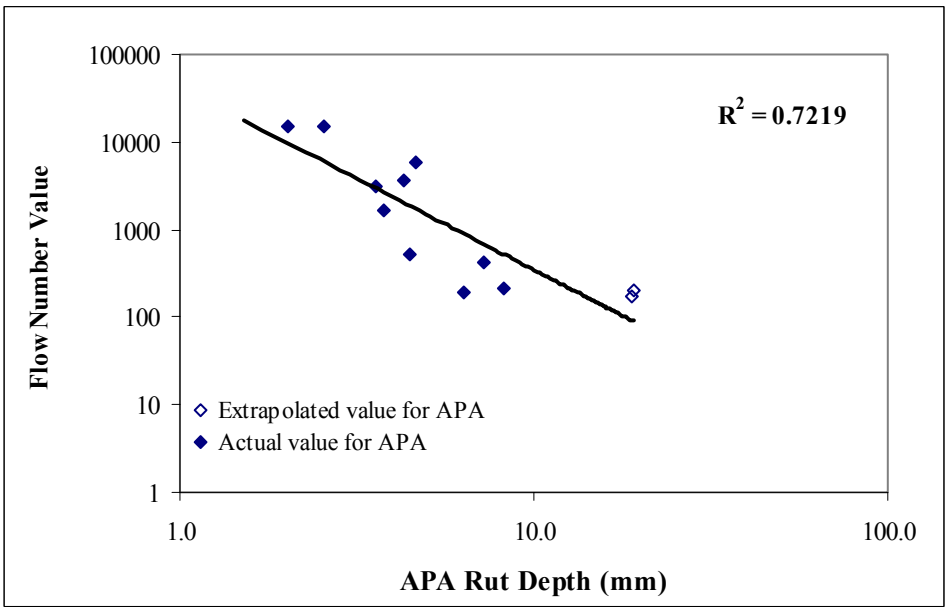

Figure G.4. APA Rut Depth versus Flow Number Value.

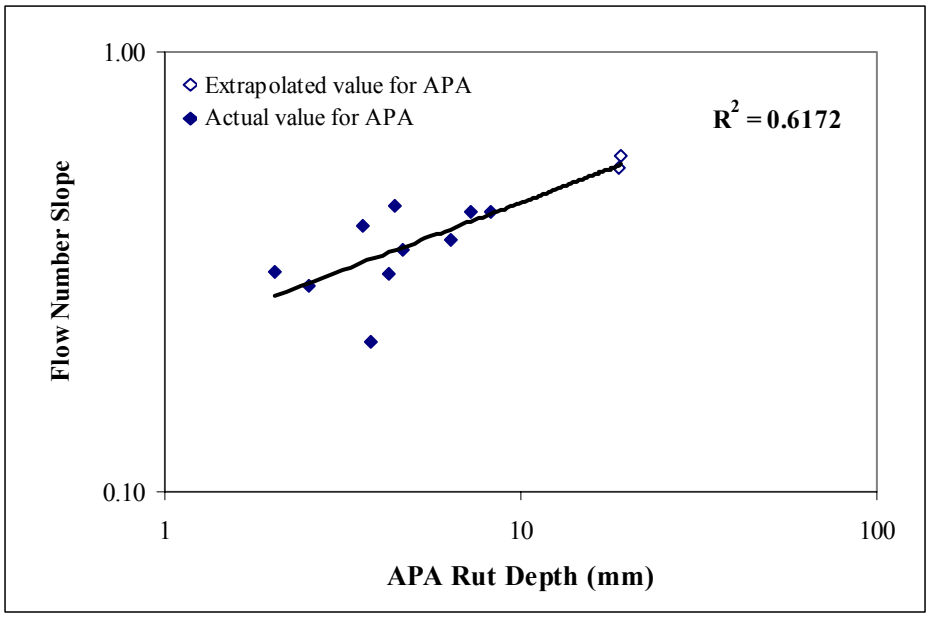

Figure G.5. APA Rut Depth versus Flow Number Slope.

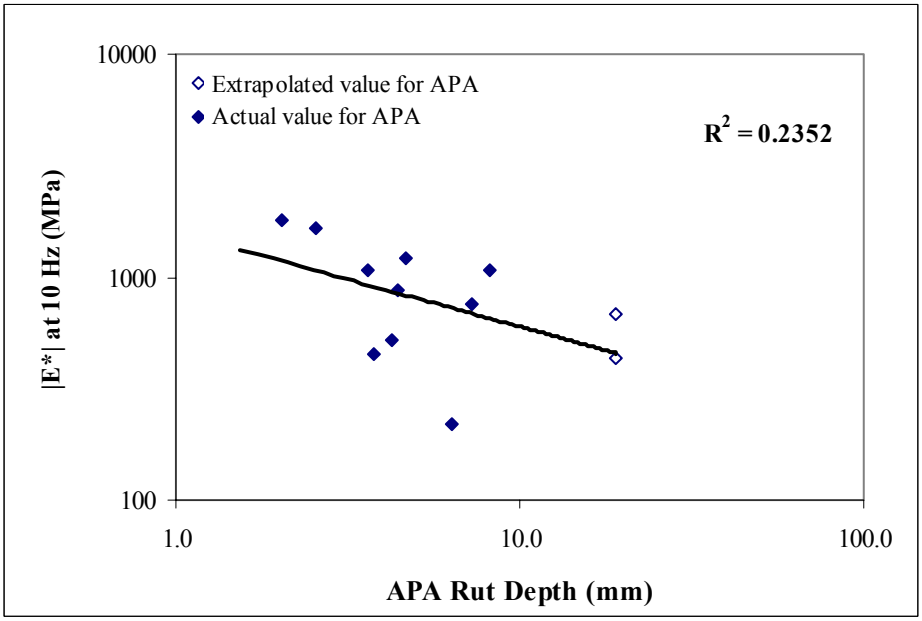

Figure G.6. APA Rut Depth versus |E*| at 10 Hz.

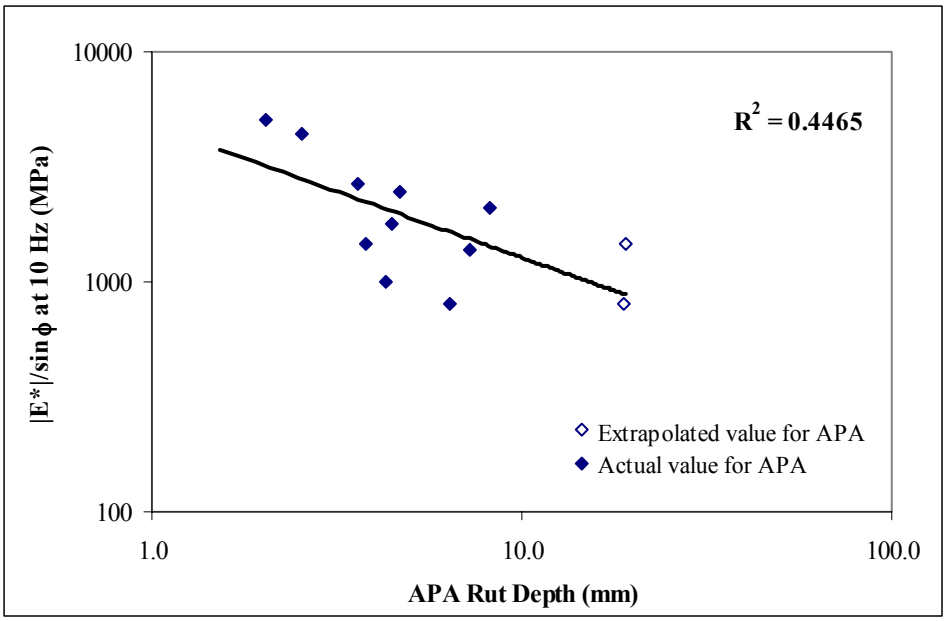

Figure G.7. APA Rut Depth versus |E*|/sin ϕ at 10 Hz.

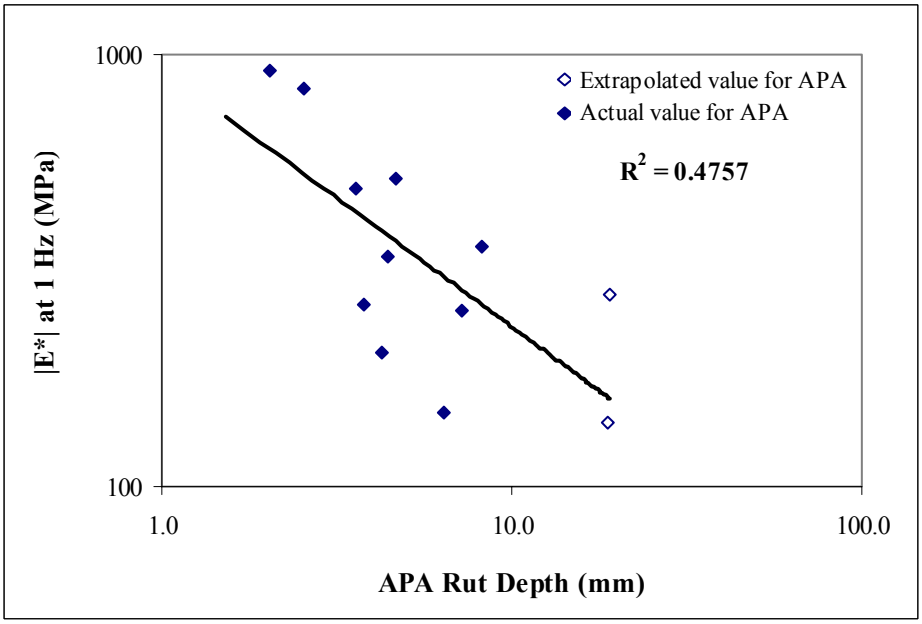

Figure G.8. APA Rut Depth versus |E*| at 1 Hz.

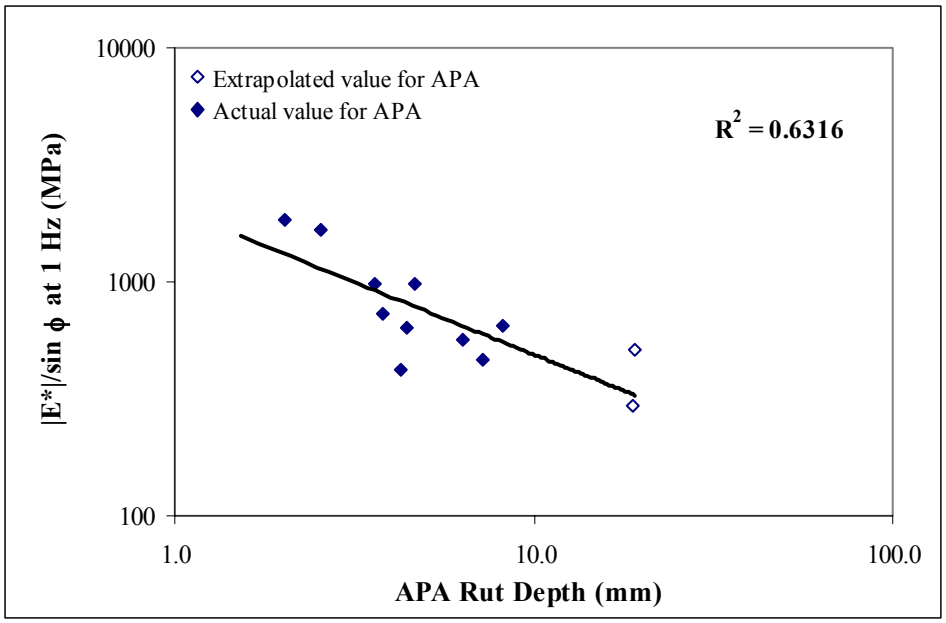

Figure G.9. APA Rut Depth versus |E*|/sin ϕ at 1 Hz.

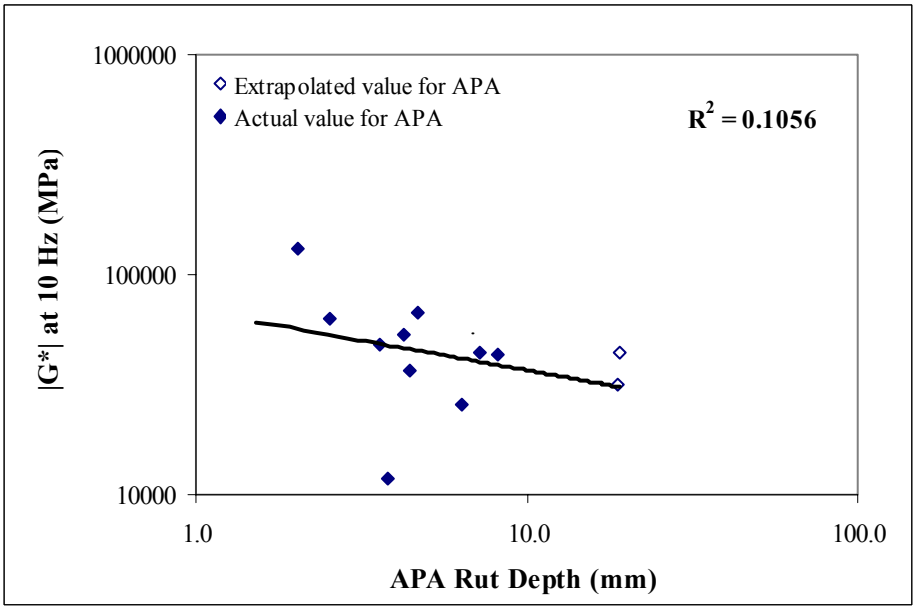

Figure G.10. APA Rut Depth versus |G*| at 10 Hz.

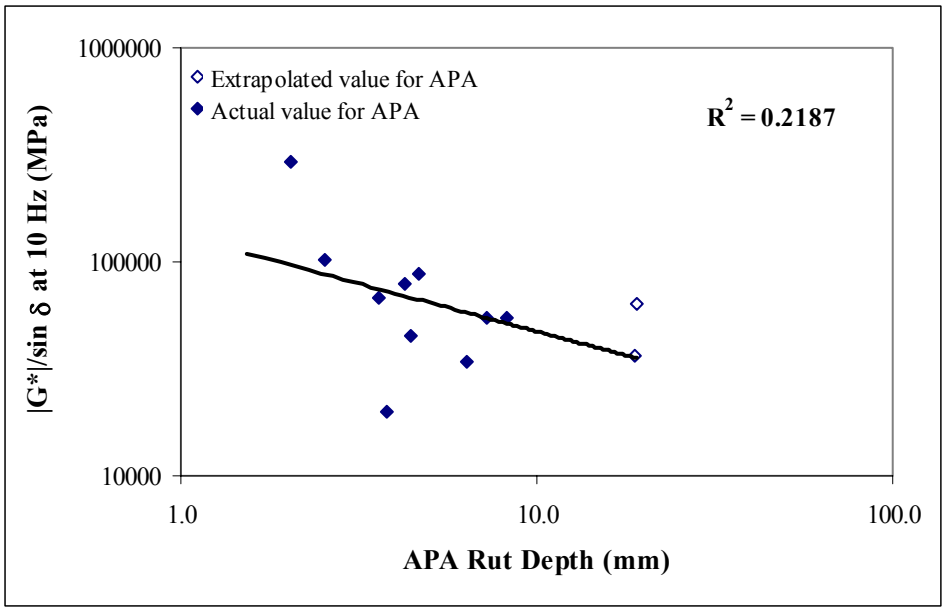

Figure G.11. APA Rut Depth versus |G*|/sin δ at 10 Hz.

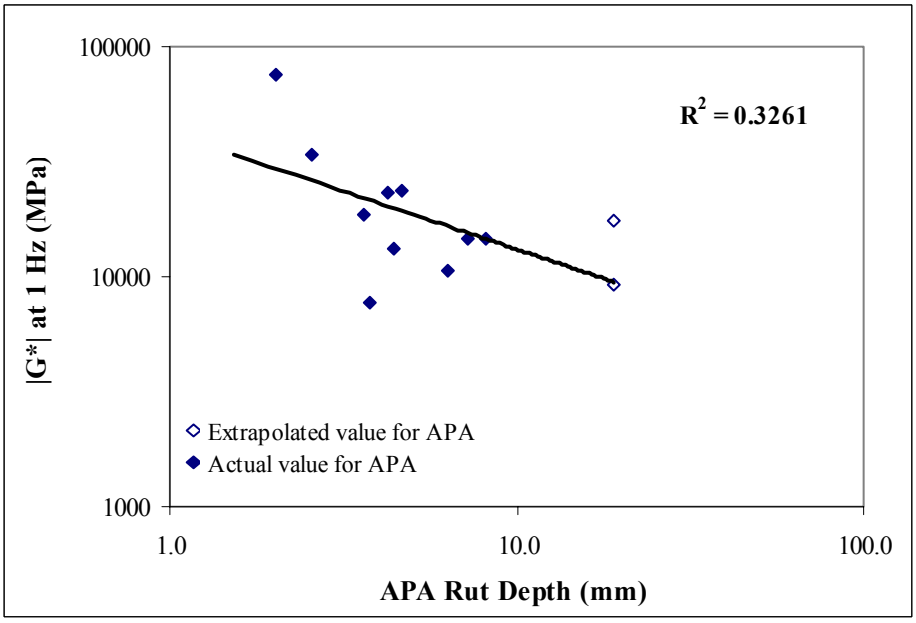

Figure G.12. APA Rut Depth versus |G*| at 1 Hz.

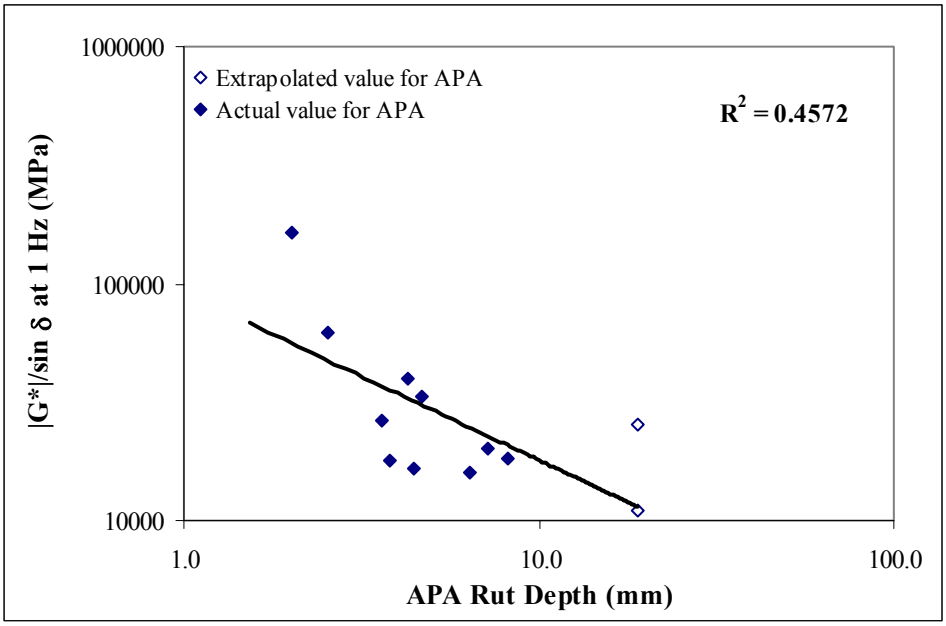

Figure G.13. APA Rut Depth versus |G*|/sin δ at 1 Hz.

APPENDIX H

CORRELATIONS OF DIFFERENT TEST PARAMETERS WITH APA CREEP SLOPE

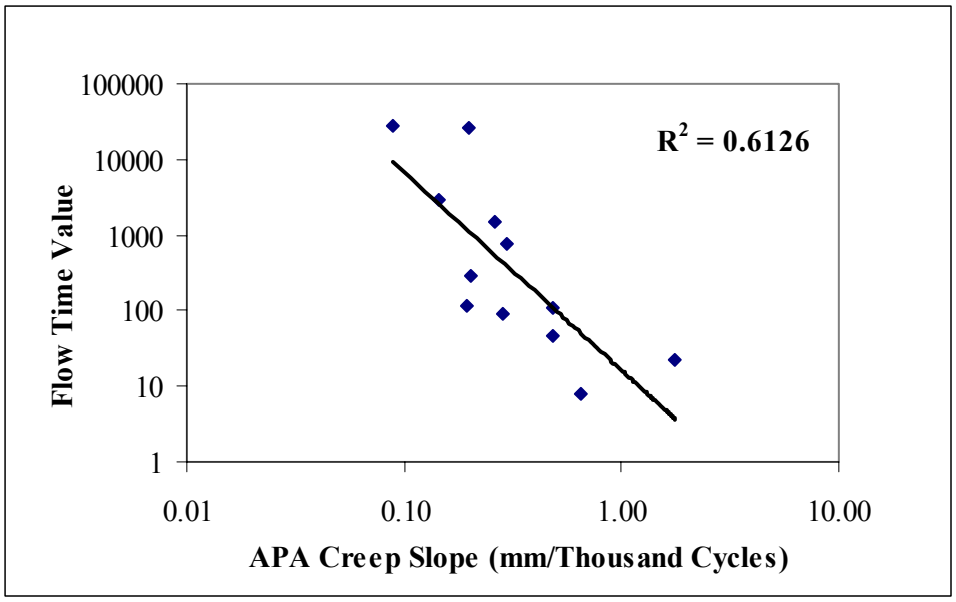

Figure H.1. APA Creep Slope versus Flow Time Value.

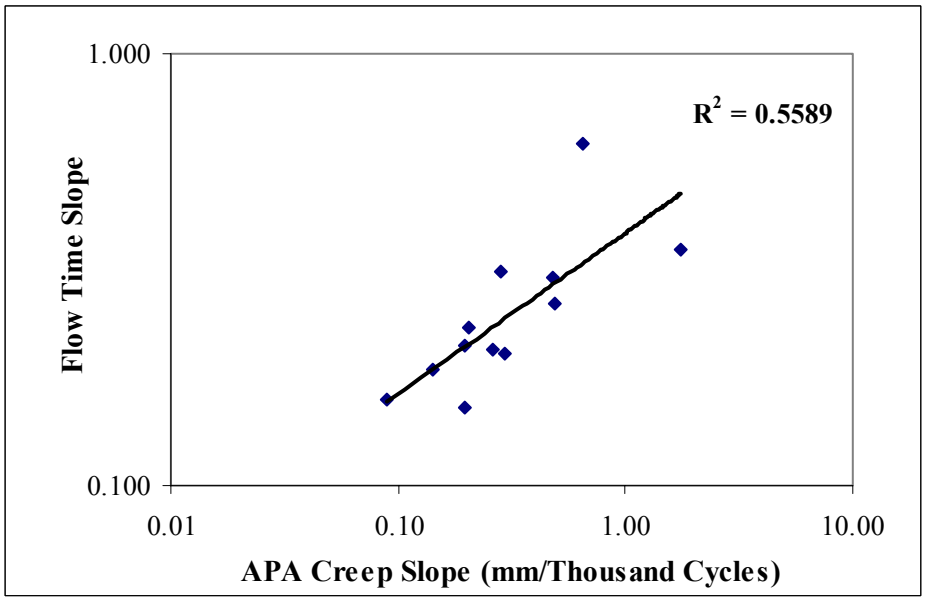

Figure H.2. APA Creep Slope versus Flow Time Slope.

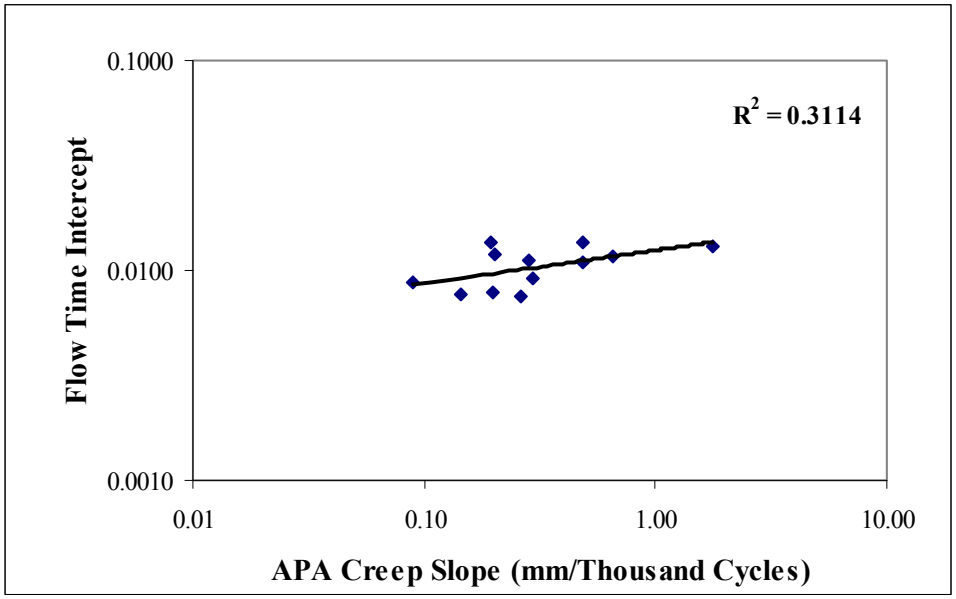

Figure H.3. APA Creep Slope versus Flow Time Intercept.

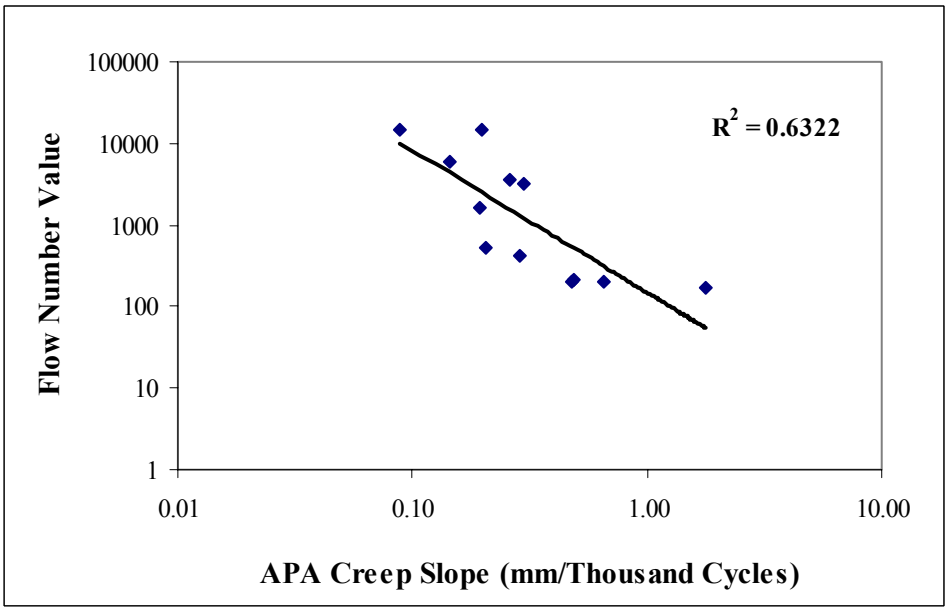

Figure H.4. APA Creep Slope versus Flow Number Value.

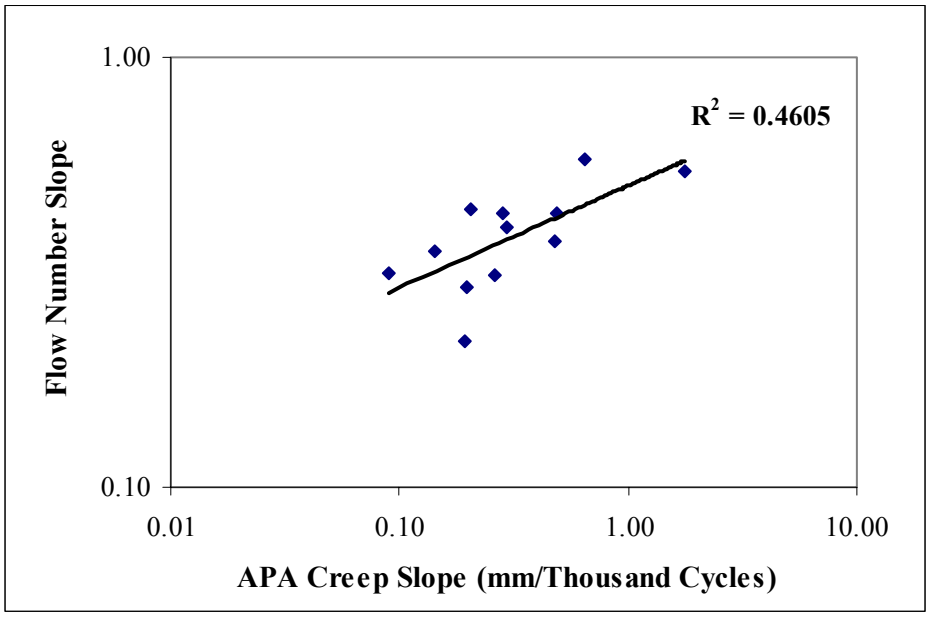

Figure H.5. APA Creep Slope versus Flow Number Slope.

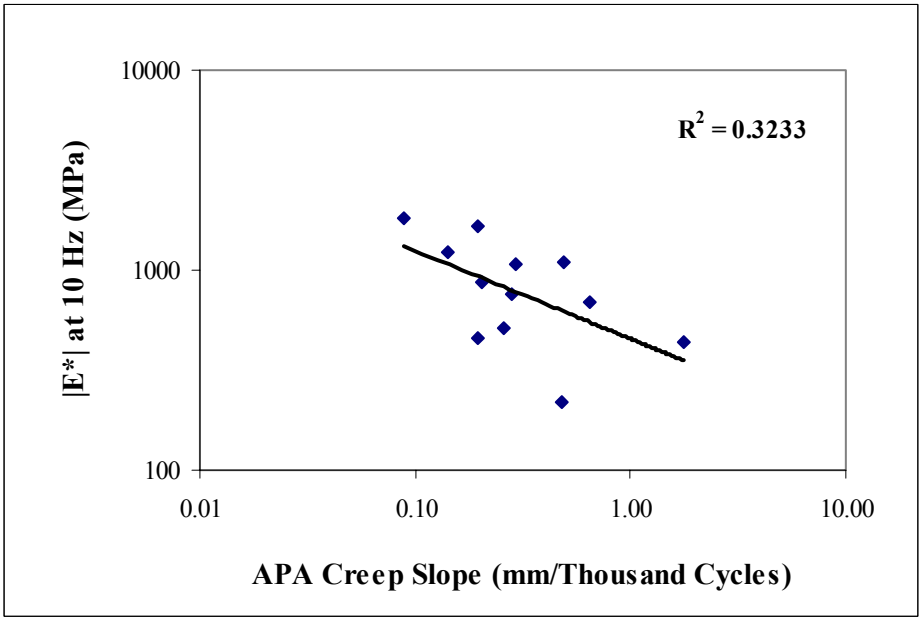

Figure H.6. APA Creep Slope versus |E*| at 10 Hz.

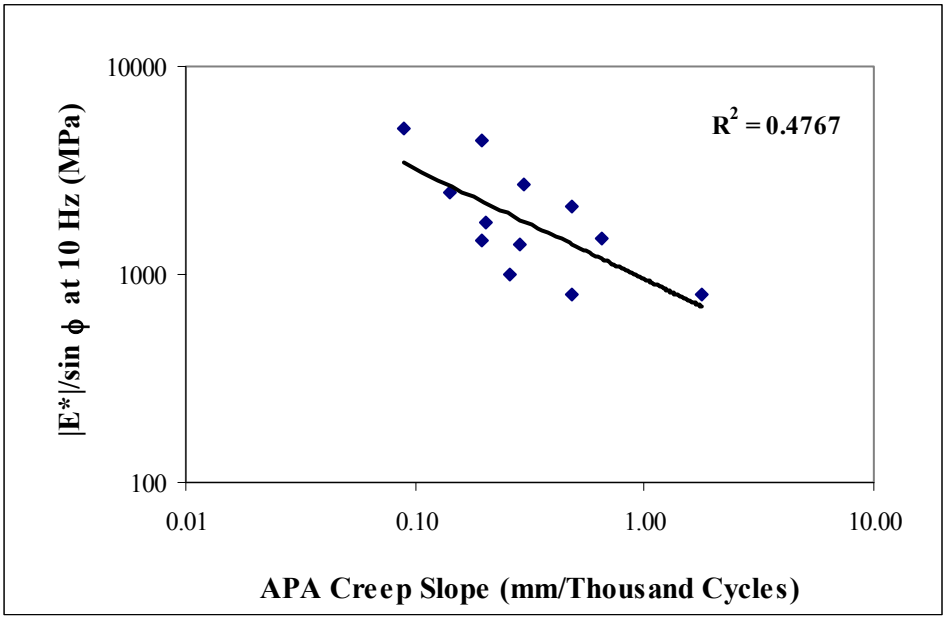

Figure H.7. APA Creep Slope versus |E*|/sin ϕ at 10 Hz.

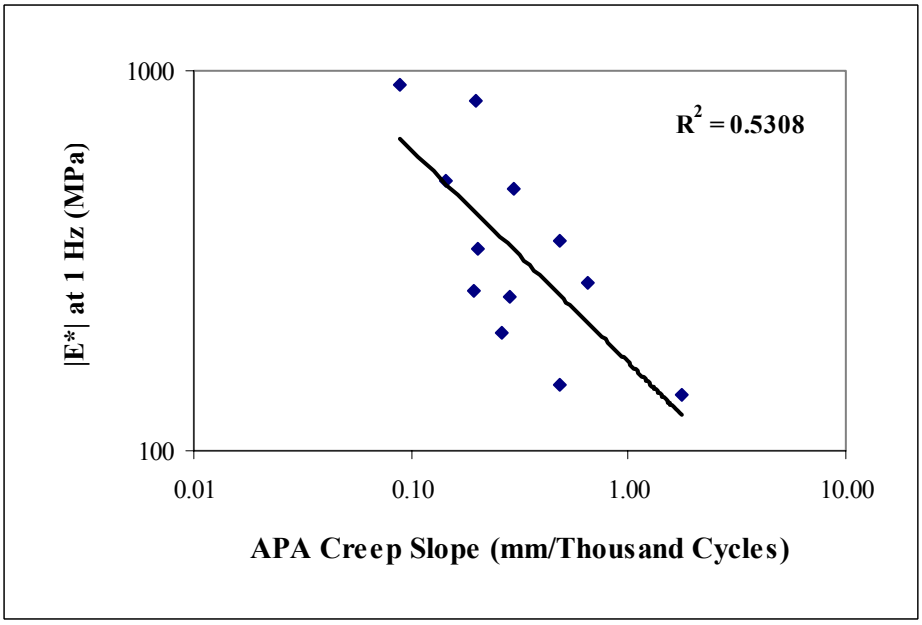

Figure H.8. APA Creep Slope versus |E*| at 1 Hz.

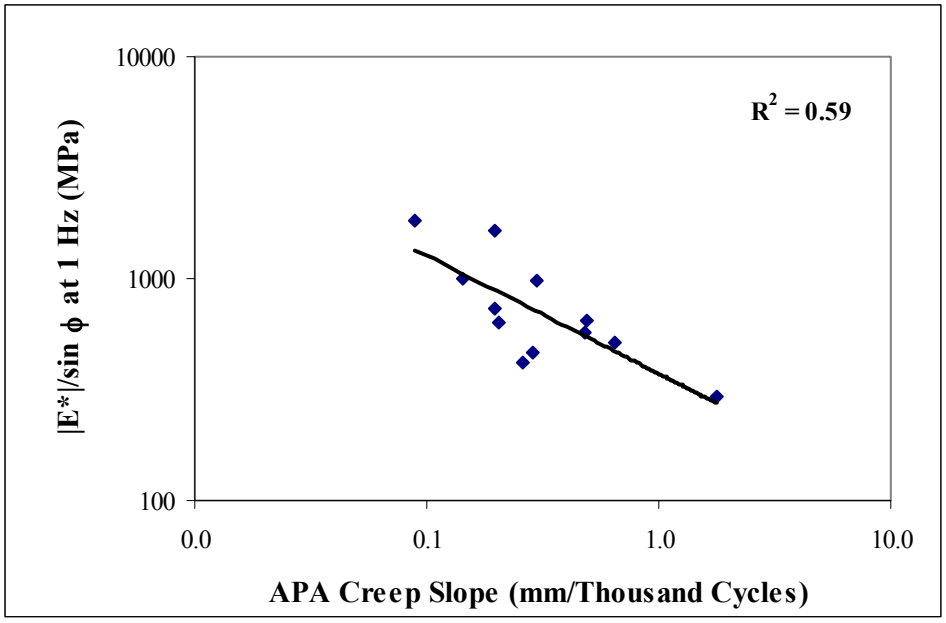

Figure H.9. APA Creep Slope versus |E*|/sin ϕ at 1 Hz.

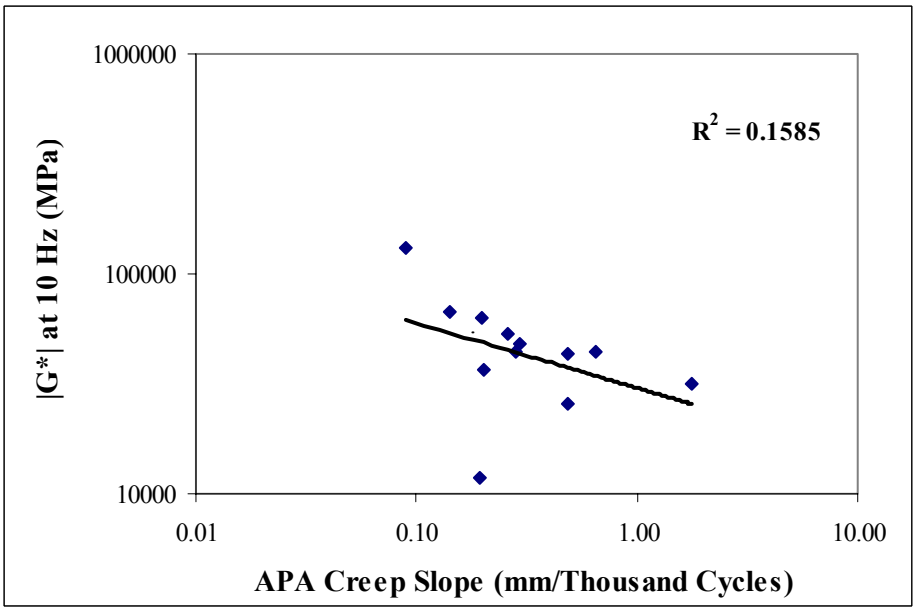

Figure H.10. APA Creep Slope versus |G*| at 10 Hz.

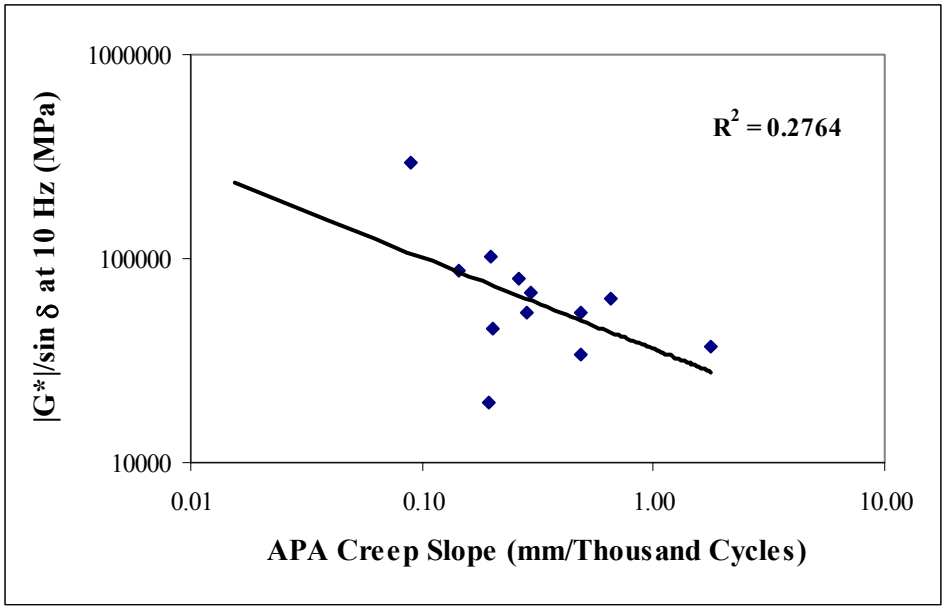

Figure H.11. APA Creep Slope versus |G*|/sin δ at 10 Hz.

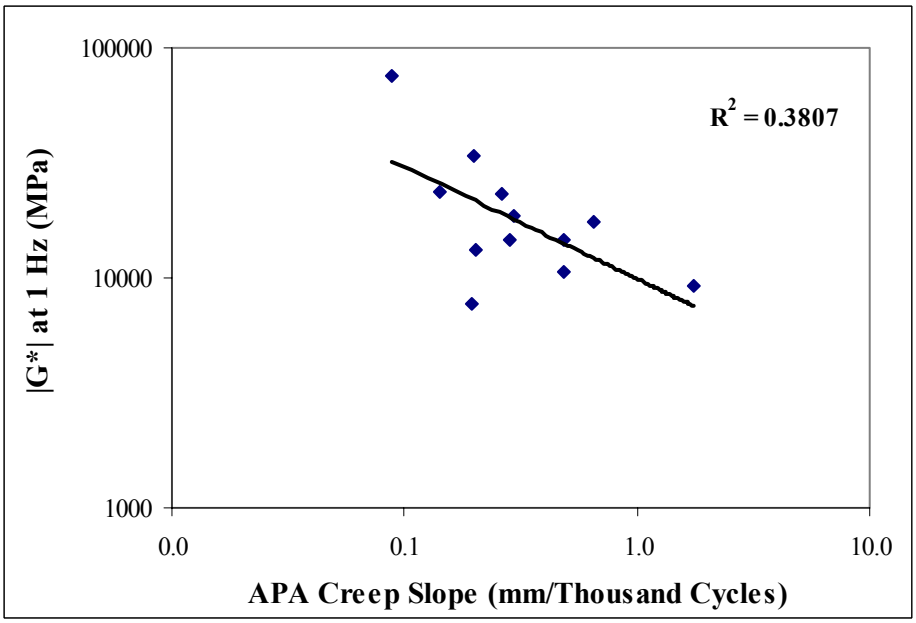

Figure H.12. APA Creep Slope versus |G*| at 1 Hz.

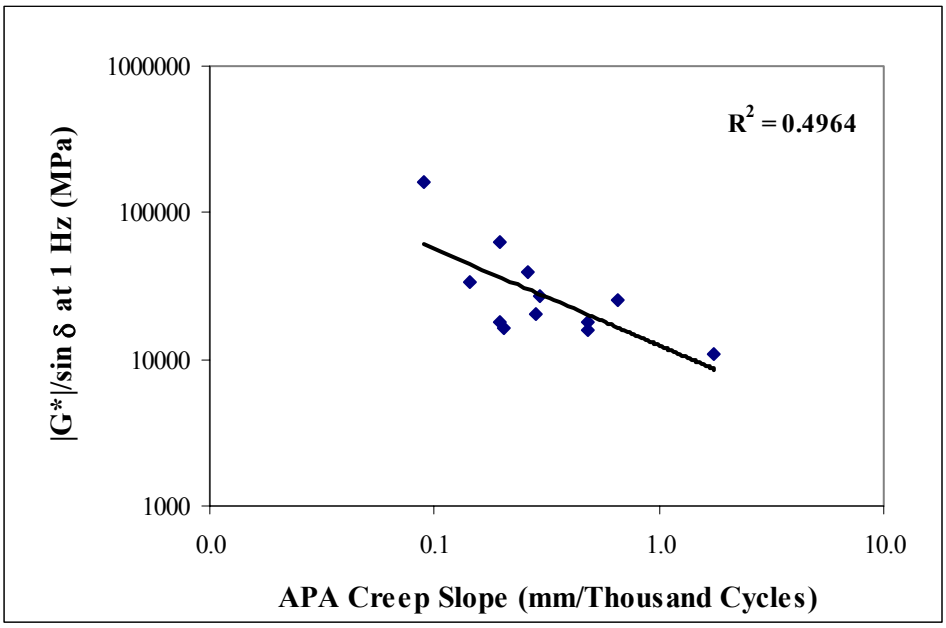

Figure H.13. APA Creep Slope versus |G*|/sin δ at 1 Hz.

APPENDIX I

CORRELATIONS OF DIFFERENT TEST PARAMETERS WITH HAMBURG WHEEL TRACKING DEVICE RUT DEPTH

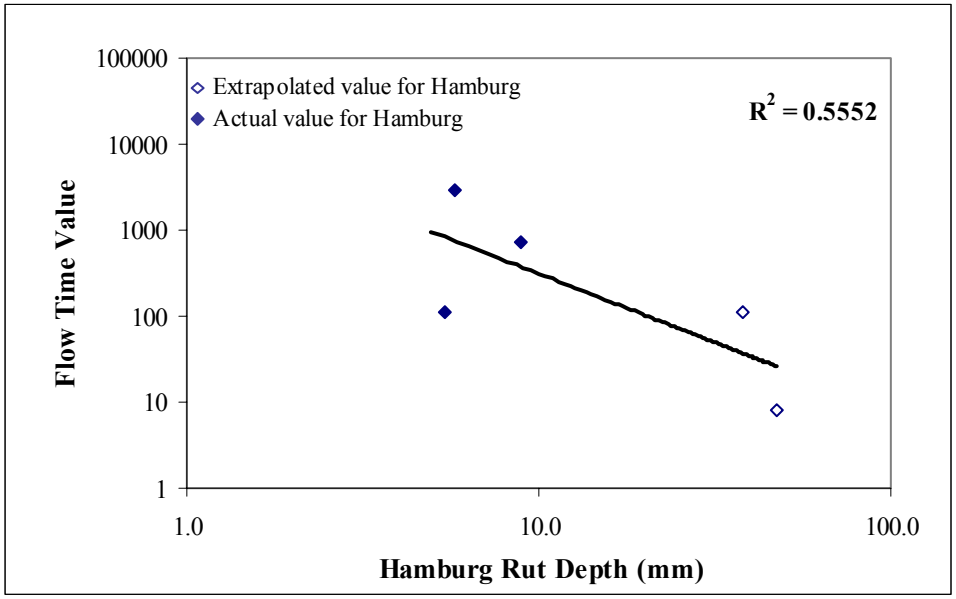

Figure I.1. HWTD Rut Depth versus Flow Time Value.

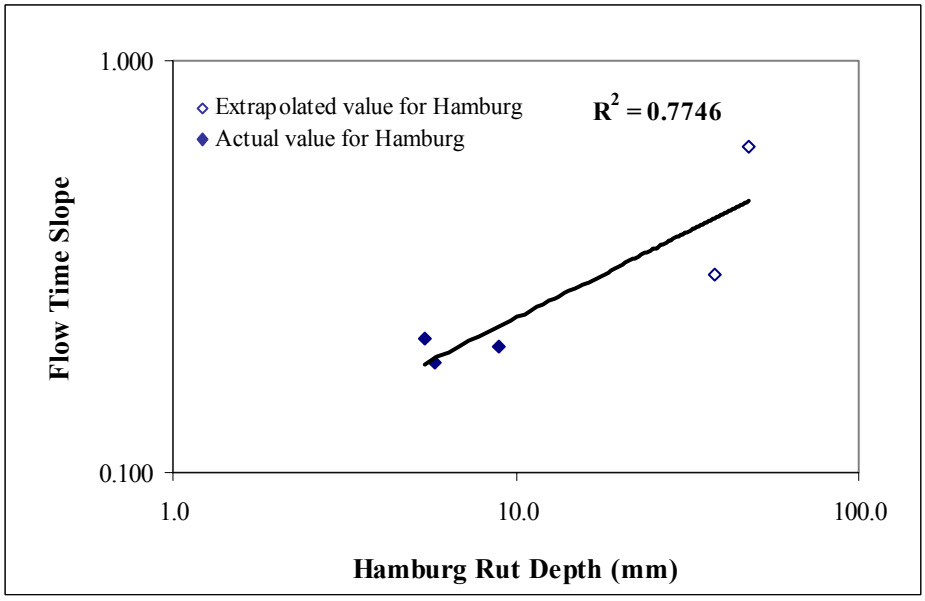

Figure I.2. HWTD Rut Depth versus Flow Time Slope.

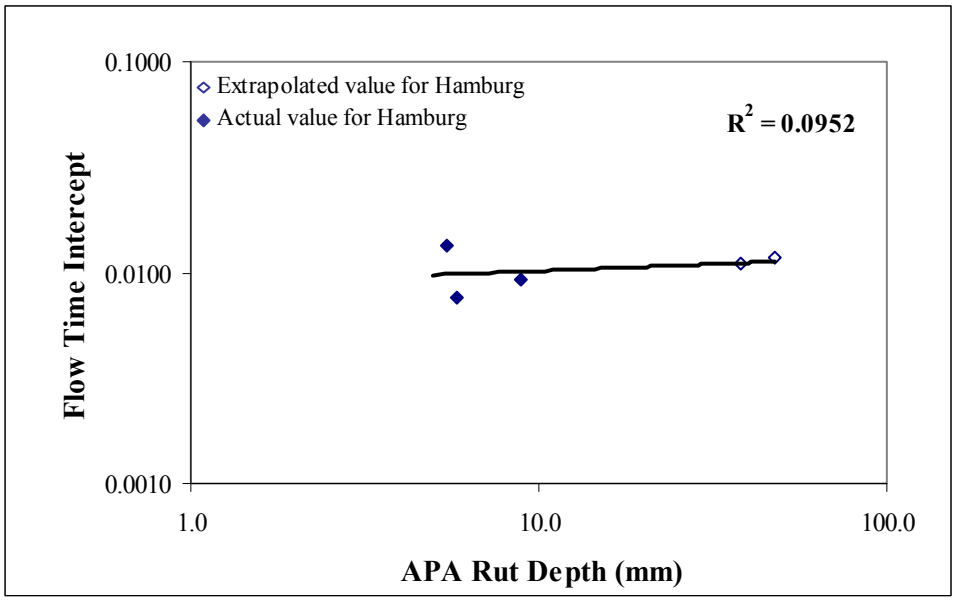

Figure I.3. HWTD Rut Depth versus Flow Time Intercept.

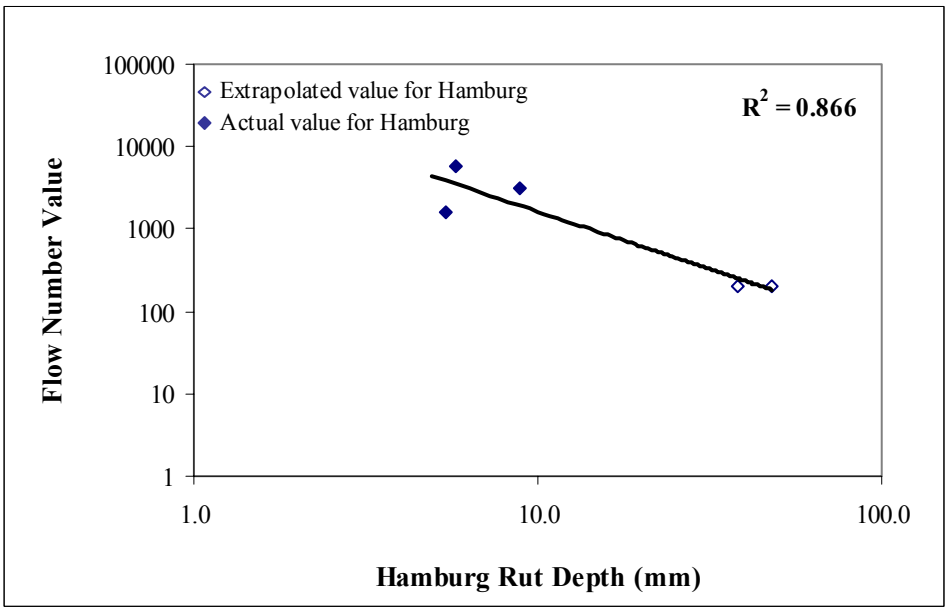

Figure I.4. HWTD Rut Depth versus Flow Number Value.

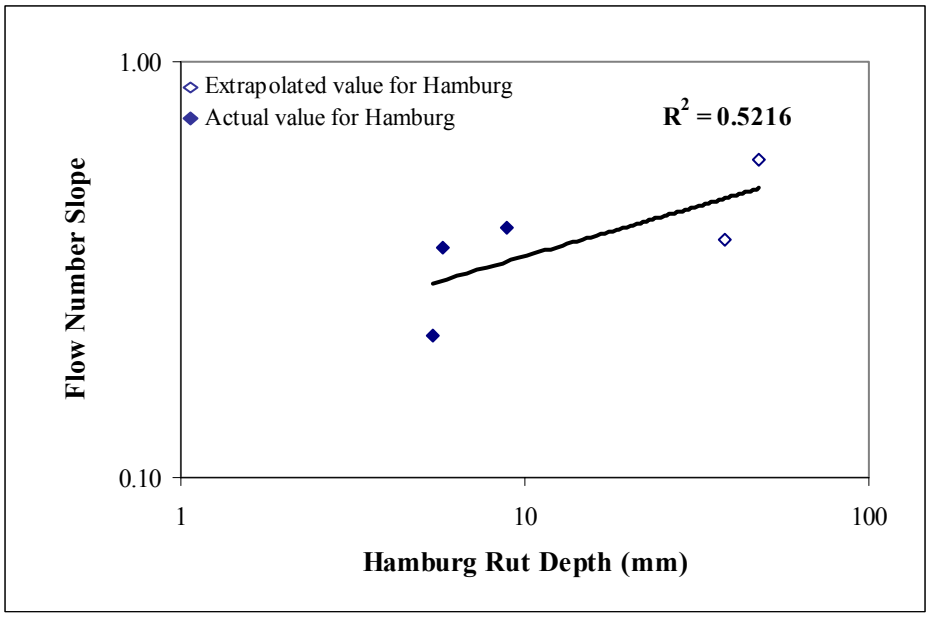

Figure I.5. HWTD Rut Depth versus Flow Number Slope.

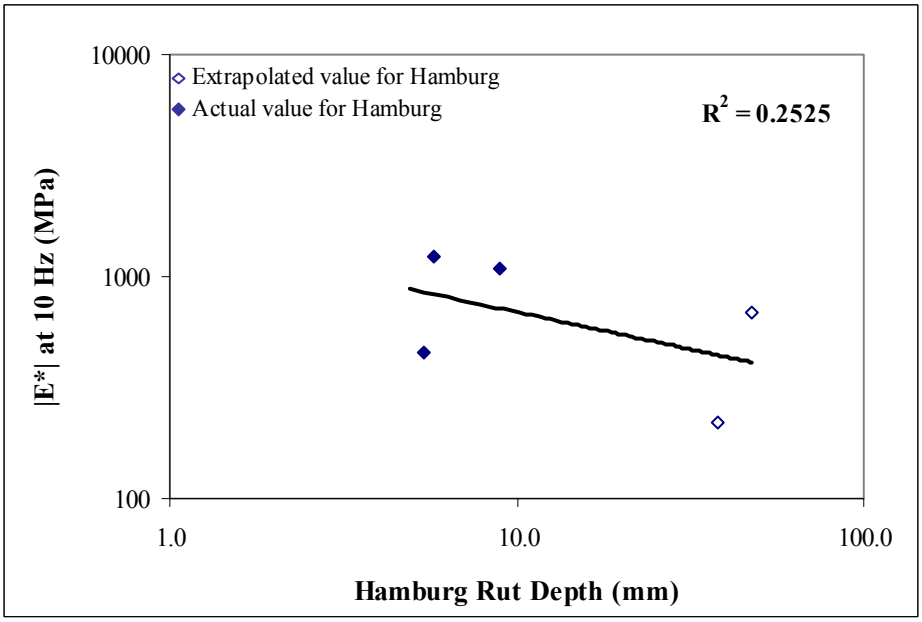

Figure I.6. HWTD Rut Depth versus |E*| at 10 Hz.

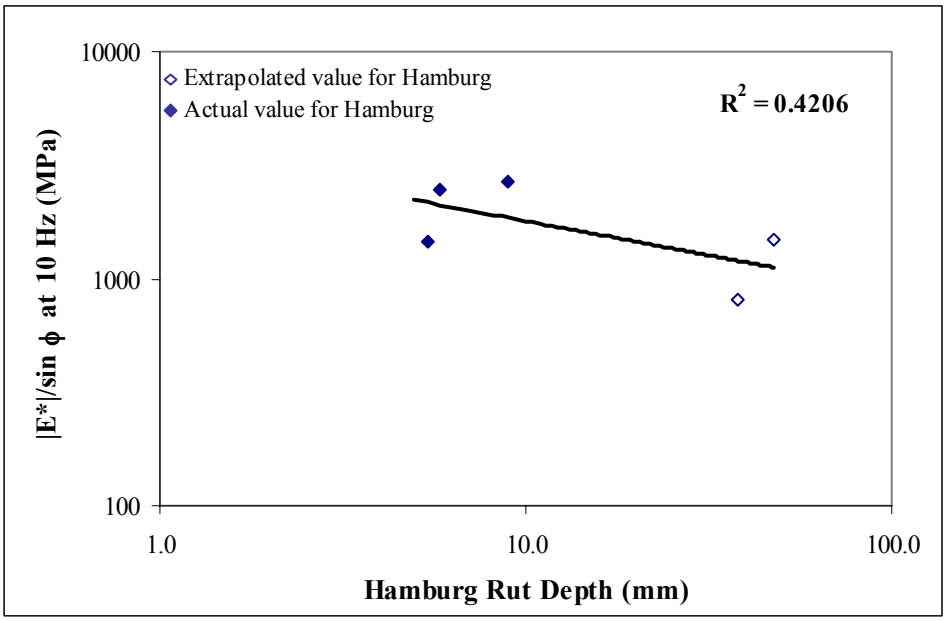

Figure I.7. HWTD Rut Depth versus |E*|/sin ϕ at 10 Hz.

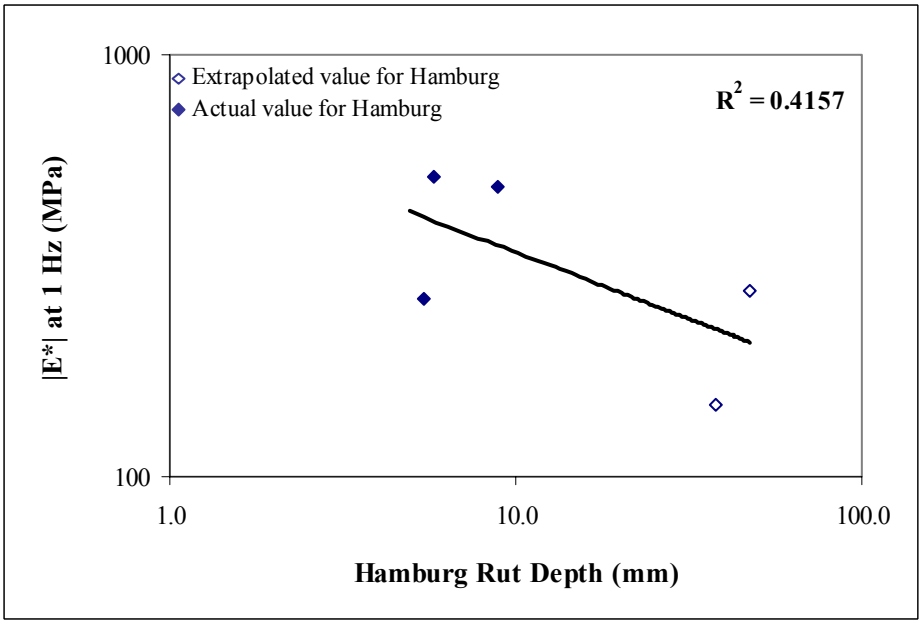

Figure I.8. HWTD Rut Depth versus |E*| at 1 Hz.

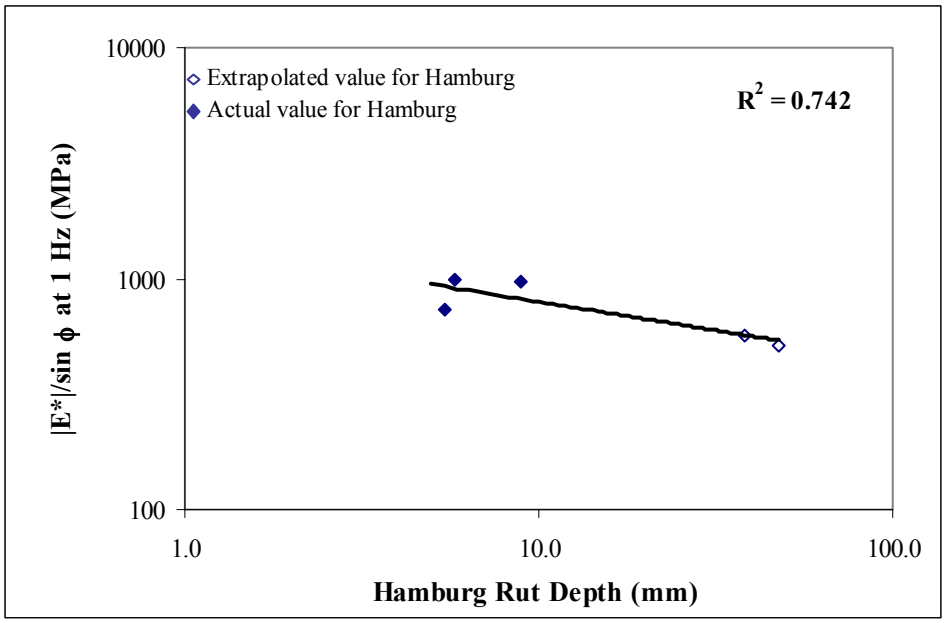

Figure I.9. HWTD Rut Depth versus |E*|/sin ϕ at 1 Hz.

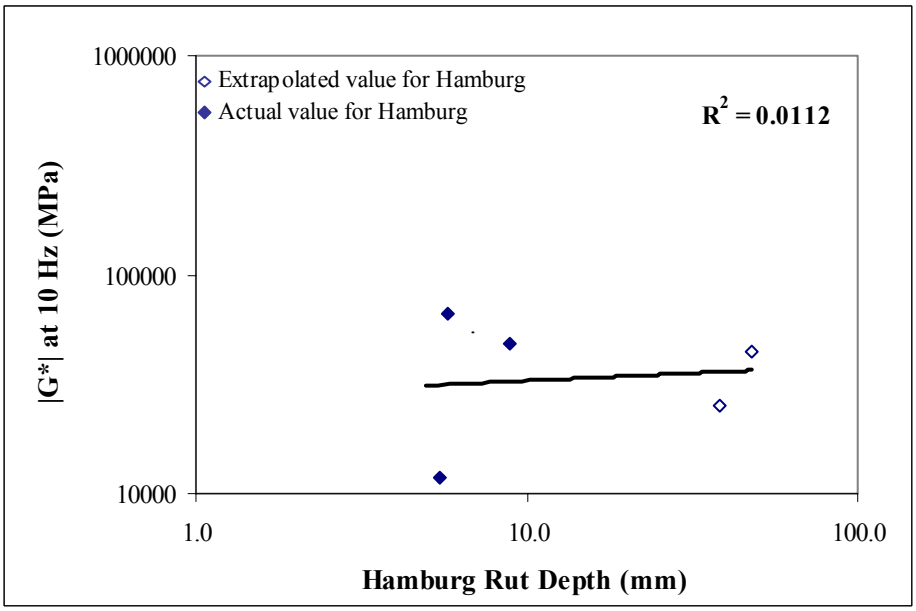

Figure I.10. HWTD Rut Depth versus |G*| at 10 Hz.

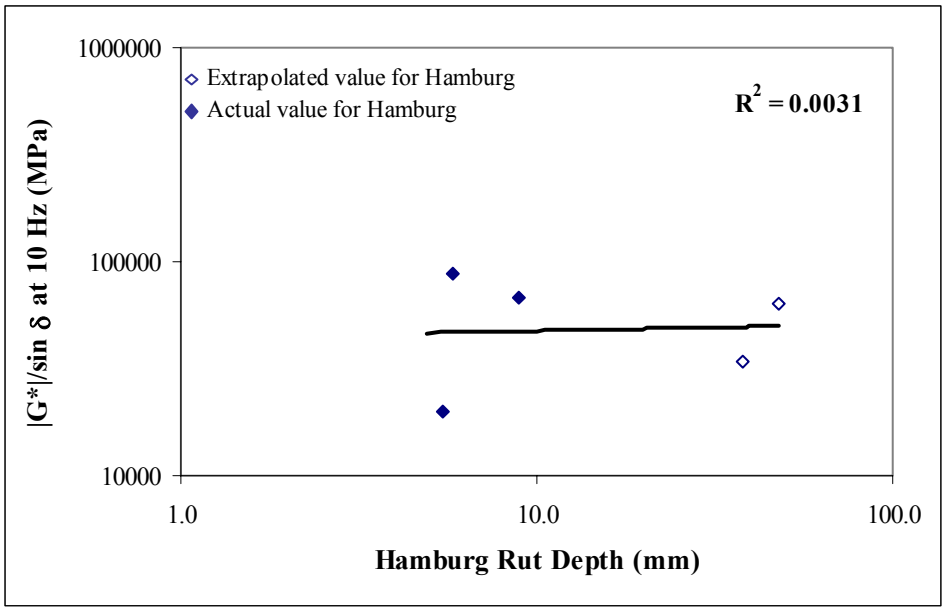

Figure I.11. HWTD Rut Depth versus |G*|/sin δ at 10 Hz.

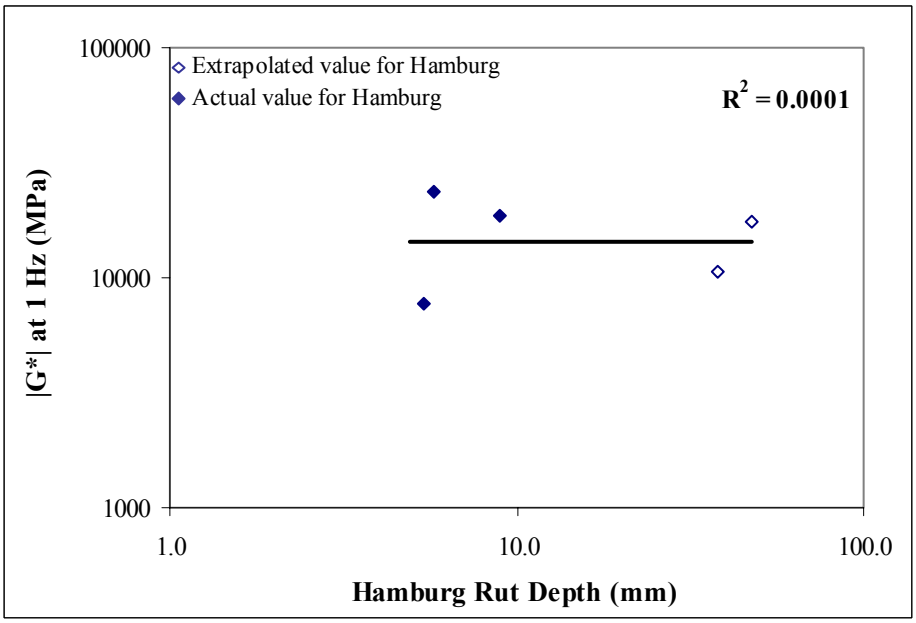

Figure I.12. HWTD Rut Depth versus |G*| at 1 Hz.

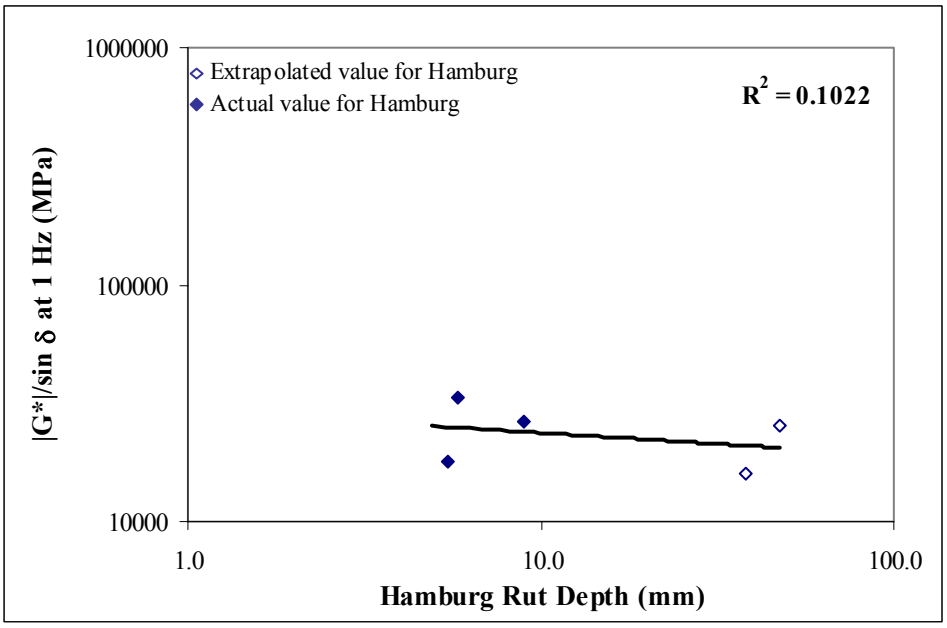

Figure I.13. HWTD Rut Depth versus |G*|/sin δ at 1 Hz.

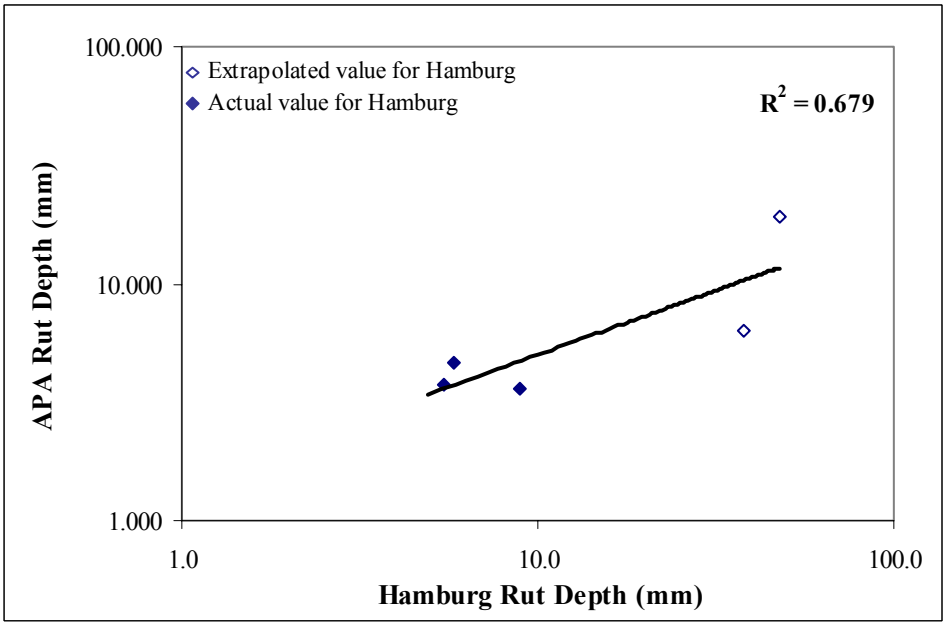

Figure I.14. HWTD Rut Depth versus APA Rut Depth.